# Molecular Mechanism of RNA-Mediated Gene Silencing in Human Cells: A Dissertation

Chia-Ying Chu
*University of Massachusetts Medical School*

## Let us know how access to this document benefits you.

# MOLECULAR MECHANISM OF RNA-MEDIATED GENE

# SILENCING IN HUMAN CELLS

## A Dissertation Presented

## By

## CHIA-YING CHU

**Submitted to the Faculty of the**

**University of Massachusetts Graduate School of Biomedical Sciences, Worcester**

**in partial fulfillment of the requirements for the degree of**

## DOCTOR OF PHILOSOPHY

**OCTOBER 9, 2008**

**DEPARTMENT OF BIOCHEMISTRY AND MOLECULAR PHARMACOLOGY**

# MOLECULAR MECHANISM OF RNA-MEDIATED GENE SILENCING IN HUMAN CELLS

A Dissertation Presented
By

**Chia-Ying Chu**

This signatures of the Dissertation Defense Committee signifies
completion and approval as to style and content of Dissertation

---
Tariq M. Rana, Ph.D., Thesis Advisor

---
Craig C. Mello, Ph.D., Member of Committee

---
Danesh Moazed, Ph.D., Member of Committee

---
Joel D. Richter, Ph.D., Member of Committee

---
Zuoshang Xu, Ph.D., M.D., Member of Committee

The signature of the Chair of the Committee signifies that the written dissertation meets
the requirements of the Dissertation Committee

---
Alonzo Ross, Ph.D., Chair of Committee

The signature of the Dean of the Graduate School of Biomedical Sciences signifies that
the student has met all graduation requirements of the school

---
Anthony Carruthers, Ph.D.,
Dean of the Graduate School of Biomedical Sciences

**Department of Biochemistry and Molecular Pharmacology**

October 9th, 2008

# DEDICATION

To my father and mother,

Hung-Hsuan Chu and Shu-Chin Chen

# ACKNOWLEDGEMENT

supports. I also thank my great classmates in year 2002 of GSBS. We shared lots of fun, passed the courses and exams together, and made me feel I am not lonely to study abroad.

Finally, I dedicate this work to my family in Taiwan, especially my parents, for their unconditional love, support, and encouragement.

# ABSTRACT

Small non-coding RNAs regulate gene expression at posttranscriptional level in eukaryotic cells. Two classes of such small (~21-25 nt) RNAs that have been extensively studied in gene silencing are short interfering RNAs (siRNAs) and microRNAs (miRNAs). RNA interference (RNAi) is process whereby double-stranded RNA induces the sequence-specific degradation of homologous mRNA. The RNAi machinery can also be programmed in human cells by introducing 21-nt siRNA duplexes that are assembled into RNA-induced silencing complexes (RISC). In this dissertation, systematic analysis of siRNAs with deletions at the passenger and/or guide strand reveals that a short RNAi trigger, 16-nt siRNA, induces potent RNAi in human cells. The 16-nt siRNA more effectively knocked down mRNA and protein levels than 19-nt siRNA when targeting the endogenous CDK9 gene. In vitro kinetic analysis of human RISC indicates that 16-nt siRNA has a higher RISC-loading capacity than 19-nt siRNA. These results suggest that 16-nt duplexes can be designed as potent triggers for RNAi.

RISC can be programmed by small interfering RNAs (siRISC) to cleave a perfectly complementary target mRNA, or endogenous microRNAs (miRISC) to inhibit translation by binding imperfectly matched sequences in the 3'-untranslated region (3'-UTR) of target mRNA. Both RISCs contain Argonaute2 (Ago2), which localizes to cytoplasmic mRNA processing P-bodies. This dissertation shows that RCK/p54, a DEAD box helicase, interacts with Ago2, in

affinity-purified active siRISC or miRISC, facilitates formation of P-bodies. Depletion of RCK/p54 disrupted P-bodies and dispersed Ago2 throughout the cytoplasm, but did not significantly affect siRNA-mediated RNAi. Depleting RCK/p54 releases general and miRNA-induced translational repression. These findings imply that miRISC-mediated translation repression requires RCK/p54, also suggest that location of miRISC to P-bodies is not required for miRNA function, but is the consequence of translation repression.

To elucidate the function of RCK/p54 in miRNA-mediated gene silencing, analysis of a series of YFP-tagged RCK/p54 mutants reveals the motif required for P-body localization, interaction with Ago2, and/or facilitating the miRNA-mediated translation repression. Additionally, rabbit reticulocyte lysate system was used to recapitulate the miRISC function in a cell-free system and confirmed the requirement of RCK/p54 for miRNA function in vitro. Analysis of Ago2 distribution in the polysome profiling in RCK/p54-depleted cells, compared to that in normal cells, revealed that RCK/p54 facilitates miRISC by trapping it at translation initiation complex. These data suggest that interaction of RCK/p54 with Ago2 is involved in the repression of translation initiation of miRNA function.

# TABLE OF CONTENTS

# LIST OF FIGURES

**Chapter IV:**

# CHAPTER I

# INTRODUCTION

**ABSTRACT**

RNA interference (RNAi) is the mechanism by which double stranded RNA (dsRNA) complexed with RNA binding proteins triggers sequence-specific gene silencing. The first hints of RNA-mediated gene silencing were observed in the early 1990s in several studies in plants and flies. The potent and specific silencing phenomenon induced by dsRNA was first defined in *C. elegans* by the Fire and Mello groups (Fire et al. 1998). The results of the Fire and Mello groups rapidly became the focus of studies on how RNAs mediate gene silencing in different eukaryotic cell types, from yeast to human. In addition to exogenously introduced dsRNA, different types of small non-coding endogenous regulatory RNA, with 19-31 nucleotides in length, have been identified as triggers for gene silencing. These small regulatory RNAs are divided into several classes according to either their interacting proteins or their origins (Table I.1). Studies on these small RNAs and their function in sequence-specific silencing have provided insights into the epigenetic regulation of gene expression in development and disease. As the RNAi field has quickly expanded, researchers have worked to identify the key effectors and cofactors, to elucidate the mechanism of sequence-specific silencing, to reveal the cellular functions of RNAi, and to exploit it as a potential therapeutic.

This chapter summarizes the significant aspects of major classes of small non-coding regulatory RNAs: small interfering RNAs (siRNAs), microRNAs

**Table I.1 Classes of small RNAs involved in gene silencing.**

| Class | Length (nt) | Mechanism | Organism | References |
|---|---|---|---|---|
| Small interfering RNA (siRNA) | 19-21 | Target mRNA cleavage | Vertebrates, fly, worm, plant, and yeast | (Rana 2007) |
| MicroRNA (miRNA) | 19-25 | Translational repression, mRNA decay | Vertebrates, fly, worm, plant, and yeast | (Bartel 2004) |
| Repeat-associated siRNA (rasiRNA) or piwi-interacting RNA (piRNA) | 24-31 | Transposon control and/or transcriptional silencing | Vertebrates, fly, worm, and plant | (O'Donnell and Boeke 2007) |
| Trans-acting siRNA (tasiRNA) | 21-22 | mRNA cleavage | Fly, plant, and yeast | (Peragine, et al. 2004) |
| Small-scan RNA (scnRNA) | ~28 | DNA elimination | tetrahymena | (Mochizuki, et al. 2002; Taverna, et al. 2002) |

(miRNAs), Piwi-interacting RNAs (piRNAs), and the newly identified endogenous siRNAs (endo-siRNAs). Here, we focus on their biogenesis, structure features, coupled effectors, and the mechanisms of each small regulatory RNA pathway to reveal the fascinating ways by which gene-silencing is controlled and fine-tuned at epigenetic level.

## 1. Small interfering RNAs (siRNAs)

## 1.1 RNA as the trigger for gene silencing

RNAi is triggered by small interfering RNAs (siRNAs), and it is considered as a conserved anti-viral mechanism that can be found in many organisms in response to foreign dsRNAs (reviewed in (Mello and Conte 2004)). When long dsRNA enters eukaryotic cells, it is processed by Dicer to form a ~21-nt RNA duplex. These substrates for Dicer cleavage are not only viral RNA or viral replication intermediates, but some endogenous RNA transcripts with long stem loop structures, such as microRNA precursors (see below), can also be recognized by Dicer and its cofactor. Cleavage of these dsRNA structures by Dicer results in a ~21-nt siRNA with 19-nt base pairs, a 2-nt overhang at the 3'end, and a phosphate group at the 5' end. Since Dicer processes linear dsRNA duplex or hairpin RNA, DNA constructs that encode small hairpin RNAs have been developed as an alternative method to induce RNAi. Moreover, synthetic 21-nt siRNAs that have structures similar to the post-Dicer cleavage products can be introduced into cells and enter the RNAi pathway (reviewed in (Carmell

and Hannon 2004)). However, it has been shown that Dicer substrate dsRNAs are more potent RNAi triggers than these 21-nt siRNAs (Kim et al. 2005; Siolas et al. 2005), possibly because Dicer processing is coupled with other co-factors and facilitates the siRNA loading onto siRNA-induced silencing complex (siRISC).

Following Dicer cleavage, only one strand of the siRNA duplex is assembled into the effector of RNAi, forming an RNA-protein complex called siRISC. The strand loaded onto RISC is known as the guide strand because it is complementary to the target sequence and serves as a guide for sequence-specific silencing of RNA. The other strand, called the passenger strand, is eliminated during RISC loading (Matranga et al. 2005; Rand et al. 2005). Strand-selection, an important feature during RISC loading, may be determined by the relative thermodynamic stability of two ends of siRNA (Khvorova et al. 2003; Schwarz et al. 2003b). With the assistance of other co-factors, the strand with less stability at the 5' end is loaded onto RISC, while the passenger stand is cleaved and eliminated. Guide strand siRNA is bound to the core endonuclease of active siRISC, the Argonaute protein, and directs the cleavage of target mRNA is then catalyzed by siRISC. With perfect base pairing and formation of an A-form helix structure between the siRNA guide strand and target mRNA, siRISC can then cleave a single phosphodiester bond of the target mRNA between the 10th and 11th nucleotide from the 5' end of the paired guide strand siRNA (Elbashir et al. 2001b). The RISC complex is then released for the next cycle of target

**Figure I.1 siRNA-mediated gene silencing.**

(a) In animals, such as fly and mammal, 21- to 22-nt siRNA duplexes that are processed from long dsRNAs or shRNA by the Dicer/TRBP complex are incorporated into RISC. Synthetic 21-nt siRNAs can also be introduced into cells and loaded onto RISC in a similar mechanism. Active siRISC containing the guide strand of siRNA recognizes and cleaves complementary target mRNA. After target cleavage, siRISC is recycled for multiple rounds of catalysis. (b) In plants and worms, the RNAi response is amplified by RNA-dependent RNA polymerases (RdRPs). RdRPs coupled with siRISC generate double stranded RNA using target mRNA as the template. This long double stranded RNA is subsequently cleaved by Dicer to form secondary siRNAs that can target more mRNA and amplify the RNAi effect.

**(a)**

shRNA or long dsRNA

siRNA

Dicer processing
and RISC assembly

5'-phosphorylation
and RISC assembly

**(b)**

Ago2

RISC assembly

Guide strand loading and
mature RISC formation

Ago2

Dicer processing

Target recognition

Ago2

m⁷G

AAAA

RdRP

mRNA cleavage

Amplification of dsRNA trigger
by RdRP

m⁷G

AAAA
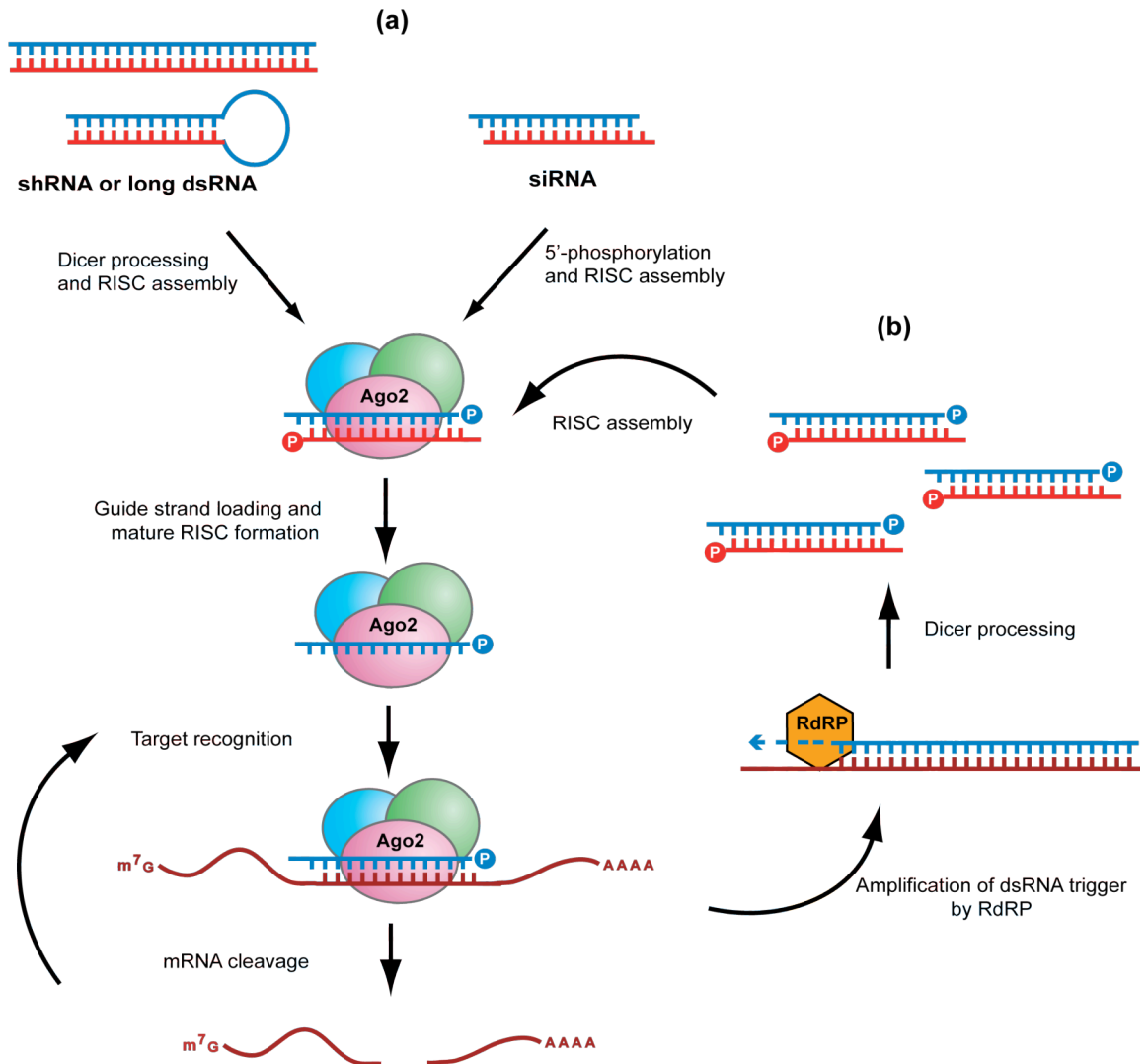
cleavage, while the cleaved target mRNA is subsequently degraded by other exonucleases in the cytoplasm (Fig I.1).

Although RNAi is a simple target-recognition and cleavage cycle in fly and human, RNAi in plants and *C. elegans* can be amplified by a mechanism that requires a specific enzyme called RNA-dependent RNA polymerase (RdRP). It has been shown that RdRP produces more dsRNA by using target mRNAs as a template with a primer-independent synthesis of complementary RNA. This RdRP-derived dsRNA can be subsequently processed by Dicer and generate more abundant secondary siRNAs for enhanced RNAi, similar to the phenomenon triggered by primary siRNAs (Reviewed in (Mello and Conte 2004) (Fig I.1b).

## 1.2 Structural features of siRNAs in RNAi pathways.

One fundamental question regarding the RNAi mechanism is why RNA duplexes, but not DNA duplexes, can induce gene silencing. This phenomenon can be explained by the differences between dsRNA and dsDNA structures (reviewed in (Rana 2007). DsRNA forms a right-handed A-form helix with 11 bp per helical turn, while dsDNA is a right-handed B-form helix with 10 bp per turn. The importance of the A-form helix in RNAi was examined by introducing modifications on synthetic siRNAs to abolish the A-form structures of siRNAs. Synthetic siRNA with a 2-nt bulge structure in the passenger strand that can disrupt the A-form helical geometry can still enter RISC and induce RNAi.

However, if the bulge is on the guide strand when it pairs with target mRNA, the RNAi effect is abolished, indicating that helical geometry is critical for target recognition but not for the RISC loading stage (Chiu and Rana 2002b). To further understand the features of siRNA structure required for RNAi, siRNAs with chemical modifications at various functional groups have been used in RNAi assays. These results confirmed that a central A-form helix is required for target cleavage of siRISC in human and Drosophila RNAi, and provide a guideline to develop modified and stable siRNAs with high potency.

Other than A-form helical geometry between the guide strand and target mRNA, the terminal structures of siRNAs are also important for RNAi activity. Since Dicer processes dsRNA or shRNA to generate siRNAs with a phosphate group at the 5' end and a hydroxyl group at the 3' end, the synthetic siRNA with the same features can function as exogenous trigger of RNAi. To understand the requirement of terminal structure for RNAi, several modifications were engineered at the 3' or 5' end of both guide stand and passenger strand (Chiu and Rana 2002b). Results of these experiments showed that only the 5'-phosphate group of guide strand is irreplaceable. However, capping at the 5'end of the passenger strand and the 3' end of both strands with other functional groups does not change the efficacy of siRNAs. Interestingly, siRNAs with a hydroxyl group at the 5' end of guide stand still induce RNAi because the hydroxyl group can be phosphorylated by endogenous RNA kinases, resulting in a structure that is the same as Dicer products. The requirement for 5'-phosphate

on the guide strand was further confirmed by the crystal structure of Argonaute proteins associated with siRNA, which showed that the guide strand RNA is anchored onto RISC via its 5' phosphate binding to the phosphate binding domain of Argonaute proteins (Ma et al. 2005). Additionally, recent studies have shown that siRNAs in Drosophila are 2'-*O*-methylated at the 3' end by the Hen1 protein to increase siRNA stability after being loaded onto RISC (Saito et al. 2007). This finding is in agreement with previous studies that 3' modification does not affect the RNAi activity in human cells.

Taken together, the structure requirements for siRNA are well characterized, and provide a guideline to design modified siRNAs that are both stable and potent (Table I.2). Efforts to examine the effects of chemical modifications of siRNA have provided insight into the application of RNAi as not only a powerful tool in biology research but also as a potent therapeutic reagent in the future.

## 1.3 Argonaute proteins are the key components in siRISC

In the RISC complex, the effector protein that directly binds siRNAs is Argonaute. Argonaute proteins perform the cleavage activity of RNAi and also mediate translation repression in miRNA pathways (see below). The human Argonaute family contains eight protein members. Four of these family members are grouped as a germ-line specific PIWI subset, which associate with 24-30 nt small RNAs called piRNAs (see below). The other four members, Ago1, Ago2,

**Table I.2 Guideline of chemically modified siRNAs**

| Modification at guide strand | Modification at passenger strand | RNAi efficiency[a] | Reference |
|---|---|---|---|
| 5'-end capping | Unmodified | - | d, e, f |
| Unmodified | 5'-end capping | ++ | d, e, f |
| 3'-end capping | Unmodified | ++ | d, e, f |
| Unmodified | 3'-end capping | ++ | d, e, f |
| 2'-deoxy | Unmodified | - | g |
| Unmodified | 2'-deoxy | + | g |
| 2'-fluoro-Pyrimidines | 2'-fluoro-Pyrimidines | ++ | g, h, i, j |
| 2'-O-methyl | Unmodified | - | g, h, i, j, k |
| 2'-O-methyl at position 2 from the 5'end | Unmodified | ++[b] | l |
| Unmodified | 2'-O-methyl | + | g, h, i, j, k |
| 2'-O-(2-methoxyethyl) | Unmodified | - / +[c] | i |
| Unmodified | 2'-O-(2-methoxyethyl) | ++ | i |
| 3-methyl-U | Unmodified | - | g |
| C5-Br-U | Unmodified | ++ | g |
| C5-I-U | Unmodified | ++ | g |
| Phosphorothioate backbone | Unmodified | + | g, h, i |
| Unmodified | Phosphorothioate backbone | ++ | g, h, i |

[a]: RNAi efficiency is presented as: ++, over 50% silencing effect; +, 20-50% silencing effect; -, less than 20% silencing.
[b]: reduced off-target effect
[c]: depending on the position of the modified base.
[d]:(Chiu and Rana 2002); [e]:(Schwarz, et al. 2002); [f]:(Czauderna, et al. 2003); [g]:(Chiu and Rana 2003); [h]:(Braasch, et al. 2003); [i]:(Prakash, et al. 2005); [j]:(Morrissey, et al. 2005); [k]:(Amarzguioui, et al. 2003); [l]:(Jackson, et al. 2006);

Ago3 and Ago4, are expressed ubiquitously and all of them are capable of binding to miRNAs or siRNAs. Although the amino acid sequence and functional domain of these proteins are highly conserved, only Ago2 exhibits the endonuclease activity to cleave target mRNA during RNAi (Liu et al. 2004; Meister et al. 2004b).

Crystal structure of full length *P. furiosus* Ago reveals that the Ago proteins contain four domains: the N-terminal, PAZ, middle, and PIWI domains (reviewed in (Tolia and Joshua-Tor 2007)). The PAZ domain recognizes the 3'end of single-stranded RNA, whereas the other three domains create a unique structure, providing a positively charged groove for guide strand RNA and target mRNA base-pairing. The PIWI domain is an RNase H-like domain, and functions as the catalytic core for substrate cleavage. The cleavage reaction requires the conserved Asp-Asp-His motif, with the assistance of $Mg^{2+}$ ions and water molecules, through an SN2 reaction mechanism. Cleavage by the PIWI active motif leaves a 5'phosphate group and a 3' hydroxyl group.

**1.4 Catalysis of animal siRISC**

Catalytic analysis of human siRISC has been studied by using RISC complexes that are assembled in multiple ways: by transfection of siRNAs into HeLa cells to produce *in vivo*-assembled holo-siRISC (Brown et al. 2005), by *in vitro*-assembly of siRISC by incubating siRNAs with immuno-purified Ago2 complex (Martinez and Tuschl 2004), or by assembly of siRNAs with

recombinant Ago2 (Rivas et al. 2005). While all of these examples have shown that siRISC is a multi-turnover enzyme, the kinetic parameters are different in each case, indicating that these three siRISC complexes are catalytically different enzymes (reviewed in Rana 2007). This difference can be explained by the composition of each siRISC. Since the holo-siRISC is assembled *in vivo*, interacting with other proteins in the complete RISC complex may limit the structure flexibility of Ago2 and result in a lower enzymatic activity. In the study of holo-siRISC, it has been revealed that the presence of target mRNA in the programming stage does not affect the concentration of assembled siRISCs or the RISC catalysis (Brown et al. 2005). This data supports the concept that the two rate-limiting steps of siRNA function, RISC loading and target recognition, take place independently in different complexes.

A big challenge of RNAi is how to induce efficient sequence-specific silencing without increasing off-target effects. To solve this issue, research on the molecular features of both siRNA sequences and target structures has provided insights into the design of siRNAs. Several algorithms have been proposed according to experimental results from different studies using systematically designed siRNAs targeting one single gene (Amarzguioui and Prydz 2004; Reynolds et al. 2004; Ui-Tei et al. 2004). Analysis of the sequence-position specificity on the 21-nt duplex allowed to determine several criteria, which may indicate a better design for siRNA sequences (reviewed in (Birmingham et al. 2007). While the sequence requirement of siRNA has been summarized, some

exceptions exist for sequences that follow the design rules, suggesting that there are other mechanisms which also influence the RNAi efficacy.

Other than the sequence feature for siRNAs, several studies also provide the evidence that target accessibility can dictate the RNAi activity. Early studies using the rigid TAR structure of HIV-1 RNA as a target for siRISC cleavage resulted in a reduced cleavage activity, which provides evidence that the target RNA structure contributes to siRISC activity (Brown et al. 2005). Additionally, when 2'-*O*-methyl antisense oligos complementary to the 5' or 3' regions of target site were used as clamps for disrupting the TAR structure, the target RNA was cleaved. Since the clamps block possibility of RISC scanning from either 5' or 3' directions, this study also suggests the target recognition of siRISC occurs by diffusion instead of a scanning model as ribosome does. Recently, the requirement of target accessibility and molecular basis for target recognition and cleavage by human RISC has been examined in greater detail (Ameres et al. 2007).

## 2. Micro-RNAs (miRNAs)

### 2.1 miRNA genome and biogenesis

The first miRNA gene was discovered in 1993, when the Ambros lab cloned the *C. elegans* lin-4 gene that encodes two tiny RNA products (Lee et al. 1993). Since then, thousands of miRNA genes from different species have been identified using direct cloning and computational approaches. MiRNA loci, which

are found in both non-coding genes and in the introns of coding genes, are distributed among all chromosomes. Biogenesis of miRNAs starts in the nucleus, where primary miRNAs are transcribed by RNA polymerase II (pol II) as transcripts with 5' $m^7G$ capping structures and 3' poly-A tails (reviewed in (Kim 2005). About 50% of all miRNA identified are grouped in clusters, and these clusters are generated as polycistronic primary transcripts. The long primary transcripts of miRNA genes (pri-miRNA), with an extended hairpin structure, are subsequently processed by the Drosha-DGCR8 (DiGeorge syndrome critical region gene-8) complex, also known as Drosha-Pasha complex in Drosophila and *C. elegans*.  Like other RNase III family endonucleases, Drosha contains two RNase III domains and a dsRNA-binding domain for catalytic function. DGCR8, a ds RNA-binding protein (dsRBP), however, functions as a ruler for this complex, measuring the cleavage site for Drosha (Han et al., 2006). The Drosha-DGCR8 complex cleaves pri-miRNAs at the 11-nt position from the base of stem structure, resulting in a 70-nt long, stem-loop structured miRNA precursor (pre-miRNA) with a 5' phosphate end and a 2-nt 3' overhang.

Although most pre-miRNAs are processed by Drosha, some miRNAs are derived from a different pathway. In Drosophila and mammals, it has been recently determined that a specific group of miRNA loci, which are called "mirtrons", are localized in the introns of coding genes and generate intronic hairpins during pre-mRNA splicing (Okamura et al. 2007; Ruby et al. 2007).  As a result of RNA splicing, the intronic hairpin forms a pre-miRNA-like structure that

bypasses Drosha cleavage. Mirtron-encoded pre-miRNAs are then exported and processed in a shared pathway with Drosha-cleaved pre-miRNAs.

After this primary processing step in the nucleus, pre-miRNAs are delivered to the cytoplasm for the next step of miRNA maturation. The transportation of pre-miRNAs is mediated by the nuclear export factor, Exportin-5 (Exp5), which partners with the GTP-bound cofactor Ran protein, which drives pre-miRNA through the nuclear pore to the cytoplasm (Yi et al. 2003; Bohnsack et al. 2004; Lund et al. 2004). Exportin-5 was first identified as a minor transporter for tRNAs when the major tRNA transporter, Exportin-t, does not function well (Bohnsack et al. 2002). Exportin-5 also exports some viral RNA with similar stem-loop structures and 3' overhangs, such as the adenoviral RNA VA1. The structural requirement for pre-miRNA delivery to the cytoplasm by Exp-5 has been identified as an RNA structure composed of a 16 bp stem-loop and a short 3' overhang (Zeng and Cullen 2004). Following export from nucleus, pre-miRNAs are then processed by Dicer for miRNA maturation in the cytoplasm (Fig. I.2).

Dicer is a cytoplasmic RNase III enzyme that cleaves long dsRNAs into ~22-nt duplexes of mature miRNA and miRNA passenger strand (miRNA/miRNA*) with a 5' phosphate and 2-nt overhangs at its 3' end. Dicer is highly conserved in most eukaryotic species, but in some organisms it is expressed as multiple homologs with distinct functions involved in different RNAi mechanisms. For instance, it has been shown that Drosophila Dicer-1 is involved

**Figure I.2 miRNA-mediated gene silencing.**

Pri-miRNAs are transcribed by RNA Pol II, processed into pre-miRNAs by Drosha/DGCRB in nucleus and exported into cytoplasm by EXP5-Ran. The hairpin pre-miRNAs are subsequently cleaved by Dicer/TRBP to ~22-nt miRNA/miRNA* duplexes, which are then loaded into RISC. Active miRISC then recognizes the 3'UTR of target mRNAs with imperfect base-pairing and induces translation repression through three possible mechanisms. (1) Post-initiation repression: miRISC inhibits protein translation after the initiation step and prevents protein synthesis. (2) Initiation repression: miRISC binds to the cap structure of target mRNA and blocks the initiation of protein translation by preventing the association of translation initiation factor eIF4E to mRNA 5' cap. In this case, miRISC also blocks the assembly of 80S ribosome. (3) Destabilizing target mRNA: Recognition by miRISC induces deadenylation and decay of the target mRNA. Destabilization and increased turnover of target mRNA results in reduced protein synthesis. In all three possible mechanisms, miRISC-targeted mRNAs are sequestered in P-bodies for storage or decay, although the mRNA degradation might also happen outside P-bodies.

microRNA gene

Transcription by Pol II

Drosha-DGCR8

Exp5-Ran

Processing by Dicer

RISC assembly

RISC

**microRNA biogenesis**

**Nucleus**

m⁷G — AAAA

Target RNA

m⁷G — AAAA

**1. Post-initiation repression**

m⁷G — AAAA

**2. Initiation repression**

**3. Target mRNA Destabilization**

Block 80S assembly
Prevent initiation

De-adenylation & degradation

mRNA degradation

storage

**P-body**
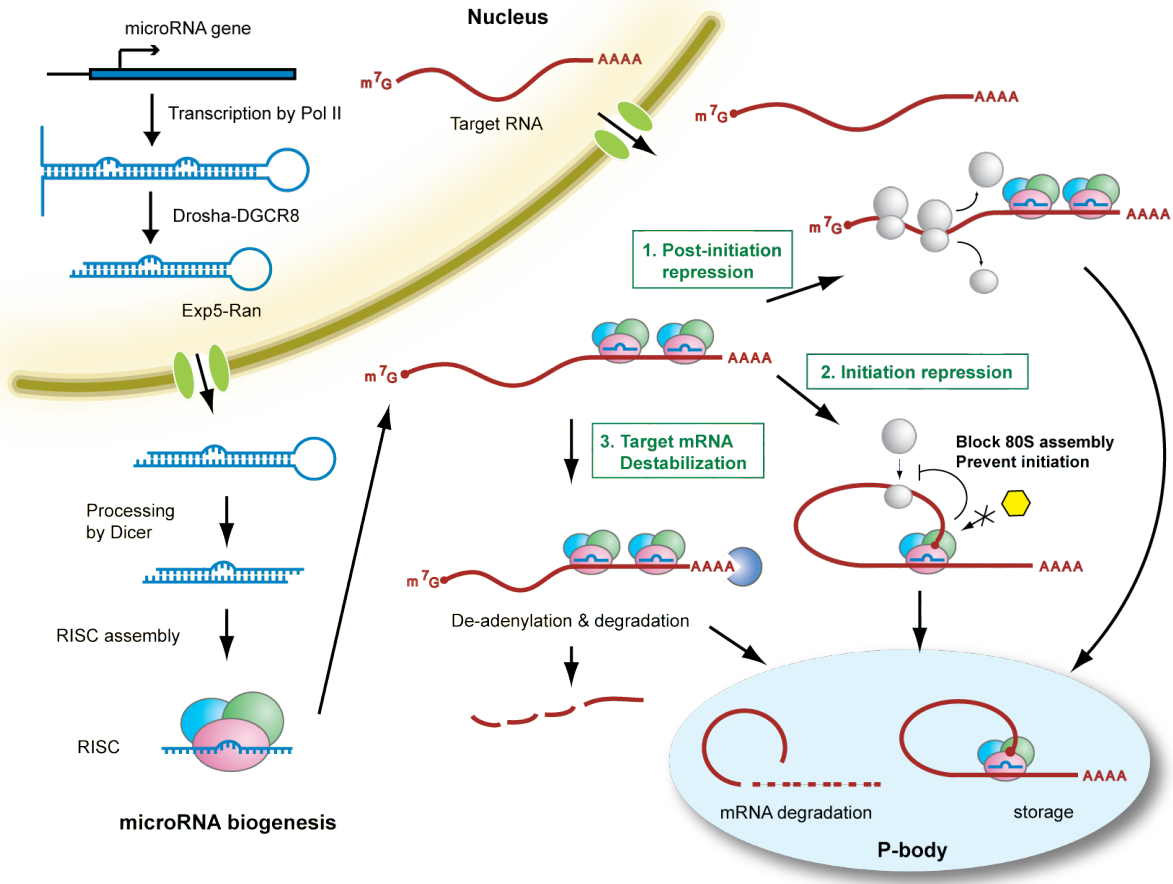
in miRNA maturation, while Dicer-2 is required for the siRNA pathway (Lee et al. 2004). Like Drosha and other RNase III family proteins, Dicer also interacts with dsRNA-binding proteins that may facilitate miRNA processing. In Drosophila, Dicer-1 and its interacting protein, Loquacious (Loqs), collaborate to facilitate miRNA maturation (Forstemann et al. 2005; Saito et al. 2005). In mammalian cells, Dicer associates with transactivation-response element RNA-binding protein (TRBP) and protein activator of the interferon-induced protein kinase (PACT) (Chendrimada et al. 2005; Lee et al. 2006). Since purified Dicer alone maintains cleavage activity *in vitro*, it has been proposed that these Dicer-interacting proteins are not required for RNase activity. Instead, the complex of Dicer and its interacting proteins play important roles in the next stage, where the miRNA/miRNA* duplex undergoes unwinding and loading onto the functional complex, miRNA-induced silencing complex (miRISC).

Similar to the unwinding process of siRNA as described above, only one strand of miRNA/miRNA* duplex can be successfully incorporated onto RISC, while the other strand is released and eliminated. The relative thermodynamic stability of the ends of miRNA duplexes may determine the strand selection. That is, the strand with less stability at the 5' end is loaded onto RISC, while the other strand is released and degraded. Several interesting questions remain with regard to the miRISC assembly stage. First, the mechanism of duplex unwinding is still unknown. Although Dicer contains DEAD-box helicase domain, there is no direct evidence that it is required for RNA unwinding. In Drosophila, a putative

RNA helicase, Armitage, has been shown to enhance miRNA maturation. A recent study illustrated that RNA helicase A (RHA) interacts with RISC and functions as a co-factor that facilitates siRNA and miRNA loading onto RISC in human cells, but a detailed mechanism for this loading step is still unclear (Robb and Rana 2007). RHA may directly unwind dsRNA for RISC loading or it may also remodel RISC complexes to enhance the miRNA loading.

The second interesting question about miRISC assembly is how cellular factors can distinguish the miRNA and siRNA pathways. Although miRISC contains several proteins such as Dicer, TRBP, PACT, and Gemin3, only Argonaute proteins are directly associated with miRNAs. Drosophila Ago1 and Ago2 play distinct roles involved in two separate pathways: Ago1 is part of miRISC and Ago2 is part of siRISC (Okamura et al. 2004). Recent studies reveal the molecular mechanism of sorting miRNA/miRNA* or siRNA duplexes into two different complexes (Förstemann et al. 2007; Tomari et al. 2007). The internal bulge structures of RNA duplex determine the final functional complex in Drosophila RNAi. The duplex of miRNA/miRNA* usually forms bulge structures at the imperfect matched sequence and binds Ago1 in siRISC, while the perfectly matched siRNA duplex enters siRISC with Ago2. In human cells, however, the Ago family contains four proteins, Ago1-4, and all of them can associate with miRNA, suggesting that the miRNA pathway may be mediated by all Ago proteins.

## (X) 3.2 Target recognition of miRNAs

While siRNAs require perfect match for the target cleavage, a key feature of miRNA-target mRNA interaction is imperfect base pairing between the miRNA guide strand and the target mRNA. Given that imperfect matches usually create bulge structures at mismatched nucleotides, the sequence specificity for target recognition is determined by the base-paired nucleotides located at position 2-8 of the miRNA's 5' end, referred to as the "seed sequence" (Doench and Sharp 2004). The requirement for miRISC function is only 7-nt long; so one miRNA could possibly recognize multiple mRNAs because several mRNA sequences could harbor the same complementary sequences to a single miRNA sequence. Indeed, miRNAs have been predicted by computational analysis of genome databases and miRNA sequences to regulate the expression of more than one third of human proteins (Lewis et al. 2005).

Specificity of miRNA for targeting protein-encoded genes has been validated by using experimental and computational approaches to develop several algorithms for miRNA-target recognition (Table I.3). In addition to the target site's perfect match with the miRNA seed region, miRNA targeting is enhanced by five other features of the target site (Grimson et al. 2007): (1). mRNAs with multiple miRNA target sites at the 3'UTR are more efficiently repressed. When two sites are closer together, the repression effects are stronger. (2). Additional base-pairing at nucleotide 12-17 of miRNA's 5'end can increase the miRNA effect on target repression. (3). Local AU-rich nucleotide

**Table I.3 Online sources of miRNA target prediction programs**

| Program | Website | Organism | Reference |
|---|---|---|---|
| DIANA-microT | http://www.diana.pcbi.upenn.edu/ | All | (Kiriakidou, et al. 2004) |
| MicroIspector | http://mirna.imbb.forth.gr/microinspector/ | All | (Rusinov, et al. 2005) |
| MiRanda | http://www.mircorna.org/ | Fly, zebrafish, and human | (Enright, et al. 2003; John, et al. 2004) |
| MiRNA-Target gene prediction at EMBL | http://www.russell.embl.de/miRNAs/ | fly | (Brennecke, et al. 2005) |
| PicTar | http://pictar.bio.nyu.edu/ | Worm, fly, and vertebrates | (Grun, et al. 2005; Krek, et al. 2005; Lall, et al. 2006) |
| RNAhybrid | http://bibiserv.techfak.uni-bielefeld.de/ | All | (Rehmsmeier, et al. 2004) |
| TargetBoost | http://demo1.interagon.com/demo | Worm and fly | (Saetrom, et al. 2005) |
| TargetScanS | http://www.targetscan.org/ | Worm, fly, and vertebrate | (Lewis, et al. 2005; Lewis, et al. 2003) |

context also correlates with miRNA targeting efficacy. (4). The position of 3'UTR miRNA targeting sequences should be at least 15nt downstream from the stop codon of the target mRNA (5). The position of target should be away from the center of long UTRs. Overall, a better knowledge of the mechanism of miRNA targeting will help the biochemical and genetic studies of regulatory miRNA functions in different cellular pathways.

## 2.3 Mechanism of miRNA-mediated gene silencing

In plants and a few animal cases, miRNAs can direct the cleavage of their target mRNAs if they are perfectly matched. However, most miRNAs in animals function as translational repressors. After a miRNA recognizes the 3'UTR of its target, how miRISC interferes with gene expression remains controversial. Evidence of miRISC regulating gene expression by accelerating mRNA degradation, repressing protein synthesis, and sequestering mRNA to storage compartments suggest several models for miRNA function (Fig I.2).

The first model suggests a post-initiation repression mechanism, where the miRISC may attenuate or stop the elongation of translation. This hypothesis was supported by evidence that lin-4 miRNA down-regulated lin-14 encoded protein in the *C. elegans* larva without changing lin-14 mRNA levels (Olsen and Ambros 1999). Analysis of mRNA polysome profiles has revealed that the repressed lin-14 mRNA was found in polysome fractions, suggesting that miRNA mediates protein expression after initiation of translation. Similar results have

been observed in mammalian cells when reporter constructs with miRNA target sites were transfected and expressed (Nottrott et al. 2006). Further support for a post initiation repression mechanism came from studies of human cells, using a polycistronic reporter construct with both cap- and internal ribosome entry site (IRES)-dependent reporter genes showing that both types of genes were associated with polysomes and can be repressed by miRNA (Petersen et al. 2006). Finally, polysome profile studies of HeLa cells showed that miRNA, together with its target mRNAs, are found in polysome fractions of cell lysates, indicating that miRNAs interact with translating mRNAs (Maroney et al. 2006). These findings suggest a mechanism where miRNA blocks translation after initiation step, but the details of how miRNA induces translation repression is still unclear. One possible explanation could be that after ribosomes are released from mRNAs, the transcripts associated with miRISC are relocated to processing bodies (P-bodies) for storage or decay (see below).

The second hypothesis of miRNA-mediated translation repression is that miRISC functions at the initiation step. This hypothesis was first proposed in studies of human cells where translation initiation was inhibited by endogenous let-7 miRNA or by Ago2 tethered at the 3'UTR of reporter mRNA (Pillai et al. 2005). In contrast to the data from other groups, this report showed that cap-independent translation by IRES resists miRNA-mediated gene silencing and suggests that miRNA represses translation at the initiation stage. Recently, *in vitro* recapitulations of miRNA-mediated repression in cell-free systems including

rabbit reticulocyte lysates, Drosophila embryonic lysates, human 293 cell lysates, and mouse Krebs-2 ascites lysates revealed that 5' cap structure of target mRNA is important for miRNA function (Wang et al. 2006; Mathonnet et al. 2007; Thermann and Hentze 2007; Wakiyama et al. 2007). Target mRNAs with an ApppG cap structure instead of a normal m7GpppG were resistant to miR-2-mediated repression in fly or *let-7*-mediated repression in mammals. In another approach, affinity purification of TRBP showed that eIF6 complexes with TRBP in human miRISC (Chendrimada et al. 2007). Given that eIF6 is a 60S ribosome-interacting protein that blocks the assembly of 80S ribosome during translational initiation, depletion of eIF6 abolishes miRNA-mediated gene silencing in human cells and lin-4 mediated translation repression of lin-14 and lin-28 in *C. elegans*. The involvement of eIF6 in miRISC function provides further evidence for miRNA repressing translation by a mechanism that repress translation initiation.

Other support for this mechanism comes form recent approaches indicating that human Ago2 directly interacts with mRNA cap structure and contains a cap-binding motif (MC) similar to that of eIF4E, a translation initiation factor that binds to the cap in normal translation initiation (Kiriakidou et al. 2007). Two phenylalanine residues, F470 and F505, in the MC domain of Ago2 have been shown to contribute to cap-binding efficacy. Mutations at these two amino acid residues abolish the specific binding of Ago2 to m7GTP-Sepharose and its function in translation repression, without affecting miRISC assembly and catalytic activity of Ago2. These findings, in agreement with *in vitro* miRISC

recapitulation results, support a model in which Ago2 competes with eIF4E for cap-binding and miRISC functions at initiation stage. Interestingly, sequence alignment and analysis of Argonaute proteins in fly reveals that, Ago1 contains similar cap-binding domain, while Ago2 does not. This result may explain the distinct function of fly Ago1 and Ago2 in two separate (miRNA and siRNA) pathways.

A third mechanism for miRISC-mediated translation repression implies the destabilization of target mRNA. In some cases, degradation rates of target mRNAs increase with miRNA-mediated gene repression, suggesting miRNAs may trigger target destabilization by a deadenylation mechanism (Bagga et al. 2005; Behm-Ansmant et al. 2006; Wu et al. 2006). Those miRNA-regulated mRNAs may also translocate to P-bodies for accelerated decay.

In human cells, localization studies of Ago proteins indicate that Ago proteins are not only distributed in the cytoplasm but also concentrated at some specific cytoplasmic foci known as mRNA processing bodies (P-bodies) (Liu et al. 2005b; Sen and Blau 2005). P-bodies (also known as GW or DCP bodies) contain non-translating mRNAs as well as proteins involved in mRNA remodeling, translation repression, decapping, and 5'to 3' exonuclease activity (reviewed in (Eulalio et al. 2007a)). It has been shown that miRISC and target mRNA are localized to P-bodies and these data suggest that P-bodies serve as the place for target mRNA storage or decay in miRNA-mediated gene silencing pathway. While several P-body components, such as GW182 and RCK/p54,

function in translational repression by miRISC (Jakymiw et al. 2005; Liu et al. 2005a; Rehwinkel et al. 2005; Chu and Rana 2006),  the consequence of P-bodies structure for miRNA function, however, is somewhat elusive.

Disruption of P-bodies by depleting Lsm1, a P-body scaffold protein, results in the dispersal of Ago2 throughout the cytoplasm without affecting siRISC and miRISC functions (Chu and Rana 2006). Together with recent similar results (Eulalio et al. 2007b), this evidence suggests that localization of miRISC and target mRNA in P-bodies is not a prerequisite or trigger for miRNA-mediated silencing, but rather a consequence for miRNA function. The functional significance of P-bodies in miRNA–mediated gene silencing is that they provide an environment plentiful with high concentration of enzymes for RNA decay, such as the CCR4/NOT deadenylase, DCP1/DCP2 decapping complex, and general translational repressors (eIF4ET, RCK/p54). Although RNA degradation starts before entering P-bodies, relocation of target mRNA to P-bodies may accelerate RNA decay in downstream processes of miRNA functions. Another function of P-bodies in translational repression is to provide a storage compartment for sequestered mRNA. Some miRNA-controlled mRNAs can be released from P-bodies in response to stress conditions (Bhattacharyya et al. 2006), suggesting that repression by miRNA is a dynamic and reversible phenomenon in the cytoplasm and that miRNA-repressed mRNAs are capable for resuming active translation.

To date, experimental evidence supports at least three models for miRNA-mediated gene silencing as summarized above. The complexity of miRNA sequence and function in the regulation of cellular physiology, make these mechanisms of miRNA-mediated mechanisms act simultaneously or synergistically to repress transaltion. Given that relatively few examples have been studied, it is possible that some other cofactors or conditions can also modulate miRNA function that remain to be uncovered in the future.

## 3. Piwi-interacting RNAs (piRNAs)

### 3.1 Germline-specific Argonaute proteins and their associated small RNAs

The Argonaute protein family has many members that can be divided into several subsets according to sequence homology: the Argonaute subfamily, the Piwi subfamily, and the *C. elegans*-specific subfamily. As described earlier, the core effector for miRISC or siRISC belongs to the Argonaute subfamily, such as Ago1 and Ago2 in Drosophila and Ago1-4 in human.

The second subset of Argonaute proteins, the Piwi proteins, is expressed specifically in certain animal tissue. Unlike the ubiquitously expressed Argonaute subfamily proteins, Piwi proteins are found in germ-line cells of animals. These Piwi proteins share some functional similarities in different organisms. Genetic studies in fly(Cox et al. 1998), zebrafish and mouse showed that the Piwi proteins are involved in germline development (Deng and Lin 2002; Kuramochi-Miyagawa et al. 2004; Carmell et al. 2007; Houwing et al. 2007). In fly, the Piwi

subfamily includes Ago3, Aubergine, and Piwi, whereas the mouse Piwi subfamily contains MIWI, MILI, and MIWI2.

Like other members of Argonaute family, the Piwi proteins also bind to small RNAs. Recent studies have revealed that a new set of endogenous small 24-30nt RNAs, called PIWI-interacting RNAs (piRNAs), are associated with Piwi proteins (reviewed in (Hartig et al. 2007)). Sequence and structure analysis of cloned piRNAs from immunopurified Piwi proteins implicate several interesting features of piRNA, unique from miRNA. First, piRNAs contain a high percentage of uridine nucleotide at the 5' end. Second, the genomic mapping of piRNAs in fly and mouse showed that piRNA genes are concentrated at several genomic loci and that adjacent clusters of piRNA reveal the same orientation with a strand bias. Third, the 3'end of piRNAs is 2'-*O*-methylated.

## 3.1 Biogenesis of piRNAs

Since the 24-30 nt piRNAs are longer than miRNAs, it is believed that production of piRNA is Dicer-independent. This possibility is supported by genetic studies in fly and zebrafish (Vagin et al. 2006; Houwing et al. 2007). Insight into the mechanism of how Piwi proteins control piRNA production comes from large-scale sequencing of piRNAs isolated from purified Piwi proteins. Genetic mapping of these sequenced piRNAs indicated that piRNA genes are located in several pericentromeric or telomeric heterochomatin loci containing retrotransposons. Strand bias is found in the piRNAs from different Piwi proteins.

For example, the fly Aub- and Piwi-associated piRNAs have sequences similar to that of the anti-sense strand of retrotransposons, while Ago3-bound piRNAs are similar to the sense strand (Brennecke et al. 2007; Gunawardane et al. 2007). Interestingly, the first 10 nucleotides of sense strand piRNAs associated with Ago3 are complementary to the first 10 nucleotides of Aub-interacting antisense strand piRNAs, suggesting that a unique mechanism is involved in the production of two piRNA populations (see below). Additionally, the Aub and Piwi-bound piRNAs contain a high percentage of U at their 5'end, while the Ago3-bound piRNAs contain a high percentage of A at the 10th nucleotide from the 5' end (Brennecke et al. 2007; Gunawardane et al. 2007).

Giving that all Piwi proteins exhibit the cleavage activities, a unique amplification loop for piRNA biogenesis has been proposed (Fig I.3). Ago3 associated with sense strand piRNA directs the cleavage of long transcripts of RNA, resulting in the formation of 5' end of antisense piRNAs. This 5' end product of Ago3 cleavage is subsequently bound to Aub or Piwi and cleaved at ~24 to 30 nt from the 5' end to generate the antisense strand of piRNAs. The Aub or Piwi complexed with antisense strand piRNAs then function as a slicer to bind and then cleave sense-strand RNAs, resulting in the 5' end of sense strand RNA coupled with Ago3 protein. This 5' end processing is then followed by the processing at 3' end, and more mature sense-stranded piRNAs are generated.

Although this ping-pong model explains the amplification of both strand piRNAs, it is still unclear how 3' end cleavage is performed. Mutation of two

**Figure I.3 Model for piRNA biogenesis**

Primary piRNA transcripts, such as transposon regulatory regions of heterochromatin, are incorporated into Piwi and Aub and trigger the piRNA amplification loop. Piwi and Aub bind anti-sense strand piRNA and cleave the target transcript to generate the 5' end of sense strand piRNA that is subsequently associated with Ago3. After 3' end cleavage and 3'-*O*-methylation, the Ago3-bound sense strand complex with piRNA functions as another slicer, which recognizes and cleaves the anti-sense strand precursor, to generate more Piwi/Aub-associated anti-sense strand piRNAs.

primary processing of piRNAs

Piwi/Aub 2' OMe
5'

U Piwi/Aub 2' OMe
5'
A

Ago3

antisense piRNA

U Piwi/Aub 2' OMe
5'

Ago3
3' A 5'

3' truncation
2'-O-methylation at 3' end

3' truncation
2'-O-methylation at 3' end

U Piwi/Aub
5' 3'

2' OMe Ago3
A 5'

sense piRNA

Piwi/Aub

2' OMe
A 5'
U
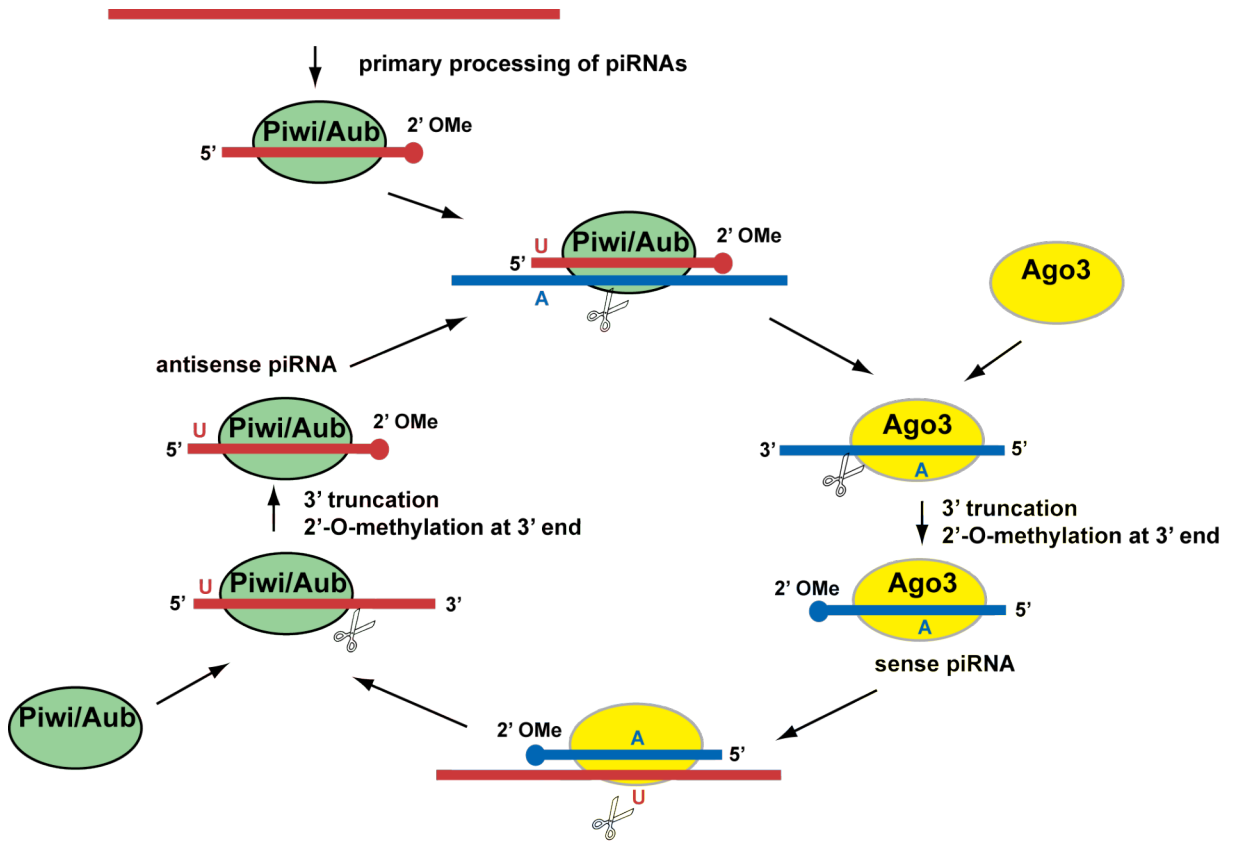
Drosophila genes, *zucchini* and *squash*, results in the loss of piRNAs, suggesting the encoded putative nucleases, Zucchini and Squash, may be involved in the processing of 3' end during piRNA maturation (Pane et al. 2007).

## 3.3 3'-end modification of piRNAs

It has been revealed that in mouse, fly and zebrafish, piRNAs are 2'-*O*-methylated at their 3' ends (Kirino and Mourelatos 2007; Ohara et al. 2007). This 2'-*O*-methylation of 3' termini is also found in plant miRNAs and Drosophila siRNAs. The methylation of fly piRNAs and siRNAs is performed by a single-strand-specific methyltransferase, Pimet/DmHen1 (Horwich et al. 2007; Saito et al. 2007). It has been shown that Pimet/DmHen1 can interact with Aub, Piwi, and Ago3, but not Ago1, suggesting it has a role in piRNA maturation. Mutation of Pimet/DmHen1 results in slightly shortened piRNAs, indicating that the 2'-*O*-methylation can protect the piRNAs and siRNAs from targeting by other exonucleases and can also interfere with the interaction between piRNAs and other proteins. Nonetheless, the genetic evidence that *pimet/hen1* mutant flies are fertile and viable implicates that the 3' end modification may not be crucial for piRNA function.

## 3.4 Biological functions of piRNAs

Genetic studies in mouse and fly provide evidence of how piRNAs function in germline development. Mouse Piwi proteins, including MIWI, MILI and MIWI2,

are expressed specifically in male testis at different stages of spermatogenesis (Kuramochi-Miyagawa et al. 2001; Carmell et al. 2007). Knockout mutations of MIWI, MILI, and MIWI2 result in the arrest of spermatogenesis at different stages. In MILI-deficient mice, spermatogenesis is arrested at early pachytene stage of spermatocytes, while in MIWI-knockout mice, it is stopped at the round spermatid stage. The loss of germ cells phenotype is observed in all Piwi-deficient mice and is accompanied by a derepression of transposable elements, suggesting that the MILI-, MIWI-, and MIWI2-associated piRNAs are involved in maintaining germline stem cells as well as transposon control (Aravin et al. 2007; Carmell et al. 2007).

Biological function of piRNAs has also been elucidated in *Drosophila* system as well. PiRNAs were first identified as rasiRNAs, which silence genomic tandem repeats and transposons in Drosophila (Aravin et al. 2001), as depleting all proteins involved in piRNA production induced a significant over-expression of retrotransposons (Aravin et al. 2001; Vagin et al. 2006). Cloning and genomic mapping of piRNAs implicate the biogenesis of piRNAs as well as the mechanism of how piRNAs involved in the repression of selfish genetic elements (Brennecke et al. 2007). One discrete genomic locus of piRNA clusters is the *flamenco* locus, which has been shown to control the activity of *gypsy*, *Idefix*, and *ZAM* retrotransposons. Mutation of the *flamenco* locus leads to a decrease of mature piRNA levels (Brennecke et al. 2007), and *gypsy* RNA levels are increased in Piwi mutants (Sarot et al. 2004), suggesting that the silencing of

retrotransposons requires Piwi proteins and piRNAs, and is coupled with the biogenesis of piRNAs, while the detail mechanism of other piRNAs are still unknown.

In addition to the repression of genetic elements, it has been shown recently that Piwi and piRNAs may play roles in activation of heterochromatin in Drosophila (Yin and Lin 2007). Localization studies showed that Piwi, unlike other Piwi family proteins, is mainly distributed in the nucleus of fly oocytes, suggesting that nucleus is the functional compartment for piRNAs bound to Piwi (Saito et al. 2006; Brennecke et al. 2007). It has been shown that Piwi promotes euchromatic histone modification and piRNA transcription in heterochromatin in subtelomeric regions. Depletion of Piwi results in the loss of euchromatic histone modification and the accumulation of heterochromatin, indicating that Piwi can modify the heterochromatin to become euchromatin, and increase its transcription (Yin and Lin 2007). This finding, which contradicts the known role of piRNAs in gene silencing, suggests that the epigenetic control by small RNAs may be through multiple mechanisms, either silencing or activation of target genes, at the transcriptional or post-transcription level of gene expression.

## 4. Endogenous siRNAs (endo-siRNAs)

### 4.1 Discovery of endogenous siRNAs

The classic phenomenon of RNAi in animals has been considered a mechanism of protection against viruses or other external infections. While some

animals, such as *C. elegans*, can use RdRP to generate siRNAs that correspond to some genomic loci, the origins of siRNAs in fly and mammals have been mostly considered as exogenous, either encoded by viruses or experimental introduced. Yet, recent studies in Drosophila and mouse have revealed that a new class of endogenous siRNAs (Endo-siRNAs) exists in these animals that lack RdRP (reviewed in (Golden et al. 2008; Okamura and Lai 2008)).

In Drosophila, endo-siRNAs were recently identified by several groups with different approach methods. Czech *et al.* and Kawamura *et al.* immunoprecipitated fly Ago2 from tissue and cells to identify the endogenous small RNAs associated with Dicer-2/Ago2 siRNA pathways(Czech et al. 2008; Kawamura et al. 2008). Both groups found that these Ago2-associated RNAs are different from previously identified miRNAs or piRNAs. Sequence analysis of these RNAs revealed that most of the Ago2-associated endo-siRNAs are derived from transposable elements, while some of the endo-siRNAs may be related to hairpin or convergent transcribed RNA precursors. Two other groups did bioinformatic approaches(Chung et al. 2008; Okamura et al. 2008b). Okamura *et al*. analyzed deep sequencing data to predict the duplex structures in fly genome that might give rise to siRNAs, and verified the expression of these duplexes. In addition, Chung *et al.* analyzed the deep sequencing data of ~21nt siRNAs and focus on the possible transposon-derived sequences. Both group have concluded that these loci are able to generate endogenous siRNAs.

The third method, performed by the Zamore group, was based on the chemical feature of small RNAs(Ghildiyal et al. 2008). In fly, siRNAs are 2'-O-methylated at the 3' end and are resistant to periodate oxidation, while miRNAs are not. Ghildiyal *et al.* therefore used periodate oxidation and β-elimination to deplete the endogenous miRNAs and deep sequenced the siRNA-enriched small RNA pool. Their data indicated that these Ago2- and Dicer-dependent endo-siRNAs, with ~21nt in length, correspond to transposon and heterchromatic sequences in somatic cells, suggesting that endo-siRNA functions in suppression of selfish gene in somatic cells.

## 4.2 Genomic sequence and biogenesis of endo-siRNAs

Current reports indicated that the Drosophila endo-siRNAs are derived from several sources. First, deep sequencing results of Ago2-associated and 3'-terminal 2'-O-methylated endo-siRNAs matched to the genome of transposon elements in somatic cells(Czech et al. 2008; Ghildiyal et al. 2008; Kawamura et al. 2008). One interesting finding is that some genomic sequences that correspond to endo-siRNA were also identified as piRNAs in germ line cells. However, unlike piRNAs, which have an existing strand bias associated with Piwi proteins, sequences of endo-siRNAs revealed an almost equal numbers of sense and anti-sense siRNAs matched to the transposon region. This result suggests that endo-siRNAs contribute to repression of transposon elements in somatic

cells as piRNAs do in germ line, but the biogenesis of endo-siRNAs and piRNAs are through different mechanisms.

The second source of endo-siRNAs is from convergent transcripts, also known as the *cis*-natural antisense transcripts (*cis*-NAT)(Czech et al. 2008; Okamura et al. 2008a). The convergent transcripts, which are bidirectionally transcribed across the same genomic DNA, are complimentary to each other and form duplexes at 3'UTR region. Since *cis*-NATs give rise to long double strand RNA structures, they are apparently processed by Dicer-2 and associated with Ago2 as siRNAs.

The third genomic loci for endo-siRNAs is the structured or hairpin RNA (hpRNA)(Okamura et al. 2008b). In some loci, the transcription of long inverted repeats results in a hairpin RNA with long double stranded stem structure that serves as the substrate of Dicer2, followed by interaction with Ago2, processing as endo-siRNAs. These hairpin structures (~400 bp in length) are typically much longer than miRNA precursors.

Studies of endo-siRNA biogenesis give us an unexpected result. The exogenous siRNA pathway has been well-defined in Drosophila, where Dicer-2 complexes with R2D2 for the duplex processing into RISC which contains Ago2 as the slicer. In the case of endo-siRNAs, the accumulation and function of endo-siRNAs are Dicer-2 and Ago2-dependent. Strikingly, it is Loquacious, the partner of Dicer-1 in miRNA pathway, instead of R2D2, that participates the biogenesis of endo-siRNAs(Chung et al. 2008; Czech et al. 2008; Okamura et al. 2008b). In

addition, immunoprecipitaion of Loquacious also co-purified Dicer-2, suggesting that a portion of Dicer-2 may complex with Loquacious involved in the processing of endo-siRNAs(Czech et al. 2008). This result indicates that the interactions of Drosophila Dicer proteins with their partners are not as simple as what had been observed before. The mechanism of how Dicer-2 determines its different binding partners for endo- or exo-siRNAs remains unknown.

## 4.3 Function of Endo-siRNA

The function of endo-siRNAs has been identified mostly as the transposable element-derived siRNAs. Mutation or knockout of endo-siRNA cofactors such as Dicer-2 and Ago2 provides insight into the function of endo-siRNAs. In recent studies, depletion or mutation of Dicer-2 and Ago2 results in an increase amount of certain transposon elements, suggesting that endo-siRNAs contribute to the suppression of transposon in somatic cells, similar to that of piRNAs in the germ line(Chung et al. 2008; Czech et al. 2008; Ghildiyal et al. 2008; Kawamura et al. 2008).

However, the functions of *cis*-NAT or hpRNA-derived endo-siRNAs are still not clear. It is possible that these subclasses of endo-siRNAs autoregulate the expression of their source transcripts, or it may guard the cell physiology in a "passive" way, to prevent any unexpected cellular response to long double stranded RNA, such as the inducing of PKR pathway.

**4.4 Endo-siRNAs in mouse oocytes**

In addition to the discovery of endo-siRNAs in Drosophila, two recent papers reported the existence of endo-siRNAs in mouse oocytes(Tam et al. 2008; Watanabe et al. 2008). To identify the analogous of male piRNA system in female germ line cells, Tam *et al.* and Watanabe *et al.* profiled the total small RNAs in mouse oocytes and found a population of endo-siRNAs that match transposons. Their results provided evidence that endo-siRNAs repress transposons in the female germ line as piRNAs do in the male germ line. In addition, these two labs also identified a population of mouse oocytes specific endo-siRNAs that are derived from pseudogenes. Some protein-encoded spliced mRNAs hybridize to the anti-sense transcript of homologous pseudogenes, and form double-stranded RNAs that can be processed by endogenous Dicer and Ago2. Their data suggested that these pseudogene-encoded siRNAs may regulate their corresponding protein-coding mRNA target, and has provided strong evidence for pseudogene function in gene regulation by RNAi pathway.

**5. Concluding remarks**

Although the RNAi phenomenon was discovered less than ten years ago, studies of the RNAi field have provided more and more clues to uncover the mystery of RNAi and have revealed the salient roles of small RNAs in regulation of gene expression. Structural and functional analysis of RISC components including the proteins which comprise it and various groups of small RNA

highlights the complexity of this cellular regulatory network. However, many questions regarding the details of silencing mechanism as well as the therapeutic application of RNAi are still unclear. How does miRNA mediate gene silencing within the three current translation repression models? Do other unknown factors facilitate the RISC function? Can some small RNAs function as activators of gene expression rather than repressors? How can we optimize the potency and specificity of in vivo RNAi for the application of RNAi-based therapies? Future genetic and biochemical work on these topics will help people to understand the diverse mechanisms of gene regulation by small RNAs. With the rapid and fascinating progress in the study of small RNAs biology, researchers are expecting that RNAi will be applied as a powerful tool and a new therapeutic strategy in the future.

# CHAPTER II

## POTENT RNAI BY SHORT RNA TRIGGERS

**ABSTRACT**

RNA interference (RNAi) is a gene-silencing mechanism by which a ribonucleoprotein complex, the RNA-induced silencing complex (RISC) and a double-stranded (ds) short-interfering RNA (siRNA), targets a complementary mRNA for site-specific cleavage and subsequent degradation. While longer dsRNA are endogenously processed into 21- to 24-nucleotide (nt) siRNAs or miRNAs to induce gene silencing, RNAi studies in human cells typically use synthetic 19- to 20-nt siRNA duplexes with 2-nt overhangs at the 3'-end of both strands. Here, we report that systematic synthesis and analysis of siRNAs with deletions at the passenger and/or guide strand revealed a short RNAi trigger, 16-nt siRNA, which induces potent RNAi in human cells. Our results indicate that the minimal requirement for dsRNA to trigger RNAi is an ~42Å A-form helix with ~1.5 helical turns. The 16-nt siRNA more effectively knocked down mRNA and protein levels than 19-nt siRNA when targeting the endogenous CDK9 gene, suggesting that 16-nt siRNA is a more potent RNAi trigger. *In vitro* kinetic analysis of RNA-induced silencing complex (RISC) programmed in HeLa cells indicates that 16-nt siRNA has a higher RISC-loading capacity than 19-nt siRNA. These results suggest that RISC assembly and activation during RNAi does not necessarily require a 19-nt duplex siRNA and that 16-nt duplexes can be designed as more potent triggers to induce RNAi.

**INTRODUCTION**

RNAi interference (RNAi) is an evolutionarily conserved process whereby double-stranded RNA (dsRNA) induces the sequence-specific degradation of homologous mRNA (for review, see (Rana 2007). Although RNAi was first discovered in *Caenorhabditis elegans* (Fire et al. 1998), similar phenomena had been reported in plants (post-transcriptional gene silencing [PTGS]), fruit flies, and human cells (reviewed in (Meister and Tuschl 2004). The current mechanistic model of the RNAi pathway involves initiator and effector protein complexes. During initiation of RNAi, dsRNA trigger sequences are processed by the RNase II enzyme Dicer into small 21- to 24-nucleotide (nt) short-interfering RNAs (siRNAs) (Zamore et al. 2000; Bernstein et al. 2001; Elbashir et al. 2001b). These siRNA duplexes containing 5'-phosphate and 3'-hydroxyl termini are loaded into an effector protein complex called RNA-induced silencing complex (RISC). siRNA is then unwound to activate RISC, allowing Ago2 to catalytically cleave the target mRNA at a specific site (Liu et al. 2004; Meister et al. 2004b; Song et al. 2004).

To induce target cleavage, siRNA must be perfectly complementary to its mRNA target (reviewed in (Rana 2007). siRNAs with sequences mismatched to nucleotides at the cleavage site do not induce target cleavage. Another class of short (21- to 24-nt) dsRNAs called microRNAs (miRNA) also associate with RISC but are not perfectly complementary to target sequences; when loaded into RISC, these miRNAs inhibit translation rather than inducing target cleavage

(reviewed in (Chu and Rana 2007)). Small (19- to 20-nt) synthetic ds siRNAs with dTdT overhangs have been shown to induce RNAi in numerous mammalian cell lines (Elbashir et al. 2001a). Variations in the structure and sequence of siRNA have also been shown to be well tolerated and to not adversely affect RNAi (Rana 2007). However, changes in the A-form helical structure of siRNA duplexes or siRNA-mRNA complexes are not well tolerated (Chiu and Rana 2002b, 2003), indicating that the A-form helix is important for mediating RNAi.

Kinetic analysis of the RNAi enzyme complex revealed that its cleavage activity tolerates 3-nt mismatches between the 5'-terminus of the guide strand and target mRNA (Haley and Zamore 2004), indicating the A-form helix can be shorter than 19-nt at the target recognition and cleavage stages of RISC function. However, the minimal dsRNA structure needed at these stages to induce effective RNAi has not been well determined. To map this essential region of the dsRNA A-form helical structure, we synthesized a series of siRNA duplexes with 3'- or 5'-terminal deletions in the passenger and/or guide strand and examined their RNAi activity. Here we report that the minimal dsRNA A-form helical structure required to assemble a catalytically active effector RNAi complex is a 16-nt duplex siRNA with ~1.5 helical turns. Our data indicate that this 16-nt siRNA is sufficient to induce potent RNAi with enhanced RISC-loading efficiency.

**RESULTS**

**16-nt siRNA duplexes with passenger-strand deletions are sufficient to induce RNAi *in vivo***

To determine the minimal dsRNA A-form helical structure required to assemble catalytically active RISC, we designed siRNA duplexes to target green fluorescent protein (GFP) and to have a 19-nt guide strand plus dTdT and a passenger strand harboring deletions at the 5'- or 3'-ends (PD-1 to PD-14) (Fig II.1A, Supplementary FigII.S1). The RNAi activity of these siRNA duplexes was quantitatively analyzed by a dual fluorescence reporter system (Chiu and Rana 2002b, 2003). Wild-type 19-nt siRNA (50 nM) silenced 92% of GFP expression in HeLa cells 48 h post-transfection; this RNAi activity is denoted as 100% in Fig 1 for comparison with the activity of other siRNA sequences. Analysis of 19-nt siRNAs with 5'-passenger-strand (PS) deletions showed that a 16-nt siRNA with PS deletions (PD-1) induced RNAi with ~75% efficiency whereas two other siRNAs with PS deletions, PD-2 and PD-3, did not exhibit RNAi activity.

To map the 3'-end boundary required for siRNA function, we systemically deleted the 3'-end of the passenger strand. A 16-nt siRNA with 3' PS deletions (PD-4) showed efficient RNAi (~77%). Duplexes with < 16-nt passenger strands (PD-5 and PD-6) were inactive. Since 19-nt siRNA duplexes with dTdT overhangs have improved RNAi efficiency, we determined the effect of adding dTdT to the truncated 3'-end of the passenger strand by quantifying the level of GFP knocked down by duplexes PD-7, PD-8, and PD-9 (Fig 1A). PD-7 exhibited

**Figure II.1 (A) siRNAs with passenger-strand (PS) deletions as triggers for RNAi.** Each GFP siRNA construct shown and reporter plasmids were co-transfected into HeLa cells and RNAi activity was quantified 48 h post-transfection. Relative RNAi activity represents the percentage of GFP knockdown induced by 50 nM siRNA with passenger-strand deletions relative to the inhibition induced by 50 nM 19-nt wild-type siRNA (designated 100%). Each siRNA was tested for knockdown in duplicate in 2 independent experiments. **(B) Effects of guide-strand and two-strand deletions on RNAi activity.** The relative RNAi activity of each GFP siRNA construct shown was evaluated as described in (A).

**A**



**B**
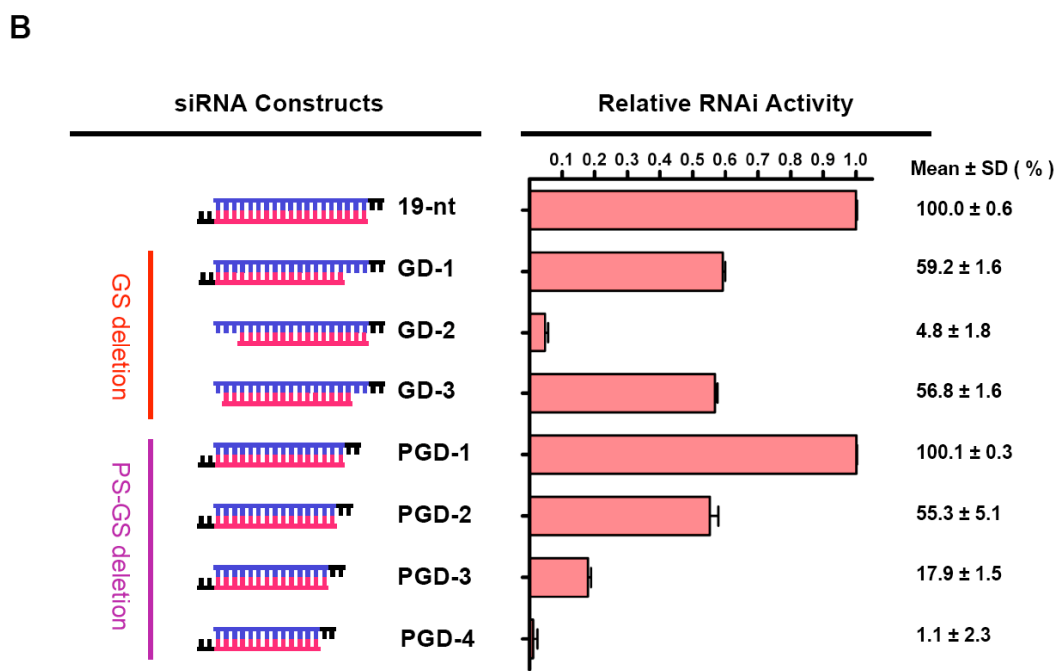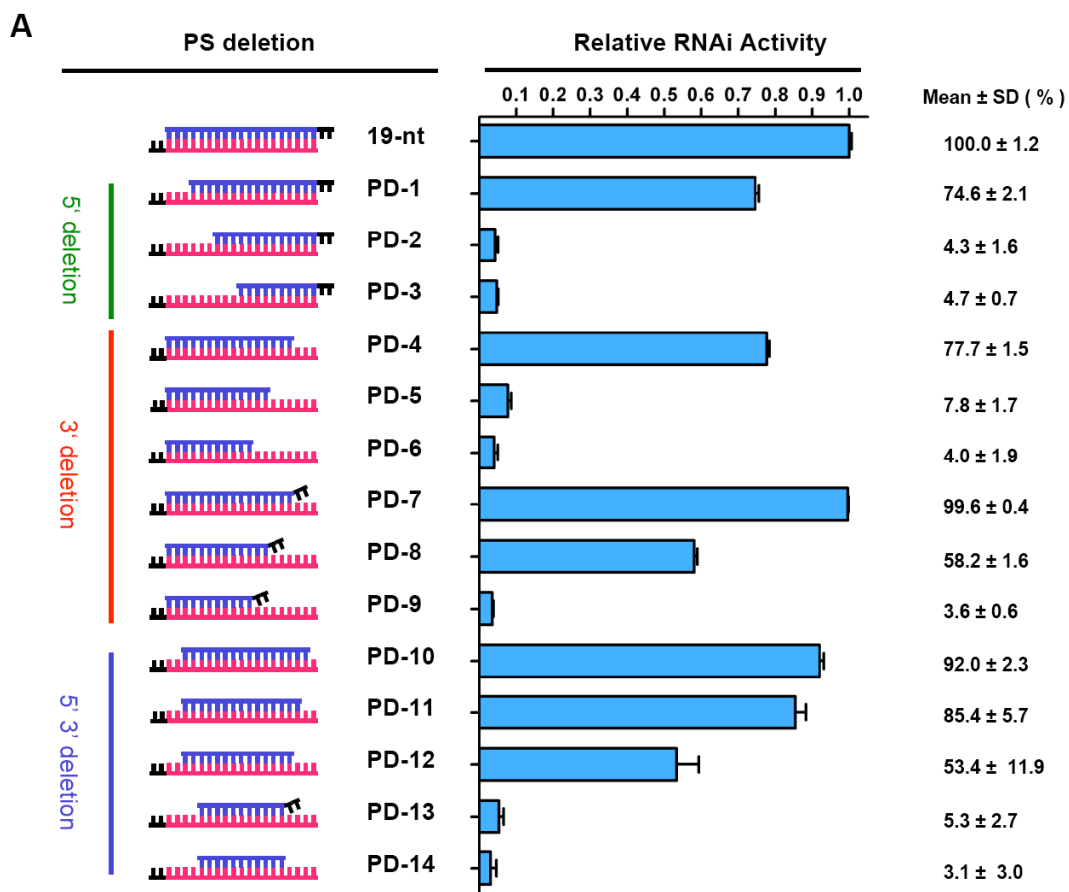
RNAi activity comparable to that of wild-type 19-nt siRNA, whereas adding dTdT to PD-6 (resulting in PD-9) did not increase the RNAi efficiency of this 11-nt duplex.

To address which region of the siRNA must form a duplex structure for efficient RNAi, we synthesized siRNA duplexes with deletions at both the 5'- and 3'-ends of the passenger strand and tested their RNAi activity. PD-10, a 16-nt duplex with a passenger strand at positions 3-18 was highly efficient at knocking down GFP (~92%), but an 11-nt duplex with a passenger strand at positions 5-15 (PD-14) was nonfunctional, and adding dTdT to the shorter duplex (PD-13) did not improve its RNAi function (Fig II.1A). To determine the minimal length of A-form helix at the central region of the siRNA duplex, we also synthesized siRNAs with a 15- or 14-nt passenger strand. PD-11 with a 15-nt passenger strand exhibited ~85% RNAi activity, whereas the RNAi activity for PD-12 with a 14-nt passenger strand dropped to ~53%. These findings demonstrate that efficient RNAi can be accomplished using a 19-nt guide strand and a 16-nt passenger strand. Taken together, these results suggest that a 16-nt duplex RNA structure is required for gene silencing *in vivo*.

**siRNAs with 16-nt guide strand are sufficient for RNAi activity**

To determine whether this 16-nt rule applied to the guide strand, reciprocal experiments were performed. In these experiments, we used dsRNA duplexes (GD-1 to GD-3) that harbored a 19-nt plus 3' dTdT passenger strand

and a guide strand truncated from the 5'- and/or 3'-ends (Fig 1B). Relative to the wild-type 19-nt siRNA, GD-1 exhibited less efficient RNAi (~59%). This loss of function may have been due to the 5-nt passenger-strand overhang created by deleting nucleotides 1-3 of the guide strand, since increasing 3'-overhang length is known to negatively affect RNAi (Elbashir, 2001). GD-3 also showed intermediate RNAi activity (~57%), again likely due to the loss of function contributed by the 4-nt passenger strand 3'-overhang. These results indicate that a 19-nt passenger strand and a 16-nt guide strand can induce RNAi. Surprisingly, GD-2 did not exhibit RNAi activity, suggesting that the 17th to 19th nucleotides from the 5'-end of the guide strand may be important for RISC assembly or target mRNA recognition.

**16-nt siRNA is the minimum RNA duplex for adequate RNAi in human cells**

Since our results showed that siRNAs with a 16-nt passenger or 16-nt guide strand exhibited RNAi activity, we next tested whether the 16-nt rule applied to duplexes with both strands truncated (Fig II.1B). Relative to wild-type 19-nt siRNA, 16-nt siRNA (PGD-1) induced RNAi at a high efficiency (~100%), 15-nt siRNA (PGD-2) induced knockdown at a moderate efficiency (~55%), whereas 14-nt (PGD-3) and 13-nt (PGD-4) siRNAs induced knockdown at low efficiencies (~18% and ~1%, respectively). Collectively, these results demonstrate that the threshold number of nucleotides required to induce highly efficient gene knockdown is 16.

**16-nt siRNA is sufficient to knock down endogenous genes**

The 16-nt GFP siRNA (PGD-1) exhibited wild-type (WT) levels of GFP knockdown (Fig II.1B), indicating that a 16-nt siRNA is as efficient as a 19-nt siRNA at triggering RNAi *in vivo*. To show that 16-nt siRNA can be generally used as an RNAi trigger targeting cellular protein, we synthesized the 16-nt siRNA targeting CDK9 based on its published 19-nt siRNA sequence (Brown et al. 2005) (Fig II.2A). This 16-nt CDK9 siRNA (PGD) was evaluated for RNAi efficacy by transfecting it into HeLa cells in parallel with 19-nt WT siRNA and measuring CDK9 mRNA and protein levels at 48h post transfection. PGD was shown by quantitative PCR to knock down CDK9 mRNA with higher efficiency (~90%) than 19-nt siRNA (~75%) (Fig II.2B). Consistent with this result, endogenous CDK9 protein was shown by immunoblot analysis to be reduced in HeLa cells transfected with 16-nt or 19-nt siRNA (Fig II.2C).

To determine if 16-nt siRNA enters the RNAi pathway by the same mechanism as 19-nt siRNA, we compared the extent to which RISC programmed with each siRNA cleaved its target mRNA *in vitro*. RISC was programmed by transfecting HeLa cells with 19-nt or 16-nt CDK9 siRNA, preparing cell extracts, and measuring the ability of activated siRNA-programmed RISCs (siRISCs) to cleave added 150-nt $^{32}$P-cap-labeled CDK9 mRNA target. The 19-nt and 16-nt siRISC enzyme complexes cleaved target mRNA ~32%, and ~91%, respectively (Fig. II.2D). Thus, the PDG siRISC exhibited a much higher cleavage activity with

**Figure II.2 16-nt siRNA targeting CDK9 mediates RNAi endogenous gene silencing in HeLa cells. (A)** The wild-type and 16-nt CDK9 siRNAs (19-nt WT and PGD) used to program RISC are shown. Arrowheads mark target cleavage sites defined by the 5'-end of the guide strand. siRNA sequences are shown in Supplementary Fig 1. **(B) 16-nt CDK9 siRNA more efficiently knocks down CDK9 mRNA than 19-nt WT siRNA.** HeLa cells were transfected with CDK9 mRNA 50nM CDK9 siRNA (19-nt or PGD), harvested 48 h post-transfection, and 1 $\mu$g total RNA was reverse-transcribed. CDK9 mRNA levels quantified by quantitative PCR and normalized to GAPDH mRNA are presented relative to mRNA levels in mock-transfected cells. Data represent 3 independent experiments. **(C) 16-nt CDK9 siRNA more efficiently decreases CDK9 protein expression than 19-nt WT siRNA.** Immunoblot analysis of CDK9 knockdown by 19-nt and PGD siRNAs. HeLa cells were transfected and harvested as in (B), and 120 $\mu$g total protein was analyzed by immunoblot using anti-CDK9 and anti-CycT1 antibodies. **(D) 16-nt CDK9 siRNA more efficiently programs RISC to cleave target CDK9 mRNA than 19-nt WT siRNA.** CDK9 siRISC was programmed by transfecting HeLa cells with 19-nt or 16-nt (PGD) siRNA. See Materials and Methods for details. The arrow designated "[32]P-cap-labeled target" points to full-length ^{32}P-cap-labeled CDK9 target mRNA. The arrows designated "cleavage product (19-nt)" and "cleavage product (PGD)" point to products of target mRNA cleavage by CDK9 siRISC programmed with 19-nt and 16-nt siRNA, respectively.

**A**



19-nt

16-nt

**B**



**C**



**D**
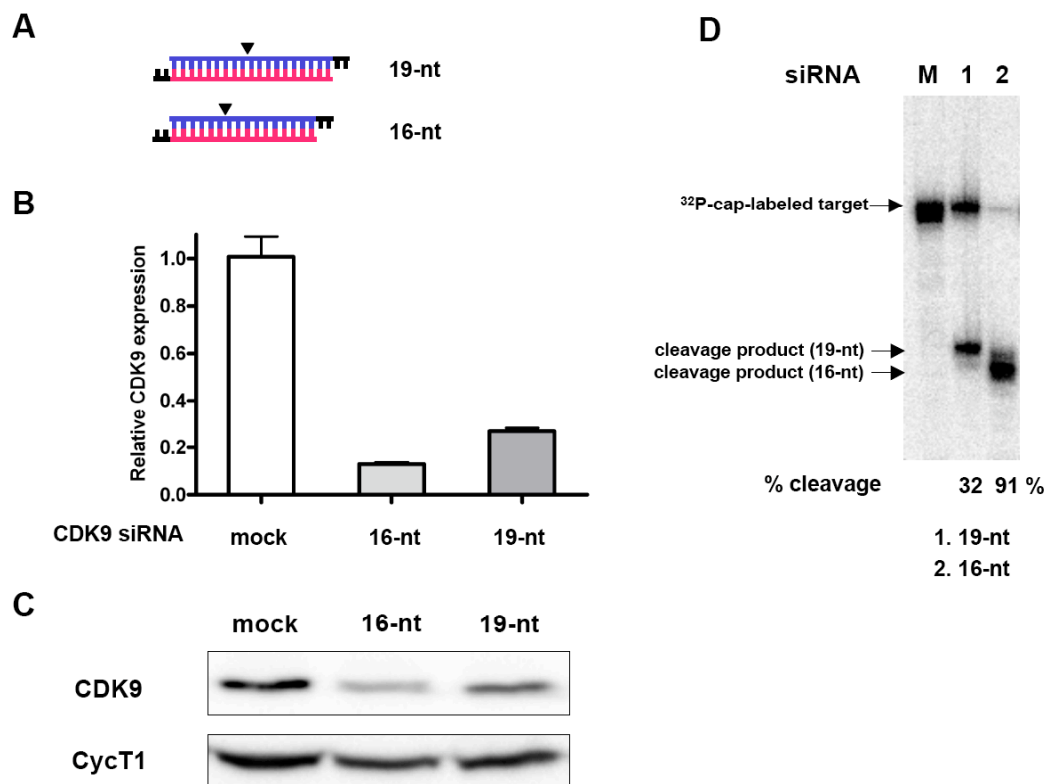
equal amounts of cell extracts, suggesting that 16-nt siRNA is a more potent RNAi trigger. The cleavage product of CDK9 PGD siRISC revealed that the cleavage site had shifted 3 nt (Fig II.2D; compare lanes 1 and 2 and arrows), consistent with previous studies (Elbashir et al. 2001c) and reflecting the new position of the 5'-end of the guide strand after truncating 3 nt.

**Kinetic analysis of programmed 16-nt siRISC**

Our results show that 16-nt siRNAs targeting GFP or CDK9 are sufficient to trigger RNAi. In addition, we tested a number of other target mRNA sequences spanning various regions of CDK9 and luciferase reporter comstructs, and compared the potency of 1-nt and 16-nt siRNAs which showed that 16-nt siRNA was a potent RNAi trigger (data not shown). The different *in vitro* cleavage efficiencies of the CDK9 16-nt RISC and 19-nt RISC (Fig II.2D) prompted us to further explore the enzymatic activity of 16-nt RISC. The substrate concentration dependence of CDK9 16-nt tiRISC cleavage activity was examined by varying the amount of target mRNA (2 nM, 10 nM, 20 nM, and 50nM) in a fixed-volume (20 $\mu$l) reaction with a constant amount of cell extract programmed with 16-nt RISC. The efficiency of RISC target cleavage increased with target mRNA concentration, saturating at higher concentrations (Figs II.3A, II.3B). The $K_m$ and $V_{max}$ of CDK9 16-nt RISC target cleavage were determined by nonlinear fitting of substrate concentration versus initial velocity to the Michaelis-Menton equation (Fig II.3B). The concentration of 16-nt RISC was determined by blocking the

cleavage activity of RISC with varying concentrations of 2'-*O*-methyl oligonucleotides complementary to the guide strand 16-nt siRNA and measuring the $IC_{50}$ (Hutvagner et al. 2004) (Fig II.3C, Fig II.S2).

Our results indicate that the 16-nt RISC is a multiple-turnover enzyme that recognizes and cleaves its target with classic Michaelis-Menton kinetics. The $K_m$ for 16-nt RISC is 17.94 nM and its $V_{max}$ is $9.72 \times 10^{-3}$ (Fig II.3D). Remarkably, the concentration of 16-nt RISC programmed in HeLa cells was 18.26 nM, indicating that 16-nt RNA programmed ~7x more RISC than 19-nt siRNA (2.5 nM) (Fig II.3C; (Brown et al. 2005)). Interestingly, rate constant ($K_{cat}$) determination showed that RISC programmed with 16-nt RNA was not catalyticaaly more efficient than 19-nt RISC (Fig II.3D). Overall, these results indicate that the reason why CDK9 16-nt RISC cleaves its target with greater efficiency is its greater capacity to program a higher concentration of RISC. These findings suggest that increases in RNAi potency correspond to an increased amount of RISC formed by a given siRNA, such as the 16-nt RNA.

**Figure II.3  Kinetic analysis of CDK9 16-nt RISC. (A) CDK9 RISC cleavage of target mRNA depends on substrate concentration.** Efficiency of target mRNA cleavage by CDK9 tiRISC programmed by 16-nt tiRNA at various substrate concentrations. **(B) CDK9 tiRISC cleavage of target mRNA shows Michaelis-Menten kinetics.** Michaelis-Menten analysis of 16-nt tiRISC. The initial velocity of cleavage product formation was determined from the slope of a curve fit to the cleavage reactions at 0-30 min as shown in (A). **(C) 16-nt RNA programs more RISC than 19-nt siRNA or 29-nt shRNA.** Concentrations of active CDK9 RISC programmed by 16-nt siRNA, 19-nt siRNA, or 29-nt shRNA were determined by 2'-$O$-Me inhibition *in vitro* cleavage assay. **(D) Kinetic analysis of 16-nt CDK9 RISC.** $K_m$ and $V_{max}$ were determined by Michaelis-Menten analysis as shown in (B).

**A**

| | 2nM | 10nM | 20nM | 50 nM |
|---|---|---|---|---|
| [Target] | | | | |
| Time (min) | 0 5 10 15 30 90 | 0 5 10 15 30 90 | 0 5 10 15 30 90 | 0 5 10 15 30 90 |

Target mRNA

CDK9 cleavage product

**B**

**C**

- 16-nt (siRNA)
- 19-nt (siRNA)
- 29-bp (shRNA)

**D**

| RISC | $K_m$ (nM) | $V_{max}$ (nM/sec) | [RISC*] (nM) | $K_{cat}$ (1/sec) |
|---|---|---|---|---|
| RISC (16-nt) | 17.64 | $9.72 \times 10^{-3}$ | 18 | $5.4 \times 10^{-4}$ |
| RISC (19-nt)* | 15.42 | $3.47 \times 10^{-3}$ | 2.5 | $1.4 \times 10^{-3}$ |

* (Brown, 2005)
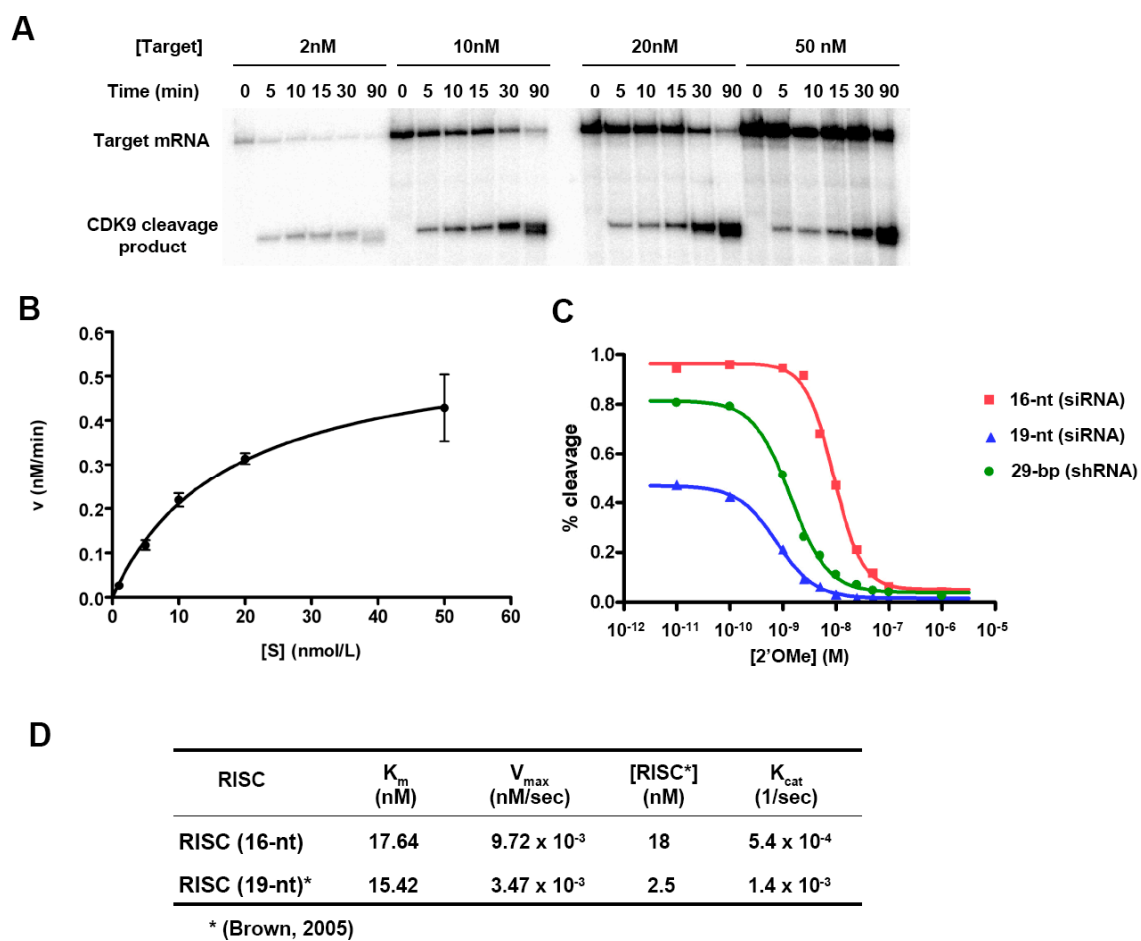
**DISCUSSION**

**A molecular ruler for RNAi**

Our results show that a 16-nt siRNA is sufficient to enter the RNAi pathway and target mRNA for site-specific cleavage, indicating that the 19-nt duplex structure is not a prerequisite for siRNA to induce RNAi. Our 16-nt recognition model is consistent with previous reports that a 16-nt mRNA target was sufficient for RNAi (Haley and Zamore 2004; Martinez and Tuschl 2004). Since a 16-nt duplex has ~1.5 helical turns and one helical turn of an A-form helix is 28 Å, our results suggest that the dsRNA structure recognized by RISC is an A-form helix of ~42 Å. Endogenous RNAi pathways involve Dicer processing of longer dsRNAs to 21- to 24-nt siRNAs or miRNAs as the native triggers for gene silencing (Zamore et al. 2000; Bernstein et al. 2001; Elbashir et al. 2001b; Hamilton et al. 2002). Our data suggest, however, that assembly of active RISC and mRNA cleavage require only 16-nt duplex siRNA, which is shorter than native triggers of RNAi.

Our results of systematically deleting nucleotides from the passenger and guide siRNA strands have several implications. First, truncating the passenger and/or guide strands to 16-nt still allows siRNA to enter the RNAi pathway, indicating that the 16-nt duplex can be recognized by, loaded into, and unwound by RISC. Second, the 16-nt duplexes induced potent RNAi, whereas siRNAs shorter than 16-nt were generally inefficient at inducing RNAi. Nonetheless, 15-nt siRNA did retain ~85% RNAi activity, suggesting that 15-nt siRNA can associate

with RISC but recognition, loading, and/or unwinding of the duplex may be defective.

A threshold size for siRNA is consistent with the crystal structure of Ago2 and the proposed Ago2-siRNA complex. The Ago2 crystal structure shows a claw shape and a "stalk" between its N-terminus and PAZ domain, which accommodates the A-form helical structures of the siRNA duplex and the siRNA-target mRNA complex (Song et al. 2004). Since recognition of siRNA depends on its A-form helical structure (Chiu and Rana 2002b, 2003), our results specify the minimal number of A-form helical turns (~1.5 turns) required for siRNA-RISC complex formation. siRNAs less than 16 nucleotides have a shorter helical structure that may not be recognized by Ago2 or may not stably associate with Ago2 during loading and/or unwinding. Correlating our results with those of future structural studies using 16-nt siRNA and Ago2 may provide further insight into the structural elements required for efficient RNAi.

## A potent trigger of RNAi

To examine if 16-nt siRNA is a real RNAi trigger for depleting endogenous proteins, we synthesized the 16-nt siRNA targeting CDK9 mRNA at the same region as 19-nt siRNA. To our surprise, the CDK9 16-nt siRNA was more effective than 19-nt siRNA in depleting target mRNA and protein (Fig II.2B, II.2C) and in programming RISC to cleave target mRNA *in vitro* (Fig II.2D). The RNAi functionality of siRNA can be predicted by the thermodynamic properties of its

strand-end base pairing (Khvorova et al. 2003; Schwarz et al. 2003b), and RISC can detect asymmetric siRNA by the thermodynamic properties of base pairing at each strand end (Tomari et al. 2004). Thus, we calculated the stability ($\Delta G$) for each end of 19-nt siRNA and 16-nt siRNA using established methods (Tomari et al. 2004). The stabilities of the 3'-guide ends were identical for the 19-nt siRNA and 16-nt tiRNAs ($\Delta G$= -7.38 kcal/mole), whereas the 5'-end of the 16-nt tiRNA guide strand was more stable ($\Delta G$= -10.53 kcal/mole) than the 5'-end of the 19-nt siRNA guide strand ($\Delta G$= -5.29 kcal/mol). These results indicate that the different RNAi efficiencies of 16-nt siRNA and 19-nt siRNA were not due to thermodynamic differences between the 5'- and 3'-ends of the guide strands that contribute to duplex unwinding at the RISC-loading stage.

Further kinetic analysis of the 16-nt siRISC complex targeting CDK9 mRNA clearly revealed why 16-nt siRNA more efficiently triggers RNAi than 19-nt siRNA *in vitro* and *in vivo*. The concentration of CDK9 16-nt siRISC was ~ 7x higher than that of 19-nt siRISC, suggesting that CDK9 16-nt tiRNA has a greater capacity than 19-nt siRNA to load into and activate RISC. We also examined the RISC concentration of CDK9 29-bp shRNA, a Dicer-processed RNAi trigger reported to be more potent than siRNA (Kim et al. 2005; Siolas et al. 2005). Surprisingly, the concentration of 16-nt tiRISC was also higher than that of 29-bp shRISC (Fig II.2C), indicating that a 16-nt RNA duplex is loaded into RISC with higher efficiency even if it bypasses the Dicer-processing mechanism.

A comparative analysis of catalytic parameters for siRISC and siRISC provided interesting features that may explain the highly potent RNAi capability of siRNA (Fig 3D). Although both 16-nt and 19-nt siRISC have similar $K_m$ values, the $V_{max}$ of 16-nt RISC is significantly higher than that of 19-nt RISC. With the higher RISC concentration for 16-nt siRNAs, which resulted in lower $K_{cat}$, comparative results showed that 16-nt RISC was not catalytically more efficiently than 19-nt RISC. We therefore concluded that the reason why CDK9 16-nt siRISC cleaves its target with greater efficiency at steady state is its greater RISC-loading capacity.

It is not clear why the loading capacity of CDK9 16-nt siRNA is so much greater than that of the CDK9 19-nt siRNA. Since 19-nt siRNA sequences are well known to vary in their RNAi efficiencies due to structure (Chiu and Rana 2002b) and thermodynamic properties (Khvorova et al. 2003; Schwarz et al. 2003a), we postulate that the sequence and structure of CDK9 16-nt siRNA favor its loading and catalytic properties. Delineating these differences in future studies and testing other 16-nt siRNAs for their capacity to load and activate RISC should enhance understanding of the siRNA properties required for potent RNAi.

Using 16-nt siRNA for RNAi-mediated knockdown studies may have several advantages. For GFP and CDK9 targets, we found that 16-nt siRNA had an equal or greater capacity for RISC loading than 19-nt siRNA. Co-transfecting synthetic 19-nt siRNA and 16-nt siRNA into cells reduced the knockdown effects typically seen with either siRNA alone (data not shown), suggesting that a limited

pool of RISC is freely available for loading. Thus, increased RISC loading and catalysis may allow synthetic 16-nt siRNA to have a competitive advantage over endogenous pools of 21- to 24-nt siRNA and miRNA generated by Dicer. The 16-nt siRNA may also have more specificity for a single target mRNA and may induce less off-target effects than 19-nt dTdT siRNA. Off-target RNAi knockdown effects can be induced even when mRNA sequences share only partial complementarity with sense or antisense siRNA strands (Jackson et al. 2003). Nonspecific target recognition may be reduced by using shorter siRNAs because they inherently have less potential to base pair with other mRNAs. Since the 16-nt tiRISC exhibits higher catalytic activity, lower concentrations can be used for transfection, also reducing off-target effects. Another advantage of using 16-nt tiRNA is that shorter RNA duplexes are more cost effective to synthesize.

In conclusion, our findings demonstrate that 16-nt siRNA duplexes are potent RNAi triggers and can now be considered for use in reverse genetic studies. Further studies on the detailed mechanisms by which 16-nt siRNA is incorporated into RISC and triggers RNAi will provide insight into the principles of RNAi pathways in human cells, particularly those involved in RISC loading and duplex unwinding. Since the current algorithms for designing siRNAs have been specifically developed for 19-nt duplexes, new algorithms should include 16-nt duplexes to create siRNAs with even higher RNAi efficiencies. Given the advantages of using 16-nt siRNA to trigger RNAi, we expect that these shorter RNA duplexes will be widely employed in biomedical studies.

## MATERIALS AND METHODS

### siRNA preparation

The sequences of GFP target-specific siRNA duplexes were designed as previously described (Chiu and Rana 2002b). 2'-bis(acetoxyethoxy)-methyl ether-protected single-stranded RNA of varying lengths were chemically synthesized by Dharmacon (Lafayette, CO). Synthetic oligonucleotides were deprotected, annealed, and purified as described by the manufacturer. Successful duplex formation was confirmed by 20% non-denaturing PAGE.

### Culture and transfection of cells

HeLa cells were maintained at 37°C in Dulbecco's modified Eagle's medium (DMEM, Invitrogen) supplemented with 10% fetal bovine serum (FBS), 100 units/mL penicillin, and 100 µg/mL streptomycin (Invitrogen). Cells were regularly passaged at subconfluence and plated 16 h before transfection at 70% confluence. Lipofectamine (Invitrogen)-mediated transient co-transfection of reporter plasmids and siRNAs were performed in duplicate 6-well plates. A transfection mixture containing 0.16 µg of pEGFP-C1 and 0.33 µg of pDsRed2-N1 reporter plasmids (Clontech), 50nM of each siRNA deletions, and 7 µl of lipofectamine in 1 ml of serum-reduced OPTI-MEM (Invitrogen) were added to each well. Cells were incubated in the transfection mixture for 4 h and further cultured in antibiotic-free DMEM. Cells were treated under the same conditions without siRNA for mock experiments.

**Dual fluorescence assay**

The function of GFP siRNAs was evaluated by a dual fluorescence assay as described (Chiu and Rana 2003). RNAi activity was quantified in total cell lysates (150 µg in 200 µl reporter lysis buffer) 48 h after transfecting cells with siRNA. GFP fluorescence was detected using a Safire plate reader (TECAN) by exciting at 488 nm and recording emissions from 504 to 514 nm. The spectrum peak at 509 nm represents the fluorescence intensity of GFP. RFP fluorescence was detected in the same cell lysates by exciting at 558 nm and recording emissions from 578 to 588 nm. The spectrum peak at 583 nm represents the fluorescence intensity of RFP. The fluorescence intensity ratio of target (GFP) to control (RFP) fluorophores was determined in the presence of siRNA duplexes and normalized to the emissions measured in mock-treated cells. Normalized ratios <1.0 indicated specific RNA interference. Relative RNAi activity represents the percentage of GFP knockdown induced by 50 nM siRNA with passenger-strand deletions relative to the inhibition induced by 50 nM 19-nt wild-type siRNA (designated 100%).

**Cytoplasmic cell extract preparation and *in vitro* mRNA cleavage assay**

To prepare cell extracts, HeLa cells were transfected with 25 nM siRNA, harvested 18 h later with trypsin, and centrifuged at 1000 x g for 5 min at 4$^{o}$C. The pellets were washed 3x with ice-cold PBS pH 7.2 and lysed by adding 3

packed-cell volumes of lysis buffer (20 mM HEPES pH 7.9, 10 mM NaCl, 1mM

MgCl$_2$, 0.5 M sucrose, 0.2 mM EDTA, 0.5 mM DTT, 0.5 mM PMSF, and 0.35%

Triton X-100). Lysis was continued for 10 min on ice. Once lysed, nuclei were

removed by centrifugation at 2500 rpm for 10 min at 4$^o$C. Cytoplasmic extracts in

supernatants were prepared by adding 0.11 volumes of cold Buffer B (20 mM

HEPES pH 7.9, 10 mM NaCl, 1 mM MgCl$_2$, 0.35 M sucrose, 0.2 mM EDTA, 0.5

mM DTT, and 0.5 mM PMSF). Extracts were quick frozen in liquid nitrogen and

stored at –80$^o$C.

To evaluate target mRNA cleavage *in vitro*, the GFP mRNA target

sequence was amplified by PCR with forward and reverse primers 5'-

GCCTAATACGACTCACTATAGACCTACGGCGTGCAGTGC-3' and 5'-

TTTTTTTTTTTTTTTTTTTTTTTTGATGGTGCGCTCCTGGACGT-3',

respectively, for transcription of a 126-nt GFP target mRNA containing a 24-nt

adenosine tail. The resulting transcript was $^{32}$P-cap-labeled, as described (Chiu

and Rana 2003). GFP target mRNA (10 nM) was incubated for 75 min at 37$^o$C in

the presence of 4 μL cytoplasmic extract ,1 mM ATP, 0.2 mM GTP, 1 U/μL

RNasin (Promega), 30 μg/ml creatine kinase, 25 mM creatine phosphate, 2 mM

MgCl$_2$, 20 mM NaCl. Buffer D (1 M KCl, 20 mM HEPES pH 7.9, 10% glycerol, 0.2

mM EDTA) was added to a final reaction volume of 20 μl.  Cleavage reactions

were stopped by adding 9 volumes of proteinase K buffer (200 mM Tris-HCl pH

7.5, 25 mM EDTA, 300 mM NaCl, and 2% [w/v] SDS). Proteinase K (Ambion)

was added to a final concentration of 0.6 mg/ml.  Reactions were incubated for

15 min at 37$^{\circ}$C.  Cleavage products were isolated by phenol/chloroform/isoamyl alcohol (25:24:1) extraction and ethanol precipitation, and resolved on a 6.5% polyacrylamide-7 M urea gel.

**SUPPLEMENTARY FIGURES**

**Figure II.S1**

**Schematics and sequences of siRNAs used in this study to target GFP and CDK9.**

## EGFP siRNAs

| CDK9 siRNA |

### passenger-strand deletions

### guide-strand deletions

**19-nt** 5'GCAGCACGACUUCUUCAAGdTdT
dTdTCGUCGUGCUGAAGAAGUUC'5

**PD-1** 5'GCACGACUUCUUCAAGdTdT
dTdTCGUCGUGCUGAAGAAGUUC'5

**PD-2** 5'CGACUUCUUCAAGdTdT
dTdTCGUCGUGCUGAAGAAGUUC'5

**PD-3** 5'CUUCUUCAAGdTdT
dTdTCGUCGUGCUGAAGAAGUUC'5

**PD-4** 5'GCAGCACGACUUCUUC
dTdTCGUCGUGCUGAAGAAGUUC'5

**PD-5** 5'GCAGCACGACUUC
dTdTCGUCGUGCUGAAGAAGUUC'5

**PD-6** 5'GCAGCACGAC
dTdTCGUCGUGCUGAAGAAGUUC'5

**PD-7** 5'GCAGCACGACUUCUUCdTdT
dTdTCGUCGUGCUGAAGAAGUUC'5

**PD-8** 5'GCAGCACGACUUCdTdT
dTdTCGUCGUGCUGAAGAAGUUC'5

**PD-9** 5'GCAGCACGACdTdT
dTdTCGUCGUGCUGAAGAAGUUC'5

**PD-10** 5'AGCACGACUUCUUCAA
dTdTCGUCGUGCUGAAGAAGUUC'5

**PD-11** 5'AGCACGACUUCUUCA
dTdTCGUCGUGCUGAAGAAGUUC'5

**PD-12** 5'AGCACGACUUCUUC
dTdTCGUCGUGCUGAAGAAGUUC'5

**PD-13** 5'CACGACUUCUUUdTdT
dTdTCGUCGUGCUGAAGAAGUUC'5

**PD-14** 5'CACGACUUCUU
dTdTCGUCGUGCUGAAGAAGUUC'5

**GD-1** 5'GCAGCACGACUUCUUCAAGdTdT
dTdTCGUCGUGCUGAAGAAG'5

**GD-2** 5'GCAGCACGACUUCUUCAAGdTdT
CGUCGUGCUGAAGAAGUUC'5

**GD-3** 5'GCAGCACGACUUCUUCAAGdTdT
GUCGUGCUGAAGAAGU'5

### both-strand deletions

**PGD-1** 5'GCAGCACGACUUCUUCdTdT
dTdTCGUCGUGCUGAAGAAG'5

**PGD-2** 5'GCAGCACGACUUCUUdTdT
dTdTCGUCGUGCUGAAGAA'5

**PGD-3** 5'GCAGCACGACUUCUdTdT
dTdTCGUCGUGCUGAAGA'5

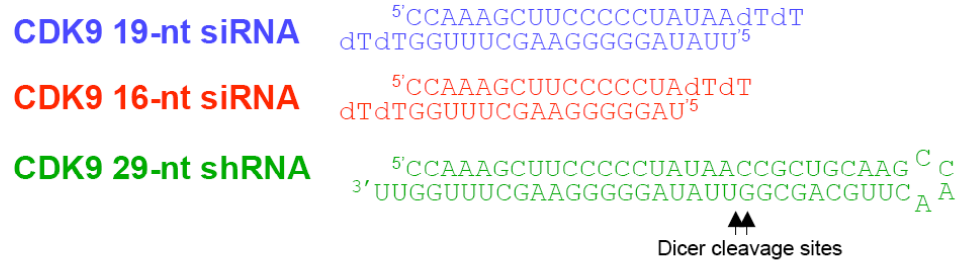**PGD-4** 5'GCAGCACGACUUCdTdT
dTdTCGUCGUGCUGAAG'5

## CDK9 siRNA

**19-nt** 5'CCAAAGCUUCCCCCUAUAAdTdT
dTdTGGUUUCGAAGGGGGAUAUU'5

**16-nt** 5'CCAAAGCUUCCCCCUAdTdT
dTdTGGUUUCGAAGGGGGAU'5

### 29-base paired shRNA

5'CCAAAGCUUCCCCCUAUAACCGCUGCAAG C C
3'UUGGUUUCGAAGGGGGAUAUUGGCGACGUUC A A

**Figure II. S2**

**Determination of 19-nt siRISC, 16-nt tiRISC, and 29-bp shRISC concentrations in HeLa cell extracts. (A) Schematics of CDK9 19-nt siRNA, 16-nt tiRNA, and 29-bp shRNA**. Arrows indicate the predicted Dicer cleavage site for shRNAs. **(B) 16-nt tiRNA programs more RISC than 19-nt siRNA or 29-bp shRNA.** HeLa cells were transfected with 19-nt siRNA, 16-nt tiRNA, or 29-bp shRNA to program RISCs targeting CDK9. Cell extracts were incubated with 150-nt $^{32}$P-cap-labeled CDK9 target mRNA and increasing concentrations of 2' $O$-methyl RNA oligonucleotides complementary to the CDK9 target site. The reactions were stopped after 120 min, and products were resolved by 6% denaturing PAGE. The concentrations of RISC were determined as shown in Fig 3C by $IC_{50}$ analysis using Prism4 software.

**A**

CDK9 19-nt siRNA

$^5$CCAAAGCUUCCCCCUAUAAdTdT
dTdGGUUUCGAAGGGGGAUAUU$^5$

CDK9 16-nt siRNA

$^5$CCAAAGCUUCCCCCUAdTdT
dTdGGUUUCGAAGGGGGAU$^5$

CDK9 29-nt shRNA

$^5$CCAAAGCUUCCCCCUAUAACCGCUGCAAG$^C$C
$^{3'}$UUGGUUUCGAAGGGGGAUAUUGGCGACGUUC$_A$A

Dicer cleavage sites

**B**
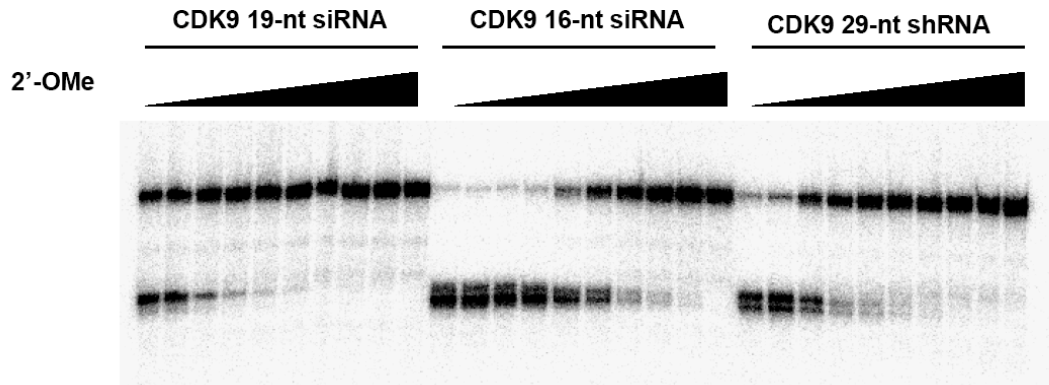
# CHAPTER III

# TRANSLATION REPRESSION IN HUMAN CELLS BY MICRO

# RNA-INDUCED GENE

# SILENCING REQUIRES RCK/P54

**ABSTRACT**

RNA-induced silencing complexes (RISC) in human cells can be programmed by small interfering RNAs (siRISC) or endogenously expressed micro RNAs (miRISC). siRISC silences expression by cleaving a perfectly complementary target mRNA, whereas miRISC inhibits translation by binding imperfectly matched sequences in the 3' untranslated region (3'-UTR) of target mRNA. Both RISCs contain Argonaute2 (Ago2), which catalyzes target mRNA cleavage by siRISC and localizes to cytoplasmic mRNA processing P-bodies. Here, we show that RCK/p54, a DEAD box helicase, interacts with argonaute proteins, Ago1 and Ago2, in affinity-purified active RISC from human cells programmed with siRNA or endogenous miRNA, directly interacts with Ago1 and Ago2 *in vivo*, facilitates formation of P-bodies, and is a general repressor of translation. Disrupting P-bodies by depleting Lsm1 did not affect RCK/p54 interactions with argonaute proteins and its function in miRNA-mediated translation repression. Depletion of RCK/p54 disrupted P-bodies and dispersed Ago2 throughout the cytoplasm, but did not significantly affect siRNA-mediated RNAi functions of RISC. Depleting RCK/p54 released general, miRNA-induced, and *let*-7-mediated translational repression of RAS protein. Therefore, we propose that translation repression is mediated by miRISC via RCK/p54 and its specificity is dictated by the miRNA sequence binding multiple copies of miRISC to complementary 3' UTR sites in the target mRNA. These studies also suggest

that translation suppression by miRISC does not require P-body structures and location of miRISC to P-bodies is the consequence of translation repression.

**INTRODUCTION**

Small non-coding RNAs play important roles in the posttranscriptional regulation of genes that code for diverse biological functions, e.g., in most metazoan organisms from nematodes to mammals (Ambros 2004; Bartel 2004; Wienholds and Plasterk 2005). Two classes of such small (~21 nucleotide [(nt)]) RNAs that have been extensively studied in gene silencing are short interfering RNAs (siRNAs) and microRNAs (miRNAs) (reviewed in (Filipowicz 2005)). Currently the best known mechanism of gene silencing is RNA interference (RNAi), an evolutionarily conserved process whereby double-stranded RNA (dsRNA) induces the sequence-specific degradation of homologous mRNA (Fire et al. 1998). The RNAi machinery can also be programmed in cells by introducing duplexes of siRNAs that are assembled into RNA-induced silencing complexes (siRISC) containing Dicer, argonautes and other proteins (Zamore and Haley 2005). Although RNAi has commonly been associated with siRNAs, this process is largely mediated in plants by miRNAs (Baulcombe 2004; Carrington 2005) and examples of miRNA-mediated RNAi have been found in mammals and viruses (reviewed in (Zamore and Haley 2005)). Growing evidence indicates that miRNAs are important in human disease, including cancers (Poy et al. 2004; Vella et al. 2004; He et al. 2005; Lu et al. 2005). For example, relatively low levels of *let*-7 miRNA up-regulate RAS protein in lung cancer cells, demonstrating a possible role of miRNA in tumorigenesis (Johnson et al. 2005).

Both classes of small RNAs are assembled into silencing complexes that contain Dicer, argonautes and other proteins (Filipowicz 2005), but they silence gene expression by two different pathways. Upon recognizing complementary mRNA, activated RISC (RISC*) forms an effector complex with the target mRNA (Zamore and Haley 2005). Antisense siRNA in RISC* serves as guide for Argonaute2 (Ago2) (Liu et al. 2004; Meister et al. 2004b; Song et al. 2004) to catalyze the cleavage of target mRNA at a site ~10 nucleotides from the 5' end of the siRNA (Elbashir et al. 2001c). Following cleavage, the target mRNA is degraded. RISC*, as a multi-turnover enzyme (Hutvagner and Zamore 2002), is recycled to cleave additional mRNA targets.

In the case of miRNAs, they are assembled into miRNA-induced silencing complexes (miRISC) that contain Dicer, argonaute proteins, transactivation-responsive RNA-binding protein (TRBP) (Chendrimada et al. 2005; Forstemann et al. 2005; Gregory et al. 2005; Haase et al. 2005), and other cellular factors (Filipowicz 2005). This assembly into miRISC has been implicated in inhibiting the translation of target mRNAs (Hammond et al. 2001; Caudy et al. 2002).

Whether siRNA-mediated RNAi or miRNA-mediated inhibition of translation is triggered depends largely on the degree of complementarity between the siRNA or miRNA and its mRNA target (reviewed in (Ambros 2004; He and Hannon 2004)). While both miRNAs and siRNAs must harbor sequences that recognize the target mRNA, miRNAs are generally not fully complementary to the mRNA target. In contrast, siRNA sequences must be completely complementary

to the mRNA target cleavage site to efficiently induce cleavage through the RNAi pathway. Interestingly, miRNAs can behave like siRNAs and induce mRNA cleavage when the miRNA sequence is completely complementary to a target mRNA (Hutvagner and Zamore 2002; Zeng et al. 2003; Yekta et al. 2004).

In human cells, the mechanism by which the endogenous miRNA and siRNA pathways are distinguished is not clearly understood. It is also unclear how miRNAs repress the translation of target mRNAs. New insights into miRNA function have recently been provided by localization of the RISC components, Ago1 and Ago2, in mRNA-processing bodies (P-bodies)(Liu et al. 2005b; Pillai et al. 2005; Sen and Blau 2005), which are cytoplasmic foci containing translationally repressed mRNP proteins. During cellular translational control, an mRNP complex is formed containing the translationally repressed mRNA and associated repressor proteins and lacking translation initiation factors (Coller and Parker 2004). These translationally repressed mRNPs accumulate in P-bodies and contain proteins that mediate the translation (Ferraiuolo et al. 2004; Andrei et al. 2005; Ferraiuolo et al. 2005), RNAi (Sen et al. 2004; Liu et al. 2005b), translation suppression (Minshall et al. 2001), and decay (Coller and Parker 2004; Cougot et al. 2004) of cellular mRNA. P-bodies, also referred to as GW or Dcp bodies, contain GW182 proteins that have recently been reported to play a role in RNAi (Jakymiw et al. 2005; Liu et al. 2005a; Rehwinkel et al. 2005). Other proteins found in cytoplasmic P-bodies and implicated in mRNA processing are RCK/p54, Lsm1, Dcp1:2 and eIF4E (Coller and Parker 2004; Cougot et al. 2004;

Andrei et al. 2005). Given that target mRNA and RISC components have been co-localized in P-bodies (Liu et al. 2005b; Pillai et al. 2005), it is possible that P-bodies are the *bona fide* site for RISC-induced target cleavage or repression of translation. However, the mechanism by which target mRNA and miRISC are directed to P-bodies and how translation is repressed by miRISC are still unknown.

One P-body protein, RCK/p54, the human homolog of yeast Dhh1p, is a member of the ATP-dependent DEAD box helicase family and was originally identified as a proto-oncogene (Akao et al. 1995). In human cells, RCK/p54 interacts in P-bodies with the translation initiation factor, eIF4E (Andrei et al. 2005). The *Xenopus* homolog of RCK/p54, Xp54, which interacts with eIF4E and forms RNA-dependent oligomers, represses the translation of mRNA in oocytes and eggs (Minshall and Standart 2004). In yeast, Dhh1p interacts with the decapping and deadenylase complex and functions in translational repression (Coller et al. 2001). Dhh1p has also recently been shown to stimulate translational repression by inhibiting production of the pre-initiation complex (Coller and Parker 2005).

Here, we show that RCK/p54 interacts with argonaute proteins, Ago1 and Ago2, in affinity-purified active RISC assemblies from human cells programmed with siRNA or endogenous miRNA, directly interacts with Ago1 and Ago2 *in vivo*, facilitates formation of cytoplasmic P-bodies, and acts as a general repressor of translation. Depletion of RCK/p54 disrupted P-bodies and dispersed Ago2

throughout the cytoplasm. We further show that depletion of RCK/p54 did not significantly affect the RNAi function of RISC, but released general, miRNA-induced, and *let*-7-mediated translational repression of RAS protein. Taken together, our results suggest that RCK/p54 is the effector molecule in miRISC that represses translation and that the specificity of this repression is dictated by the sequence of miRNA binding to complementary sites in the 3' UTR of the target mRNA.

**RESULTS**

**Human argonaute proteins interact with RCK/p54, a component of mRNA processing P-bodies**

To investigate the mechanism of micro-RNA-mediated repression of mRNA translation and to determine the interactions of P-body components with the RNAi machinery, we constructed expression vectors for the YFP-tagged P-body proteins, Lsm1, RCK/p54, Dcp2, and eIF4E. These vectors were co-expressed in HeLa cells with myc-tagged Ago2 and immunopurified using anti-myc antibodies. The protein composition of isolated complexes was analyzed by immunoblot using antibodies against GFP or myc. When total cell extracts (TCE) were analyzed to determine the protein expression efficiencies of the vectors used in these experiments (TCE panel in Fig III.1A), all YFP- and myc-tagged proteins were efficiently expressed. Analysis of immunopurified complexes revealed that Ago1, Dcp2, RCK/p54 and eIF4E formed complexes with Ago2 (anti-myc panel, Fig III.1A). Control experiments showed that YFP did not co-purify with Ago2 (Fig III.1A). Interestingly, Lsm1 did not co-purify with Ago2, but localized to P-body structures in HeLa cells (Fig III.1B).

Since P-bodies contain RNA and proteins, many protein components of P-bodies are likely to be assembled on a common RNA scaffold without forming functional protein-protein interactions. To address this possibility, HeLa cells were transfected with vectors to co-express myc-Ago2 and the YFP-tagged P-body proteins, Lsm1, RCK/p54, Dcp2, and eIF4E, subjected to RNase A

digestion, and immunopurified. Analysis of immunopurified complexes showed that Ago1 and RCK/p54 interactions with myc-Ago2 were not affected by RNase treatment, whereas the amounts of Dcp2 and eIF4E protein that co-purified with myc-Ago2 decreased significantly (anti-myc panel, Fig III.1A). Control experiments analyzing myc-Ago2 showed that equal amounts of complexes were purified (anti-myc lane, Fig III.1A). Taken together, these results suggest that Ago1 and RCK/p54 directly interacted with Ago2, whereas Dcp2 and eIF4E interactions with Ago2 were RNA-mediated. These results do not rule out the possibility that Ago1 and RCK/p54 interactions with Ago2 were mediated by adapter protein(s).

Cytoplasmic P-bodies contain RCK/p54, Lsm1, Dcp2, and eIF4E (Coller and Parker 2004; Cougot et al. 2004; Andrei et al. 2005). To confirm whether these structures also contain Ago2 as recently reported(Liu et al. 2005b; Sen and Blau 2005), we transfected HeLa cells with expression vectors containing YFP-Ago1, CFP-Ago1, YFP-Ago2, and CFP-Ago2. Transiently expressed YFP- and CFP-tagged Ago1 and Ago2 co-localized at specific foci in cytoplasm (data not shown). To examine the contents of these cytoplasmic foci, HeLa cells were transfected with expression vectors for YFP-Lsm1 and CFP-Ago2, or YFP-RCK/p54 and CFP-Ago2 and visualized 24 h later by confocal microscopy. As shown in Fig III.1B, CFP-Ago2 co-localized with YFP-Lsm1 and YFP-RCK/p54, two *bona fide* P-body proteins (Coller and Parker 2004; Cougot et al. 2004; Andrei et al. 2005). In addition, immunofluorescence experiments showed that

endogenous Ago2 co-localized with Lsm1 in P-bodies (Fig III.S1). Interestingly, overexpressing YFP-RCK/p54 increased the average number of P-bodies in every cell (Fig III.1B, compare panels a and d). To confirm that the localization of Ago2 and Lsm1 to P-bodies was not the result of overexpression in transiently transfected cells, we immunostained cells with antibodies to endogenous Ago2 and Lsm1 and found that the localization of Ago2 and Lsm1 to P-bodies (Fig III.S1) was similar to that in Fig 1B. These results show that Ago2, Lsm1, and RCK/p54 are present in P-bodies.

To visualize protein-protein interactions *in vivo*, we used fluorescence resonance energy transfer (FRET) as a probe. In FRET, a fluorescent donor molecule transfers energy via a nonradiative dipole-dipole interaction to an acceptor molecule (Clegg 2002). We used a well known donor: acceptor fluorescent-protein pair, CFP:YFP, with a Förster distance ($R_0$) of 4.9 nm (Patterson et al. 2000). To determine whether Ago1 and Ago2 interacted *in vivo* with each other and with RCK/p54, we measured the FRET efficiency between the donor, CFP-Ago2, and acceptor, YFP-RCK/p54. To do so, we used a method in which the donor signal lost during FRET is restored by deliberately photobleaching the acceptor fluorophore to abolish its capacity as an energy acceptor (Bastiaens et al. 1996; Miyawaki and Tsien 2000; Chiu et al. 2005). In cells expressing YFP-RCK/p54 and CFP-Ago2, the FRET efficiency was 21.07% ± 2.52 (Fig III.1C and D). In cells expressing CFP-Ago2 and YFP-Lsm1, FRET efficiency was not significant (1.62% ± 1.11), corroborating our

immunoprecipitation results (Fig III.1A). Furthermore, cells co-expressing YFP-RCK/p54 and CFP showed no significant FRET efficiency (1.64% ± 1.28). Similar to the YFP-RCK/p54 and CFP-Ago2 pair, YFP-Ago1 and CFP-Ago2 showed an efficient FRET (19.61% ± 4.51), indicating a direct interaction between Ago1 and Ago2 *in vivo* (Sen and Blau 2005).

Interestingly, the FRET efficiency between Ago1 and Ago2 decreased to 12.13% ± 1.6 when we used CFP-Ago1 and YFP-Ago2, indicating that the energy transfer efficiencies were sensitive to the orientation of donor: acceptor pair in the RNP complex. Moreover, only a moderate energy transfer efficiency (6.41% ± 1.96) was seen when YFP-RCK/p54 and CFP-Ago1 were used in FRET experiments, suggesting that this donor: acceptor pair was not as ideally oriented for an efficient energy transfer as the pair CFP-Ago1 and YFP-Ago2. Alternatively, RCK/p54-Ago1-Ago2 is assembled in an RNP complex where the donor: acceptor pair is affected by the location of the probe. Nonetheless, the efficiency of energy transfer was well above the background control (0.99%). As a control experiment, cells co-expressing YFP-Ago1 and CFP showed no significant FRET efficiency (0.99% ± 0.67). Taken together, these results indicate that Ago1 and Ago2 directly interact *in vivo* with each other and with RCK/p54.

**Figure III.1 Human argonaute proteins interact with RCK/p54, a component of mRNA-processing P-bodies. (A) Immunopreciptation and immunoblot analyses.** Total cell extracts from HeLa cells co-expressing myc-Ago2 and YFP-Ago1, YFP-Dcp2, YFP-RCK/p54, YFP-eIF4E, YFP-Lsm1 or YFP were treated with +/- RNase A followed by myc-Ago2 immunoprecipitation (IP). Total cell extract (TCE) and anti-myc IPs were analyzed by immunoblot using anti-GFP and anti-myc antibodies. **(B) *In vivo* localization of RCK/p54 and Ago2 to P-bodies.** HeLa cells expressing YFP-Lsm1 and CFP-Ago2 (panels **a, b,** and **c**), YFP-RCK/p54 and CFP-Ago2 (panels **d, e,** and **f**) were visualized by confocal microscopy at 24 h post-transfection. **(C) Visualization of interactions between RCK/p54 and Ago2 in P-bodies by fluorescence resonance energy transfer (FRET).** HeLa cells expressing YFP-RCK/p54 and CFP-Ago2 were fixed at 24 h post-transfection. FRET was measured by an acceptor photobleaching method. Fluorescence images of donor (CFP-Ago2) and acceptor (YFP-RCK/p54) molecules were taken before and after photobleaching YFP. FRET efficiencies were calculated as described, and data were analyzed by Leica confocal software. Arrows point to P-bodies, which are enlarged in insets. **(D) FRET efficiencies between different P-body protein donor:acceptor pairs.** HeLa cells co-expressing YFP-RCK/p54 and CFP-Ago2, YFP-Lsm1 and CFP-Ago2, YFP-RCK/p54 and CFP, YFP-Ago1 and CFP-Ago2, YFP-Ago2 and CFP-Ago1, YFP-RCK/p54 and CFP-Ago-1, as well as YFP-Ago1 and CFP were fixed and FRET efficiencies were measured.
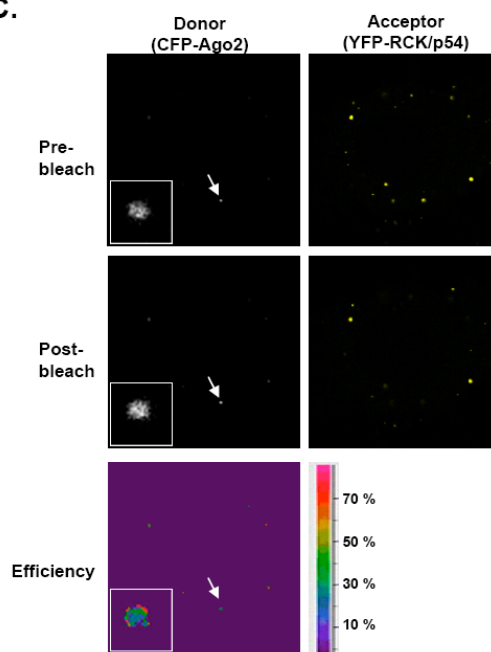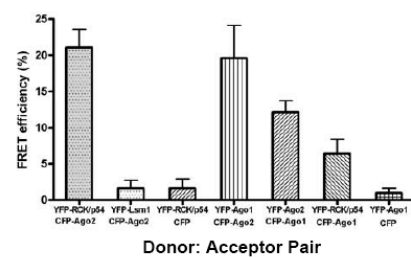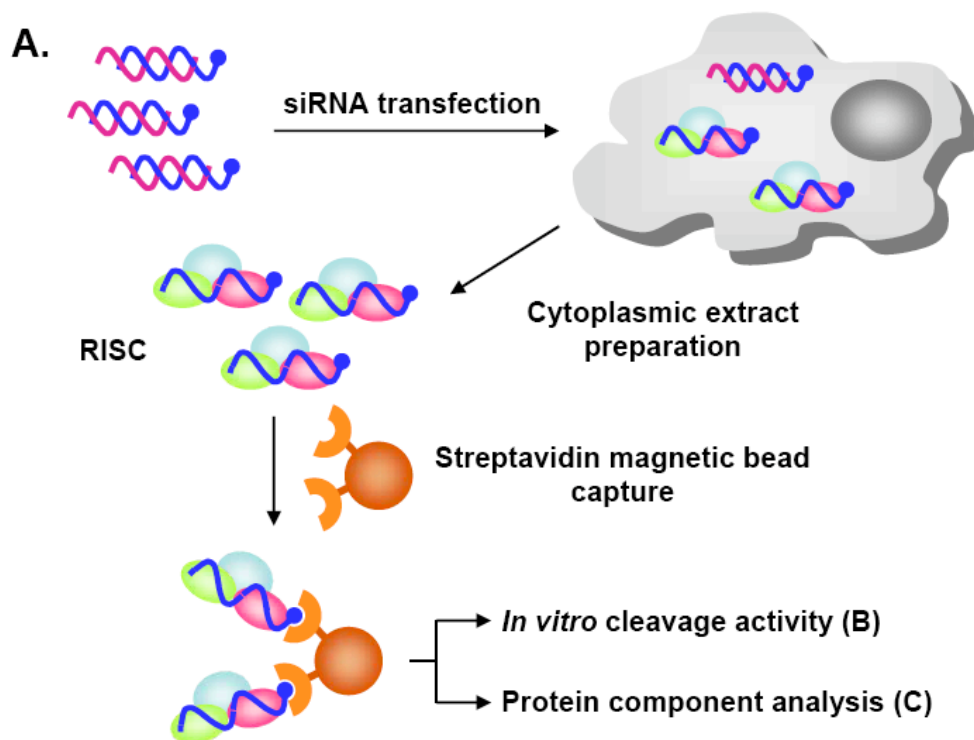
**A.**
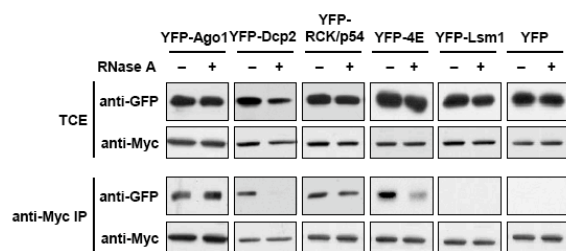


**B.**
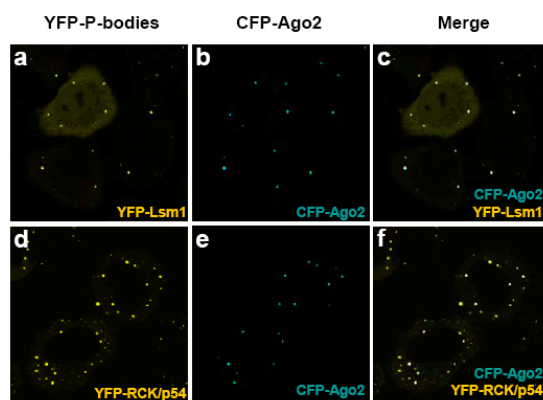


**C.**



**D.**

**RCK/p54 is a component of RISC containing the guide strand of siRNA**

To determine whether RCK/p54 is recruited into a functional RISC complex containing argonaute proteins or its association with Ago1/Ago2 is merely due to their co-localization in P-bodies, we affinity purified active RISCs, analyzed their protein composition, and assayed for RISC function (Fig III.2A). siRNA duplexes against EGFP (si-GFP) were synthesized and 3'-biotin moieties were conjugated to the 3'-end of the guide strand (si-GFP-Bi). These two duplexes (unmodified siGFP and biotin-modified si-GFP [si-GFP-Bi]) were transfected into HeLa cells, and RISCs were captured by incubating cell extracts with streptavidin-conjugated magnetic beads (Chiu and Rana 2002b, 2003). Beads and supernatants were analyzed for RISC function, i.e., the ability to cleave target mRNA *in vitro* (Brown et al. 2005). RISCs primed with siGFP or siGFP-Bi guide strands efficiently cleaved their target mRNA (Fig. III.2B, lanes 1 and 3), but only biotin-containing RISC purified on streptavidin-magnetic beads showed cleavage activity (Fig III.2B, lanes 2 and 4). These results show that active RISC can be programmed in human cells by biotin-containing guide strands of siRNAs and can be captured on magnetic beads for further analysis.

To probe the involvement of P-body proteins in this purified active RISC, its protein composition was analyzed by immunoblot using antibodies against Flag tag or endogenous Ago2, RCK/p54, eIF4E, and Lsm1. When the RNAi machinery was primed with biotin-containing siRNAs, Ago1, Ago2, and RCK/p54 were co-purified with RISC; and when the guide strand of siRNA did not contain

**Figure III.2 Isolation of active human RISC containing RCK/p54-Ago1/Ago2.**

**(A) Experimental outline to purify active human RISC.** The guide strands of siRNA complexes targeting GFP (si-GFP) were conjugated with 3' biotin (si-GFP-Bi; blue strands) and transfected into HeLa cells. RISCs were captured by incubating cell extracts with streptavidin-magnetic beads. **(B) Target mRNA is cleaved by biotin-captured RISC.** Bead (B) and supernatant (S) phases of captured RISC were incubated with 124-nt $^{32}$P-cap-labeled GFP target mRNA. The reactions were stopped after 120 min, and products were resolved on 6% denaturing polyacrylamide gels. **(C) Biotin-captured RISC contains proteins associated with mRNA processing**. Active human RISC from HeLa cells expressing Flag-Ago1 was captured by biotin-siRNA and its protein composition was analyzed by immunoblot using anti-Flag, anti-Ago2, anti-RCK/p54, anti-Lsm1, and anti-eIF4E antibodies.

**A.** siRNA transfection → Cytoplasmic extract preparation

RISC

Streptavidin magnetic bead capture

*In vitro* cleavage activity (B)

Protein component analysis (C)

**B.**

| | si-GFP | + | − |
| | si-GFP-Bi | − | + |

GFP target

GFP cleavage product

lanes 1 2 3 4

**C.**

| | si-GFP | + | − |
| | si-GFP-Bi | − | + |

anti-Flag Ago1 — S, B

anti-Ago2 — S, B

anti-RCK/p54 — S, B

anti-4E — S, B

anti-Lsm1 — S, B
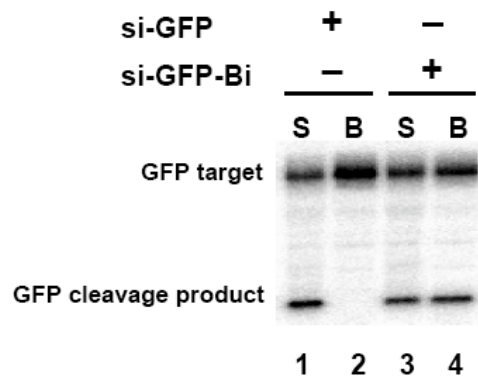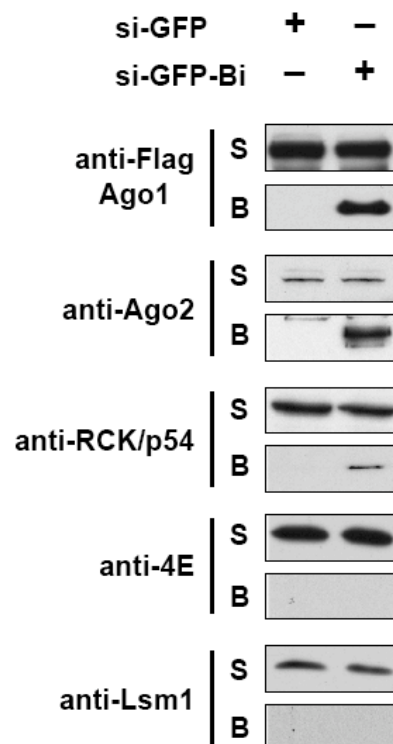
biotin, RISC did not bind to beads (Fig III.2C). Interestingly, eIF4E did not co-purify with RISC, indicating that the myc-Ago2 interaction with eIF4E that occurred in P-bodies (Fig. III.1A) was RNA-dependent, and eIF4E did not directly interact with Ago2 to assemble into active RISC by the guide stra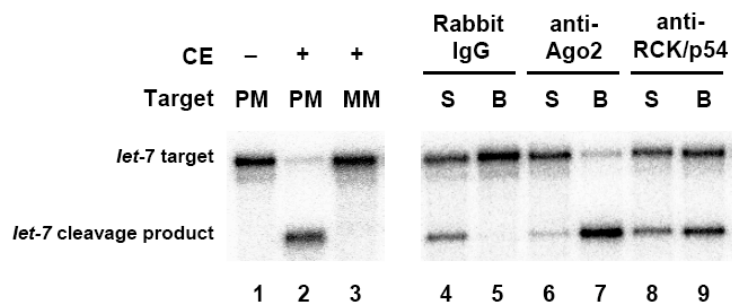nd. The data also show that Lsm1 was not a RISC component, consistent with findings shown in Fig III.1A. Together, these results identify a new argonaute-interacting protein, RCK/p54, that is recruited to RISC programmed by siRNA (siRISC).

**RCK/p54 is a component of RISC containing miRNA**

To determine the functional interactions of RCK/p54 with endogenous RISC programmed by micro RNAs (miRISC), we employed affinity purification of RISC and target mRNA cleavage capabilities of miRISC when the target has perfectly complementary sequences to the micro RNAs. Cell extracts containing *let*-7 miRISC cleaved perfectly matched radiolabeled target mRNA with high efficiencies, whereas a substrate mRNA containing a mismatched sequence was not cleaved (Fig III.3A, lanes 2 and 3). In the absence of extracts, no mRNA cleavage or degradation was detected (Fig III.3A, lane 1). After establishing the functional assay to analyze miRISC, we next affinity purified miRISC on magnetic beads using anti-Ago2 and anti-RCK/p54 antibodies and assessed the cleavage of perfectly matched *let*-7 target mRNA by the bead and supernatant phases. miRISCs purified by anti-Ago2 and anti-RCK/p54 antibodies showed efficient cleavage of *let*-7 target mRNA (Fig III.3A, lanes 7 and 9). Ago2 antibodies

**Figure III.3 RCK/p54 is a component of human miRISC. (A) Affinity-purified miRISCs associated with PCK/p54 retain cleavage activity.** To purify miRISC associated with RCK/p54, magnetic protein A beads coupled with rabbit IgG, rabbit anti-Ago2 or rabbit anti-RCK/p54 antibodies were incubated with HeLa cytoplasmic extracts. After immunoprecipitation, RISC activities were analyzed by incubating the supernatant (S) or bead (B) phases with 182-nt $^{32}$P-cap-labeled *let*-7 substrate mRNAs having a perfectly complementary or mismatched sequence to the *let*-7 miRNA. Cleavage products were resolved on 6% denaturing polyacrylamide gels. CE, cytoplasmic extract; PM, perfect match; MM, mismatch. **(B) Affinity-purified miRISCs retain cleavage activity.** *let*-7 miRISC cleavage of a perfectly matched RNA target was inhibited by 2'-*O*-Me oligonucleotides complementary to *let*-7 miRNA (*let*-7-2'-*O*-Me or *let*-7-2'-*O*-Me-biotin [Bi]). A 182-nt $^{32}$P-cap-labeled *let*-7 substrate mRNA was incubated with the supernatant (S) or bead (B) phases of captured miRISC. The reactions were stopped after 120 min, and products were resolved on 6% denaturing polyacrylamide gels. **(C) miRISCs contain proteins associated with mRNA processing.** Cytoplasmic extracts of HeLa cells expressing Flag-Ago2 and myc-Ago1 were incubated with 2'-*O*-Me oligonucleotides complementary to *let*-7 miRNA (*let*-7-2'-*O*-Me or *let*-7-2'-*O*-Me-biotin [Bi]), affinity purified by streptavidin-magnetic beads to capture *let*-7 miRISC. Supernatant (S) and beads (B) after biotin capture were analyzed by immunoblot using anti-myc, anti-Flag, anti-RCK/p54, and anti-eIF4E antibodies.

**A.**



| CE | – | + | + |
| Target | PM | PM | MM |

*let-*7 target

*let-*7 cleavage product

| 1 | 2 | 3 |

| Rabbit IgG | | anti-Ago2 | | anti-RCK/p54 | |
| S | B | S | B | S | B |
| 4 | 5 | 6 | 7 | 8 | 9 |

**B.**



| | *let-*7-2'-*O*-Me | | | *let-*7-2'-*O*-Me-Bi | |
| CE | S | B | CE | S | B |

*let-*7 target

*let-*7 cleavage product

| 1 | 2 | 3 | 4 | 5 | 6 |

**C.**



*let-*7-2'-O-Me    *let-*7-2'-O-Me-Bi

anti-Myc Ago1    S / B
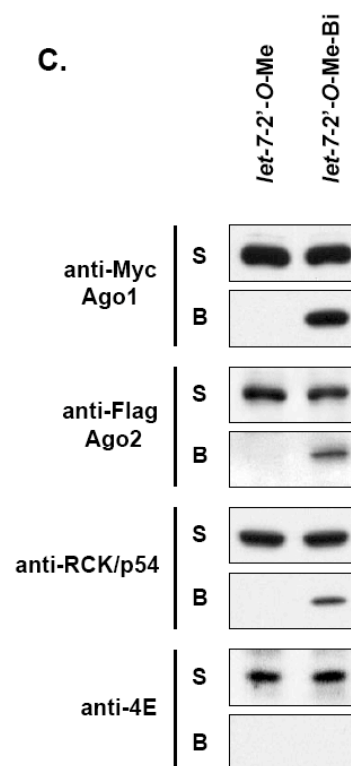
anti-Flag Ago2    S / B

anti-RCK/p54    S / B

anti-4E    S / B
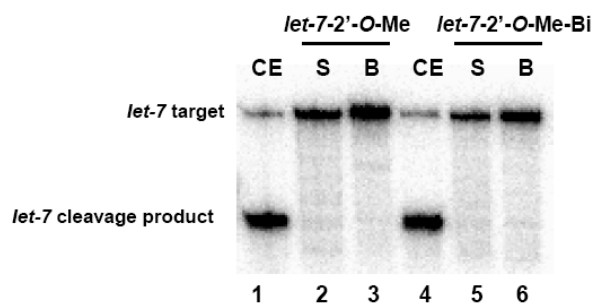
captured most of the RISC activity on beads as compared to RCK/p54 antibodies (lanes 6-9, Fig III.3A). Non-specific IgG did not purify miRISC activities on beads (lanes 4 and 5). These results demonstrate that RCK/p54 is a component of functional miRISC.

To confirm these results, we next used an alternative approach to determine whether RCK/p54 is associated with endogenous RISC programmed by miRISC. RISCs containing miRNA were isolated from HeLa cells by affinity capture as described in Fig III.2A, with the following modifications. To specifically capture endogenous miRISC, 2'-O-methyl inhibitors of *let*-7 miRNA were employed (Hutvagner et al. 2004; Meister et al. 2004a). HeLa cytoplasmic extracts expressing myc-Ago1 and Flag-Ago2 were incubated with 3'-biotinylated-*let*-7-2'-O-methyl inhibitor, which is complementary to the *let*-7 miRNA, and incubated with streptavidin-conjugated magnetic beads. As a control, cell extracts were treated with the *let*-7-2'-O-methyl inhibitor without 3'-biotinylation. After capture, beads containing miRISCs were washed with lysis buffer and split into two aliquots to determine miRISC function and protein composition. Function was determined by assaying for *in vitro* cleavage of a $^{32}$P-target mRNA that perfectly matched the *let*-7 sequence. The data in Fig III.3B (lanes 1 and 4) show that cell extracts contained active *let*-7 miRISC cleaved the perfectly matched target mRNA with high efficiencies (Hutvagner et al. 2004; Meister et al. 2004a). Incubation with *let*-7 inhibitors (with or without 3'-biotin [Bi]) blocked the cleavage activity of *let*-7 miRISC in supernatant or beads (Fig III.3B,

lanes 2-3, and lanes 5-6). These results are consistent with previous reports (Hutvagner et al. 2004; Meister et al. 2004a) that adding 2'-*O*-Me oligonucleotides complementary to *let*-7 abolishes target cleavage activity by *let*-7 in cell extracts, indicating complete hybridization of the 2'-*O*-Me probe. Immunoblot analysis of affinity-purified miRISC using anti-myc, anti-Flag, anti-RCK/p54, and anti-eIF4E antibodies (Fig III.3C) showed that myc-Ago1, Flag-Ago2, and RCK/p54 were associated with *let*-7 miRISC. As observed for the active RISC programmed with siRNA, eIF4E did not associate with miRISC. These findings reveal that RCK/p54 is a novel component of endogenous RISC programmed with either siRNA or miRNA.

**Depletion of RCK/p54 disrupts P-bodies and Ago2 localization**

To understand the function and role of RCK/p54 in the RNAi pathway, RCK/p54 was depleted in P-bodies of HeLa cells by siRNA-mediated RNAi. 24 h after transfecting cells with siRNA, real-time quantitative PCR (qPCR) showed that mRNA levels decreased by more than 90% and immunoblot analysis showed that RCK/p54 protein levels decreased significantly without affecting the levels of other P body proteins including Lsm1 and Ago2 (Fig III. S2). The effect of depleting RCK/p54 on localization of Ago2 was next examined by immunofluorescence analysis of HeLa cells expressing myc-Ago2 and siRNAs against RCK/p54. As shown in Fig III.4 (panels b, c, f, and g), depleting RCK/p54 disrupted the cellular P-body structures. In these P-body-deficient cells,

**Figure III.4   Depletion of RCK/p54 disrupts P-bodies and disperses the localization of human Ago2.**   HeLa cells were co-transfected with myc-Ago2 and siRNA against human RCK/p54 (lower panels) or CDK9 mismatch (control; upper panels). At 24 h post-transfection, cells were analyzed by immunofluorescence using antibodies against myc-Ago2 (panels **a** and **e**) and against the P-body proteins Lsm1 (panels **b** and **f**) and RCK/p54 (panels **c** and **g**). Cells were stained with Hoechst 33258 to visualize nuclei and images were digitally merged (panels **d** and **h**).

| Myc-Ago2 | Lsm1 | RCK/p54 | Overlay |
|----------|------|---------|---------|
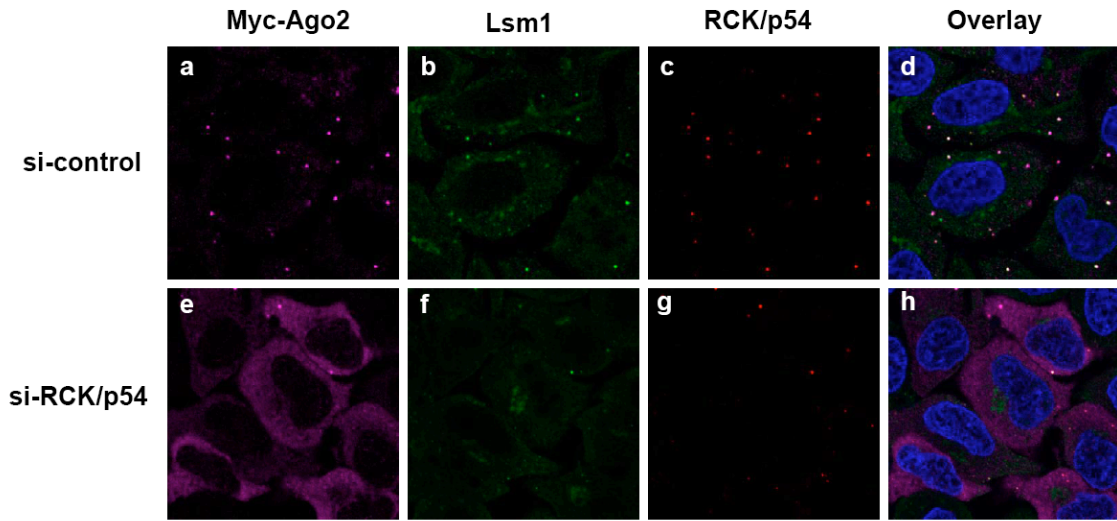
Ago2 proteins were diffused throughout the cytoplasm and no longer accumulated at specific foci (Fig III.4, panels a and e). This cytoplasmic redistribution of Ago2 suggests that its localization to P-bodies is driven in mammalian cells by factors such as RCK/p54.

**Depletion of Lsm1 disrupts P-bodies but does not affect RCK/p54 and Ago2 interactions**

The interactions between the P-body proteins, RCK/p54 and argonautes, raised the question whether P-body structures are required for these interactions. To address this question, we disrupted P-body structures by using RNAi against Lsm1 which is a P body protein but does not associate with RISC as shown in Fig III.1. HeLa cells were transfected with siRNA against Lsm1, harvested at 24, 48, and 72 h post-transfection, and total cell extracts were analyzed by immunoblot. The results show an efficient knockdown of Lsm1 compared with GAPDH (Fig III.5A). We first visualized Lsm1 and Ago2 by immunofluorescence using antibodies against Lsm1 and Myc tag that showed co-localization of Lsm1 and Ago2 in P bodies (Fig III.5B, panels a-c). To determine the status of P-body structures and RISC localization in cells after Lsm1 knockdown, Lsm1-depleted cells were analyzed by immunofluorescence which showed that P body structures were drastically disrupted, Ago2 was diffused throughout the cytoplasm, and little co-localization of Lsm1 and Ago2 was observed (Fig III.5B,
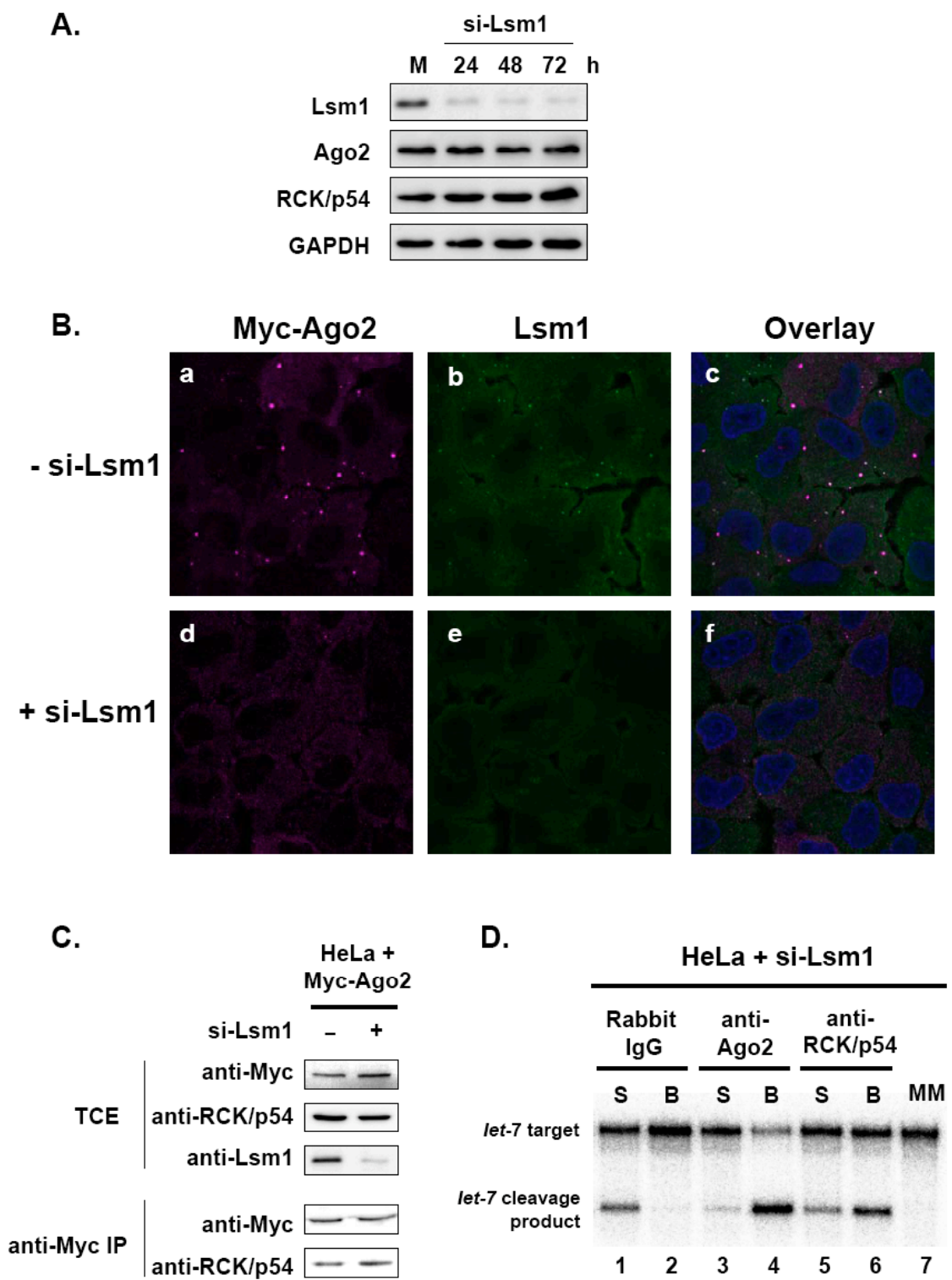
panels d-f).  These results show that P-body structures were drastically disrupted when Lsm1 was depleted by RNAi.

To determine the effect of P body disruption on Ago2 and RCK/p54 interactions, we performed immunopurification experiments after Lsm1 knock down.  HeLa cells were transfected with Myc-Ago2 and control siRNA or siRNA against Lsm1 and total cell extract were prepared at 48 h posttransfection followed by Myc-Ago2 immunoprecipitation (IP).  Total cell extract (TCE) and anti-Myc IPs were analyzed by immunoblot using anti-Myc, anti-RCK/p54 and anti-Lsm1 antibodies.  Lsm1 siRNA treatment efficiently depleted Sm1 protein levels without affecting Myc-Ago2 and RCK/p54 (Fig III.5C).  Immunoprecipitation using Myc antibodies showed that RCK/p54 interacted with Ago2 and this interaction was not significantly changed when Lsm1 was depleted in the cell (Fig III.5C).  Since P bodies were disrupted by Lsm1 depletion, these results demonstrate that Ago2 and RCK/p54 interaction does not require P bodies.

Next, we analyzed the target mRNA cleavage activities of affinity-purified miRISC from Lsm1-depleted cell extracts.  P-bodies were disrupted in HeLa cells by transfecting them with siRNA against Lsm1, and cytoplasmic extracts were prepared 48 h post-transfection.  These HeLa cell extracts were incubated with magnetic protein A beads coupled with rabbit IgG, rabbit anti-Ago2 or rabbit anti-RCK/p54 antibodies to purify miRISC associated with RCK/p54 or Ago2.  After immunoprecipitation, RISC activities were analyzed by incubating the supernatant (S) or bead (B) phases with 182-nt $^{32}$P-cap-labeled *let*-7 substrate

**Figure III.5 Depletion of Lsm1 disrupts P-bodies but does not affect the interaction between RCK/p54 and Ago2. (A) Specific knockdown of Lsm1 in HeLa cells by siRNA.** HeLa cells were transfected with siRNA against Lsm1 and harvested at 24, 48, and 72 h post-transfection, and total cell extracts were analyzed by immunoblot with antibodies against Lsm1 or GAPDH. **(B) Depletion of Lsm1 disrupts P-bodies.** HeLa cells were transfected with siRNA against Lsm1. At 48 h post-transfection, cells were analyzed by immunofluorescence using antibodies against Lsm1 and Myc tag for Ago2. Cells were stained with Hoechst33258 to visualize nuclei, and images were digitally merged. **(C) RCK/p54 interacts with myc-Ago2 in Lsm1-depleted HeLa cells.** HeLa cells were transfected with Myc-Ago2 and siRNA control or against Lsm1 and total cell extract were prepared at 48 h posttransfection followed by Myc-Ago2 immunoprecipitation (IP). Total cell extract (TCE) and anti-Myc IPs were analyzed by immunoblot using anti-Myc, anti-RCK/p54 and anti-Lsm1 antibodies. **(D) Affinity-purified RCK/p54 and Ago2 from Lsm1-depleted HeLa extracts retains miRISC activity**. 48 h after transfecting HeLa cells with siRNA against Lsm1, cytoplasmic extracts were prepared. These extracts were incubated with magnetic protein A beads coupled with rabbit IgG, rabbit anti-Ago2 or rabbit anti-RCK/p54 antibodies to purify miRISC associated with RCK/p54. After immunoprecipitation, RISC activities were analyzed by incubating the supernatant (S) or bead (B) phases with 182-nt $^{32}$P-cap-labeled *let*-7 substrate mRNAs having a perfectly matched complementary or a mismatched sequence

to the *let*-7 miRNA. Cleavage products were resolved on 6% denaturing polyacrylamide gels. MM, mismatch.

**A.**

si-Lsm1

| | M | 24 | 48 | 72 | h |

Lsm1

Ago2

RCK/p54

GAPDH

**B.**

| | Myc-Ago2 | Lsm1 | Overlay |



- si-Lsm1

a    b    c

+ si-Lsm1

d    e    f

**C.**

HeLa +
Myc-Ago2

si-Lsm1    –    +

TCE

anti-Myc

anti-RCK/p54

anti-Lsm1

anti-Myc IP

anti-Myc

anti-RCK/p54

**D.**

HeLa + si-Lsm1

| Rabbit IgG | anti-Ago2 | anti-RCK/p54 | |
| S | B | S | B | S | B | MM |

*let*-7 target

*let*-7 cleavage
product

1    2    3    4    5    6    7

mRNAs having a perfectly complementary or mismatched sequence to the *let*-7 miRNA. Cleavage products were resolved on 6% denaturing polyacrylamide gels. miRISCs purified by anti-Ago2 and anti-RCK/p54 antibodies showed efficient target *let*-7 cleavage (Fig III.5C, lanes 4 and 6). Ago2 antibodies captured more RISC activity on beads than RCK/p54 antibodies, as observed in Fig 3A (lanes 6-9). Control experiments using IgG (Fig III.5C, lanes 1 and 2) did not show any miRISC activity purified by magnetic beads, supporting specific capture by Ago2 and RCK/p54 antibodies (lanes 4 and 5). miRISC did not cleave a mismatched substrate RNA for *let*-7 (Fig III.5C, lane 7). Despite the significant loss of P-body structures in cells treated with Lsm1 siRNA, the efficiency of *let*-7 target mRNA cleavage by miRISC purified by anti-RCK/p54 antibody was not significantly affected (compare Fig III.3A, lane 9 with Fig III.5C, lane 6). These results indicate that disrupting P-bodies by depleting Lsm1 did not significantly affect RCK/p54 association with miRISC.

**Depletion of RCK/p54 does not affect RNAi activity *in vivo***

To examine whether the P-body protein RCK/p54, also a component of RISC, is involved in siRNA-mediated gene silencing, the siRNA dose dependence of RNAi-mediated gene silencing was quantified in RCK/p54-depleted HeLa cells using a dual fluorescence reporter assay. Briefly, GFP and RFP were constitutively expressed in cells transfected with reporter plasmids for EGFP and RFP, respectively. GFP expression was silenced by treating cells with

a 21-nt siRNA targeting nt 238-258 of the EGFP mRNA. The fluorescence intensity ratio of target (GFP) to control (RFP) fluorophore was determined in the presence of siRNA duplexes and normalized to that observed in control-treated cells (Chiu and Rana 2002a; Chiu and Rana 2003).

When HeLa cells were transfected with siRNA mismatched for CDK9 (control), the second transfection with GFP siRNA silenced GFP expression in a dose-dependent manner, i.e., GFP/RFP ratios decreased with increasing concentrations of siRNA (Fig III.6A, gray bars). Depleting RCK/p54 before quantifying GFP silencing resulted in moderate to no significant loss of RNAi activity, i.e., GFP/RFP again decreased with increasing concentrations of siRNA (Fig III.6A, green bars). Similarly, depleting Lsm1 (Fig III.6A, red bars) and the decapping enzyme, Dcp2 (data not shown), before quantifying GFP silencing in HeLa cells did not significantly decrease RNAi activity. In contrast, prior depletion of Ago2 completely abolished RNAi activity (Fig III.5A, blue bars), as expected and consistent with previous reports (Liu et al. 2004; Meister et al. 2004b; Song et al. 2004). These results suggest that depleting RCK/p54, which disrupts P-bodies (Fig III.4), did not significantly affect siRNA-mediated RNAi *in vivo.*

**Figure III.6 Depletion of RCK/p54 has no significant effect on RNAi activity**

*in vivo* **and** *in vitro.* **(A)** *in vivo* **effect of depleting RCK/p54, Lsm1, and**

**Ago2 on siRNA dose-dependent RNAi activity.** HeLa cells were transfected

with siRNAs against CDK9 mismatch (control), RCK/p54, Lsm1, and Ago2. 24 h

later cells were transfected again with EGFP and RFP reporter plasmids and

varying amounts (2, 10, and 50nM) of siRNA against EGFP. 24 h after the

second transfection, RNAi efficiencies were analyzed (see Materials and

Methods). To quantify the effect of depleting RCK/p54 and Ago2 on RNAi, the

ratio of GFP/RFP signals was normalized to that observed in the absence of GFP

siRNA (0 nM). Normalized ratios <1.0 indicate specific RNAi at a given siRNA

concentration. **(B) Depletion of RCK/p54 has no effect on** *in vitro* **siRISC**

**cleavage activity.** HeLa cells were transfected with siRNAs targeting RCK/p54,

Lsm1, Ago2, or CDK9 mismatch (control). 24 h after the first transfection, cells

were again transfected with 50 nM siRNA targeting EGFP. 24 h later cytoplasmic

extracts (CE) were made (see Materials and Methods), and varying amounts (20,

50, 100 µg) of total CE protein were incubated with a 124-nt, $^{32}$P-cap-labeled

GFP target mRNA. The reactions were stopped after 60 min, and products were

resolved on 6% denaturing polyacrylamide gels. **(C) Quantification of siRISC**

**cleavage activity** *in vitro* **after depletion of RCK/p54, Lsm1, or Ago2.**

Cleavage activity of siRISC targeting EGFP mRNA was quantified as a function

of protein content in extracts of HeLa cells depleted of RCK/p54, Lsm1, or Ago2.
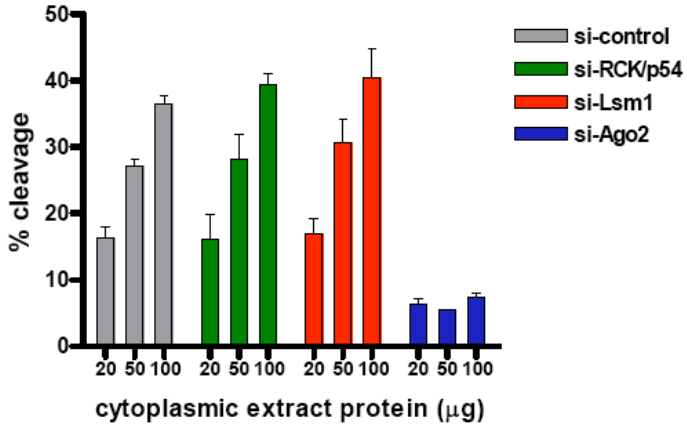
**A.**
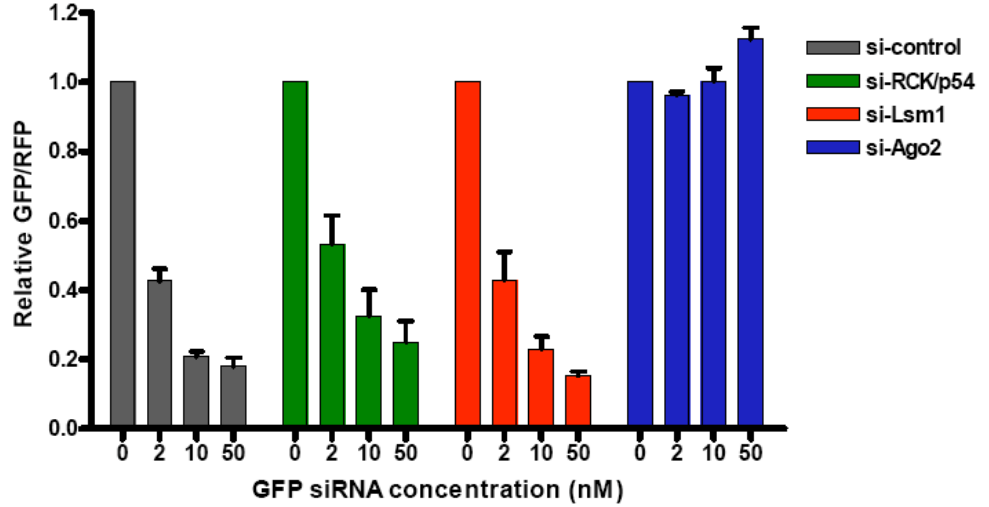


**B.**



**C.**
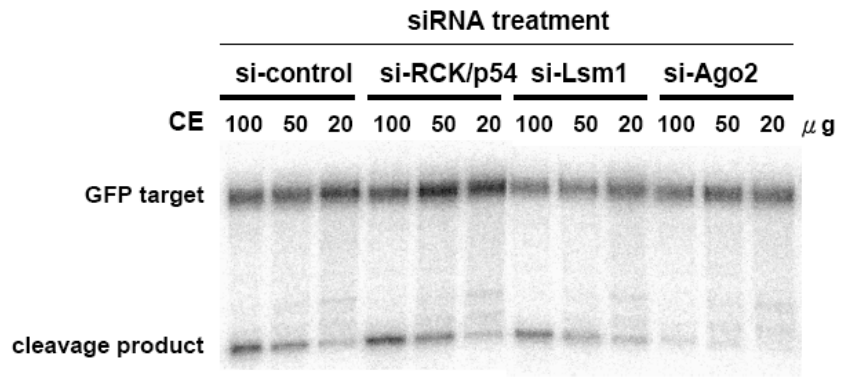
**Depletion of RCK/p54 does not affect RISC-mediated mRNA cleavage *in vitro***

To examine the role of RCK/p54 in RISC catalysis of mRNA processing, *in vitro* mRNA cleavage activity was assayed in extracts from RCK/p54-depleted HeLa cells. Cells were transfected with siRNAs against CDK9 mismatch (control), RCK/p54, Lsm1, or Ago2 and programmed 24 h later with GFP siRNA. Varying amounts of cytoplasmic extract (20-100 $\mu$g) were assayed *in vitro* for target mRNA cleavage activity. As shown in Fig III.6B and C, cleavage activity increased with increasing protein concentration of extracts from both control and RCK/p54-depleted cells, reaching a robust cleavage (37-41%) of target mRNA at the highest protein concentration (100 $\mu$g). In consistent with *in vivo* results shown in Fig 6A, Ago2 depletion abolished the target mRNA cleavage activities of RISC. These results show that RCK/p54 does not affect the slicer function of RISC in cleaving target mRNA *in vitro.*

**RCK/p54 represses general and miRNA-mediated translation**

Our results thus far demonstrate that RCK/p54 is a component of human RISC (Figs III.2 and III.3) and enhances P-body formation (Fig III.1). Our data also show that siRNA-mediated RNAi may not require RCK/p54 and P-body cytoplasmic structures. Since we also identified that RCK/p54 associates with miRISC, we hypothesized that RCK/p54 might function in miRNA-mediated suppression of translation. A recent and intriguing report (Coller and Parker

2005) identified a yeast homolog of RCK/p54, Dhh1p, which activates decapping and facilitates P-body formation, as a general translation repressor. We therefore reasoned that RCK/p54 might be a general translation repressor used by the miRNA machinery to dictate translation suppression of target mRNAs. To test this hypothesis, we first determined whether RCK/p54 was a general translation repressor in human cells. To this end, RCK/p54 expression was silenced in HeLa cells and general translational activity was analyzed by [$^{35}$S]methionine incorporation (Fig III.7A). The translational rates measured by [$^{35}$S]-labeling were significantly greater in RCK/p54-depleted cells than in control siRNA-treated cells (Fig III.7A), indicating that RCK/p54 was a translational repressor in human cells, consistent with results in yeast and reticulocyte extracts (Coller and Parker 2005).

Since RCK/p54 is a general translational repressor and a component of human RISC, we examined the effects of depleting RCK/p54 and disrupting P-bodies on siRNA- and miRNA-mediated gene silencing. To analyze siRNA- or miRNA-mediated gene-silencing events, we chose a well-established CXCR4 mRNA reporter system (Doench et al. 2003), in which siRNA- or miRNA-reporter constructs harbor 1 x perfectly matched or 4 x bulged CXCR4 siRNA target sites, respectively, in the 3'-UTR of *Renilla reniformis* luciferase (RL) mRNA (Doench et al. 2003). In this system, perfectly matched sequences are cleaved by siRISC and bulge-containing sequences are targets for translation suppression by miRISC. HeLa cells were co-transfected with siRNAs directed against P-body

proteins (RCK/p54, GW182, Lsm1, Ago2) and with siRNA or miRNA reporters in the absence or presence of 25 nM CXCR4 siRNA. At 24 h post-transfection, cells were harvested and RL activities were analyzed. RL signals were normalized to GL signals from cells co-transfected with pGL3 plasmid as control. Depletion of RCK/p54 released only miRNA-mediated gene suppression and had no effect on siRNA-mediated gene silencing (Fig III.7B). Depletion of GW182, an argonaute-interacting P-body protein, released gene suppression by miRNA, consistent with previous findings, and moderately released siRNA-mediated gene silencing (Jakymiw et al. 2005; Liu et al. 2005a; Rehwinkel et al. 2005). Ago2 depletion significantly released siRNA-mediated gene silencing and moderately released miRNA-mediated gene suppression. Knockdown of Lsm1 had no significant effect on either miRNA- or siRNA-mediated gene silencing. Taken together, these results show that RCK/p54 depletion releases miRNA-mediated translation suppression of reporter genes, but does not affect siRNA-mediated RNAi.

We next hypothesized that the expression of a specific cellular protein, known to be controlled by miRNAs, might be up-regulated in RCK/p54-depleted cells. Such a protein, human RAS, has been elegantly shown by Slack and colleagues (Johnson et al. 2005) to be regulated by the *let*-7 miRNA family. To test our hypothesis, we analyzed RAS protein levels in HeLa cells under two conditions: either *let*-7 function was inhibited by 2'-*O*-methyl oligonucleotides complementary to the *let*-7 sequence or RCK/p54 was depleted by RNAi (Fig III.7C). For control experiments, we treated cells with a CDK9 mm siRNA and a

2'-*O*-Me oligonucleotide complementary to HIV-1 TAR RNA sequence (Brown et al. 2005). Total cellular protein extracts from equal numbers of cells were prepared and analyzed by immunoblot using monoclonal anti-RAS antibodies directly conjugated with HRP (see Materials and Methods). Actin protein levels were measured as a control using HRP-conjugated anti-actin primary antibody. When cells were treated with *let*-7 inhibitor, RAS protein levels increased, consistent with previous findings (Johnson et al. 2005). Strikingly, RAS protein expression in RCK/p54-depleted cells also showed a robust increase (Fig III.7C) while RAS levels were not significantly affected when cells were treated with control siRNA or 2'-*O*-Me oligonucleotides.  RAS mRNA levels did not differ in HeLa cells after treatment with *let*-7 inhibitor, RCK/p54 silencing, or mock treatment (Fig III.S3).

To further probe our findings of endogenous RAS regulation by RCK/p54, we co-transfected HeLa cells with RAS 3' UTR reporter constructs and *let-7* 2'-*O*-Me inhibitor or siRNA against RCK/p54. For control experiments, we treated cells with a CDK9 mm siRNA and a 2'-*O*-Me oligonucleotide complementary to HIV-1 TAR RNA sequence (Brown et al. 2005). Cells transfected with a control siRNA and *let*-7 inhibitor induced more firefly luciferase expression when reporter plasmids contained 3' UTR sequences for NRAS and KRAS than for the control siRNA and a 2'-*O*-Me oligo control (Fig III.7D), consistent with a recent report (Johnson et al. 2005).  Depleting RCK/p54 by siRNA and adding a control 2'-*O*-Me oligo also released translation repression from both NRAS and KRAS

vectors. Interestingly, combining these two approaches to release translation suppression, *let*-7 2'-*O*-Me oligo and RCK/p54 depletion, did not show additive effects to induce NRAS and KRAs expression.  In all of these experiments, slightly greater firefly luciferase expression was induced from pGL3-NRAS than from KRAS vectors.  These results, combined with those of Fig III.7A-C, strongly suggest that RCK/p54 is a general translation repressor that associates with RISC to regulate miRNA-mediated translation repression.

**Figure III.7 RCK/p54 represses general and miRNA-mediated translation.**

**(A) Release of general translational repression by silencing RCK/p54.** Incorporation of [$^{35}$S]methionine into HeLa cells was used to measure general translational activity. Cells were transfected with 50 nM siRNAs targeting mismatched CDK9 (control) or RCK/p54. Mock control cells were treated with the transfection reagent only.  At 24 h post-transfection, cells were incubated for 1 h in medium lacking Met and Cys, and metabolically labeled with [$^{35}$S]methionine (see Materials and Methods). As a control for passive uptake of [$^{35}$S], mock cells were treated with 40 $\mu$g/ml of the translation inhibitor, cycloheximide (CHX). Cell incorporation of [$^{35}$S] is shown as cpm/$10^3$ cells versus time after adding [$^{35}$S]. **(B) Depletion of RCK/p54 releases translational repression in a luciferase reporter system.**  HeLa cells were transfected with siRNAs against CDK9 mm (control), RCK/p54, GW182, Lsm1, or Ago2.  24 h later, cells were co-transfected with siRNA (1 x perfectly matched [PM] site) or miRNA (4 x bulged sites) luciferase reporters in the presence or absence of CXCR4 siRNA.  RL activities were measured 24 h after the second transfection and normalized to FL activity as a control.  Repression of reporter gene by siRNA or miRNA were measured by normalizing the RL/FL signals in the present of CXCR4 siRNA to the RL/FL signals observed in the absence of siRNA. Release of gene repression by siRNA or miRNA is presented as the fold induction of relative RL/FL level compared to the RL/FL signals observed in control (si-CDK9mm) experiments.  **(C) Depletion of RCK/p54 releases repression of RAS protein translation.**  HeLa cells were

transfected with 100 nM of 2'-*O*-Me oligonucleotide (*let*-7 2'-*O*-Me inhibitor or 2'-*O*-Me control), and siRNA against RCK/p54 or CDK9 mm control. 24 h after transfection, the cells were counted and harvested (see Materials and Methods). The protein contents of total cell extracts were resolved by SDS-PAGE and analyzed by immunoblot using anti-RAS and anti-actin antibodies. **(D) Depletion of RCK/p54 releases repression of luciferase protein translation by 3'UTRs of NRAS and KRAS.** HeLa cells transfected with an *Rr*-luc-expressing vector, pRL-TK, and a *Pp*- luc-expressing vector, pGL3-control, pGL3-NRAS, or pGL3-KRAS, were co-transfected with 100 nM of 2'-*O*-Me oligonucleotide (*let*-7 2'-*O*-Me inhibitor or 2'-*O*-Me control) and siRNA against RCK/p54 or CDK9 mm control. Total cell extracts were prepared 48 h post-transfection and dual luciferase assays were performed. Relative GL (*Pp*-luc)/RL (*Rr*-luc) signals were normalized to those of pGL3-control-transfected cells and are shown as the fold induction compared to mock treatment.
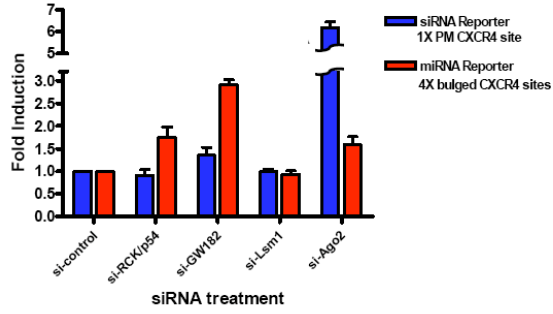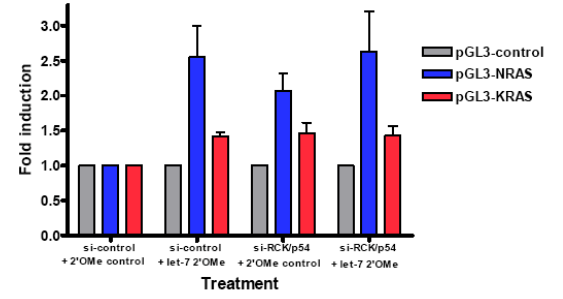
**A.**
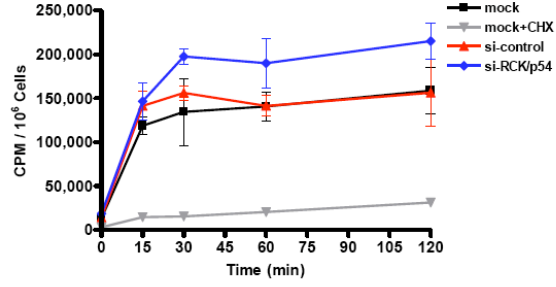


**C.**
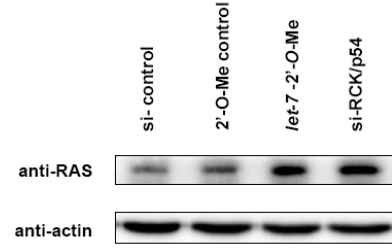


**B.**



**D.**

**Discussion**

We have identified RCK/p54 as a protein that interacts with Ago2 in affinity-purified RISC assemblies to facilitate formation of cytoplasmic P-bodies and that acts as a general translational repressor in human cells.  We have shown that depletion of RCK/p54 disrupts P-bodies and disperses the cytoplasmic localization of Ago2. Furthermore, depletion of RCK/p54 did not significantly affect the RNAi function of RISC, although general, miRNA-mediated, and *let*-7 mediated translational repression were released. Together, our results provide significant insights into RNAi mechanisms in human cells (see below).

Several recent reports show that RISC co-localizes with P-bodies, suggesting that they could be the site where RISC degrades target mRNA or represses mRNA translation. Isolation of miRNAs on polysomes also links the suppression of protein synthesis with arrest of translation initiation or elongation (Pillai et al. 2005).  These studies also demonstrated that human Ago1 and Ago2 co-localize in P-bodies with other cellular proteins, such as Dcp1a, Dcp2, GW182, Lsm1 and Xrn1. A homolog of the P-body protein GW182 in *C. elegans* is the developmental timing regulator AIN-1, which also interacts with miRISCs and may target argonaute proteins to P-bodies (Ding et al. 2005). To dissect and understand the relationship between RNAi function and P-bodies, we affinity purified RISC using myc-Ago2 and expression vectors of the YFP-tagged P-body proteins, Lsm1, RCK/p54, Dcp2, and eIF4E. Ago2 interacted with these various P-body components in ways that were RNA-dependent or RNA-independent (Fig

III.1A). Ago1 and RCK/p54 immunoprecipitated with Ago2 after RNase A treatment of HeLa cell extracts, suggesting that these proteins directly interact with Ago2. Interestingly, RCK/p54, Ago1, and Ago2 were also identified as a component of active RISC programmed with siRNA or miRNA and purified by biotin affinity to streptavidin-conjugated magnetic beads (Figs III.2 and III.3). We examined the P-body localization of Ago2 with Lsm1 and RCK/p54 by co-expressing YFP-tagged Lsm1 and RCK/p54 with CFP-Ago2. Interestingly, overexpressing YFP-RCK/p54 in HeLa cells increased the number of P-bodies (from ~8 to ~20 foci/cell). The number of P-bodies containing CFP-Ago2 also increased (Fig III.1B). These results suggested a functional relationship between RCK/p54-Ago interactions and their localization to P-bodies. To visualize protein-protein interactions *in vivo*, we used fluorescence resonance energy transfer (FRET) as a probe. In cells expressing YFP-RCK/p54 and CFP-Ago2, the FRET efficiency was 21.07% ± 2.52 (Fig III.1C and D). We also observed an efficient FRET between YFP-Ago1 and CFP-Ago2; however, FRET between RCK/p54 and Ago1 was moderate (6.41% ± 1.96). Since FRET is quite sensitive to the orientation of the donor-acceptor pair, it is possible that CFP and YFP in Ago1 and RCK/p54 are not suitably positioned for efficient energy transfer. Nonetheless, the FRET efficiency between Ago1 and RCK/p54 was significantly above the 0.9% background. Taken together, these results demonstrate that Ago1, Ago2, and RCK/p54 directly interact *in vivo*.

Where in the cell does this physical interaction between RISC and RCK/p54 take place and does it require P-body structures?  To address these questions, we disrupted P-bodies in cells by depleting Lsm1, immunopurified endogenous miRISC, and analyzed its ability to cleave a target mRNA with perfect complementarity to *let*-7 miRNA (Fig III.5). We observed no significant difference in miRISC activities purified from Lsm1-depleted and nondepleted cells (Fig III.3 and III.5) even though the P-body structures were disrupted and the total number of P-bodies per cell had significantly decreased. These results show that RCK/p54 association with RISC does not require P-bodies and suggest that localization of RISC to P-bodies is the outcome of translation repression by miRISC.

Having established the physical interactions of RCK/p54 with RISC, we questioned the functional relevance of these interactions in the RNAi pathway and how they could facilitate RISC activity. To that end, we depleted RCK/p54 in HeLa cells and analyzed RNAi activities *in vivo* and *in vitro* (Fig III.6). Depletion of RCK/p54 clearly disrupted the P-body structures and dispersed Ago2 localization throughout the cytoplasm (Fig III.4). Surprisingly, depleting RCK/p54 did not significantly affect siRNA-mediated gene silencing. Similar results showing the lack of P-body involvement in RNAi have been reported in *Drosophila* (Rehwinkel et al. 2005). In that system, depletion of the P-body proteins, GW182 or Dcp1:Dcp2 decapping complex, showed that these proteins were required for miRNA-mediated gene silencing, but RNAi efficiency was not

affected, suggesting that these two gene-silencing mechanisms were independent in *Drosophila* (Rehwinkel et al. 2005). In addition, two recent studies reported that mammalian GW182 interacts with Ago2 and plays a role in miRNA function (Liu et al. 2005a) and in siRNA-mediated RNAi (Jakymiw et al. 2005). Interestingly, depleting GW182 disrupted cytoplasmic foci and interfered with RNAi activity (Jakymiw et al. 2005). It is possible that GW182 is directly involved in human RISC function and does not spatially require P-bodies for its function. As an alternative approach to disrupting P-bodies, we treated HeLa cells with the translation inhibitor, cycloheximide, which did not significantly affect RNAi activities *in vivo* and *in vitro* (data not shown). Taken together, these results strongly suggest that functional siRNA-programmed RISC is assembled before locating to P-bodies, and P-bodies are not prerequisite sites for siRNA-mediated gene silencing.

To determine the role of RCK/p54 in miRNA-mediated translation repression, we used a CXCR4 reporter system (Doench et al. 2003), in which siRNA- or miRNA-reporter constructs harbor 1 x perfectly matched or 4 x bulged CXCR4 siRNA target sites, respectively in the 3'-UTR of *R. reniformis* luciferase (RL) mRNA. (Doench et al. 2003)In this system, perfectly matched sequences are cleaved via siRISC and bulge-containing sequences are targets for translation suppression by miRISC. We observed that depletion of RCK/p54 released only miRNA-mediated gene suppression and had no effect on siRNA-mediated gene silencing (Fig III.7B). Depletion of GW182, an argonaute-interacting P-body

protein, released gene suppression by miRNA and moderately affected reporter constructs containing perfectly matched target sequences, consistent with previous findings(Jakymiw et al. 2005; Liu et al. 2005a; Rehwinkel et al. 2005). Ago2 depletion significantly released siRNA-mediated gene silencing and moderately affected reporters containing 4x bulged sequences. Knockdown of Lsm1 had no significant effect on either miRNA- or siRNA-mediated gene silencing. These results show that RCK/p54 depletion releases miRNA-mediated translation suppression of reporter genes and that this function of RCK/p54 was not significantly affected when P-bodies were disrupted by depleting Lsm1.

To test our hypothesis that RCK/p54 mediates the translational repression of endogenous miRNA targets in P-bodies, we examined RAS protein levels in RCK/p54-depleted cells. We chose RAS because it is an endogenous target of *let*-7, and 3' UTRs of human *RAS* genes contain multiple complementary sites for *let*-7 to bind and regulate RAS expression levels (Johnson et al. 2005). Furthermore, *let*-7 inhibitors are known to enhance RAS protein expression in HeLa cells (Johnson et al. 2005). Depleting RCK/p54 in HeLa cells up-regulated RAS protein, and this increase in RAS levels was higher than that in general translation of control actin (Fig III.7C), suggesting that multiple sites of *let*-7 miRISC binding to target 3'UTR dictate the potency and specificity of translation suppression.

RCK/p54, the human homolog of yeast Dhh1p, is a member of the ATP-dependent DEAD box helicase family and was originally identified as a proto-

oncogene (Akao et al. 1995). In human cells, RCK/p54 interacts in P-bodies with the translation initiation factor, eIF4E (Andrei et al. 2005). The *Xenopus* homolog of RCK/p54, Xp54, which interacts with eIF4E and forms RNA-dependent oligomers, represses the translation of mRNA in oocytes and eggs (Minshall and Standart 2004). In yeast, Dhh1p interacts with the decapping and deadenylase complex and functions in translational repression (Coller et al. 2001). Dhh1p has recently been shown to stimulate translational repression by inhibiting production of the pre-initiation complex (Coller and Parker 2005). Dhh1p and RCK/p54 also inhibit the mRNA translation driven by internal ribosomal entry sites (IRES) *in vitro*, suggesting that this protein is a general translational repressor that may not require a cap structure for its function (Coller and Parker 2005). However, the *in vivo* function of Dhh1p required translational initiation (Coller and Parker 2005). Translation repression by miRISC and P-body localization require the 5'-cap structure in the target mRNA (Humphreys et al. 2005; Pillai et al. 2005), which provides a unique and elegant control mechanism for translation and its regulation (reviewed in (Gebauer and Hentze 2004; Holcik and Sonenberg 2005)). Recently, Petersen et al. reported an intriguing study showing that miRNA repress translation after initiation by a ribosome drop off mechanism (Petersen et al. 2006). Therefore, it is possible that RCK/p54 interacts with miRISC and blocks translation elongation by binding to the multiple target sites with high affinity and creating a barrier for elongating ribosomes (see below).

We therefore propose that the function of RISC assemblies in cells can be described by a model with two independent pathways, depending on whether RNAi is programmed by the guide strand of siRNA or miRNA. In the first pathway, the RISC recognizes a perfectly matched target mRNA and functions as siRISC (Fig III.8) by cleaving its target mRNA. This target mRNA cleavage activity and rapid turnover of siRISC induce the subsequent target mRNA degradation by exonucleases and does not require P-bodies. In the second pathway, the RISC recognizes the imperfectly matched target and functions as miRISC (Fig III.8). Multiple copies of miRISC containing RCK/p54 could initiate an oligomerization event that sequesters the whole RNP and transports it to the P-bodies. This sequestration could also explain the cooperative effects of RISC function that enhance translation repression (Doench et al. 2003). Once in P-bodies, translationally repressed mRNA could stay in oligomeric structures for storage or it could form a complex with decapping enzymes and cap binding proteins that would lead to the mRNA decay pathway. In other words, the miRNA in RISC could provide the sequence specificity and RCK/p54 could be the effector molecule that shuttles the target mRNA toward the fate of storage or processing in P-bodies. Since P-bodies are not a prerequisite for RCK/p54 to assemble into RISC or to function, it is possible that miRISC blocks protein synthesis by enhancing the ribosome drop-off during elongation of translation (Petersen et al. 2006). We propose that miRISC localization to P-bodies is the outcome of translation repression and not a prerequisite for miRISC function.

Stored mRNA in P bodies could reenter the active translation or mRNA decay pathway depending upon cellular condition or stimuli which are presently unknown. How long mRNA translation can be repressed in the cytoplasm and which factors trigger mRNA transport to P-bodies are exciting areas for future research.

Our results on the interactions between RCK/p54 and the RNAi machinery suggest an intriguing role for miRNA function in development and carcinogenesis. However, most targets of miRNA have not yet been identified. A growing body of evidence suggests that miRNAs are important in human disease, including cancers (Poy et al. 2004; Vella et al. 2004; He et al. 2005; Lu et al. 2005). For example, relatively low levels of *let*-7 miRNA up-regulate RAS protein in lung cancer cells, demonstrating a possible role of miRNA in tumorigenesis (Johnson et al. 2005). Two homologs of RCK/p54, Xp54 in *Xenopus* and Me31b in *Drosophila*, control the translation of maternal mRNA in oocytes (Ladomery et al. 1997; Nakamura et al. 2001; Minshall and Standart 2004). Altered regulation of RCK/p54 expression levels has been implicated in the development of human colorectal tumors (Nakagawa et al. 1999; Hashimoto et al. 2001) and in hepatitis C virus-related chronic hepatitis (Miyaji et al. 2003). Overexpression of RCK/p54 and Dhh1p increases the number of Ago2-containing P-bodies (Fig III.1B; (Andrei et al. 2005; Coller and Parker 2005)), suggesting that RCK/p54 is a critical factor in controlling cellular translation. Our results have identified RCK/p54 as an essential component of miRISC-mediated

translation repression and provide a functional link between miRISC and P-bodies. In the context of spatially and temporally restricted miRNA expression, this system allows for exquisite regulation of protein expression by target mRNA. Therefore, perturbations of either miRNA or RCK/p54 expression levels can have deleterious consequences for the cell. What determines the balance between active translation and repression of mRNAs targeted by miRISC, and how cells control the specificity of this repression are key directions for future investigation.

**Figure III.8 A model for human RISC function involving miRNA and siRNA.**

RISC contains Ago2 (red), Ago1 (green), RCK/p54 (blue, labeled p54), and other known (e.g., Dicer and TRBP) and unidentified proteins (pink) and is distributed throughout the cytoplasm. RISC programmed with the guide strand of siRNA (siRISC) binds to its target mRNA by perfectly matching base pairs, cleaves the target mRNA for degradation, recycles the complex, and does not require P-body structures for its function. Multiple numbers (n) of RISC programmed with miRNA (miRISC) bind to target mRNA by forming a bulge sequence in the middle that is not suitable for RNA cleavage, accumulate in P-bodies, and repress translation by exploiting global translational suppressors such as RCK/p54. The translationally repressed mRNA is either stored in P-bodies or enters the mRNA decay pathway for destruction. Depending upon cellular conditions and stimuli, stored mRNA can either re-enter the translation or mRNA decay pathways.
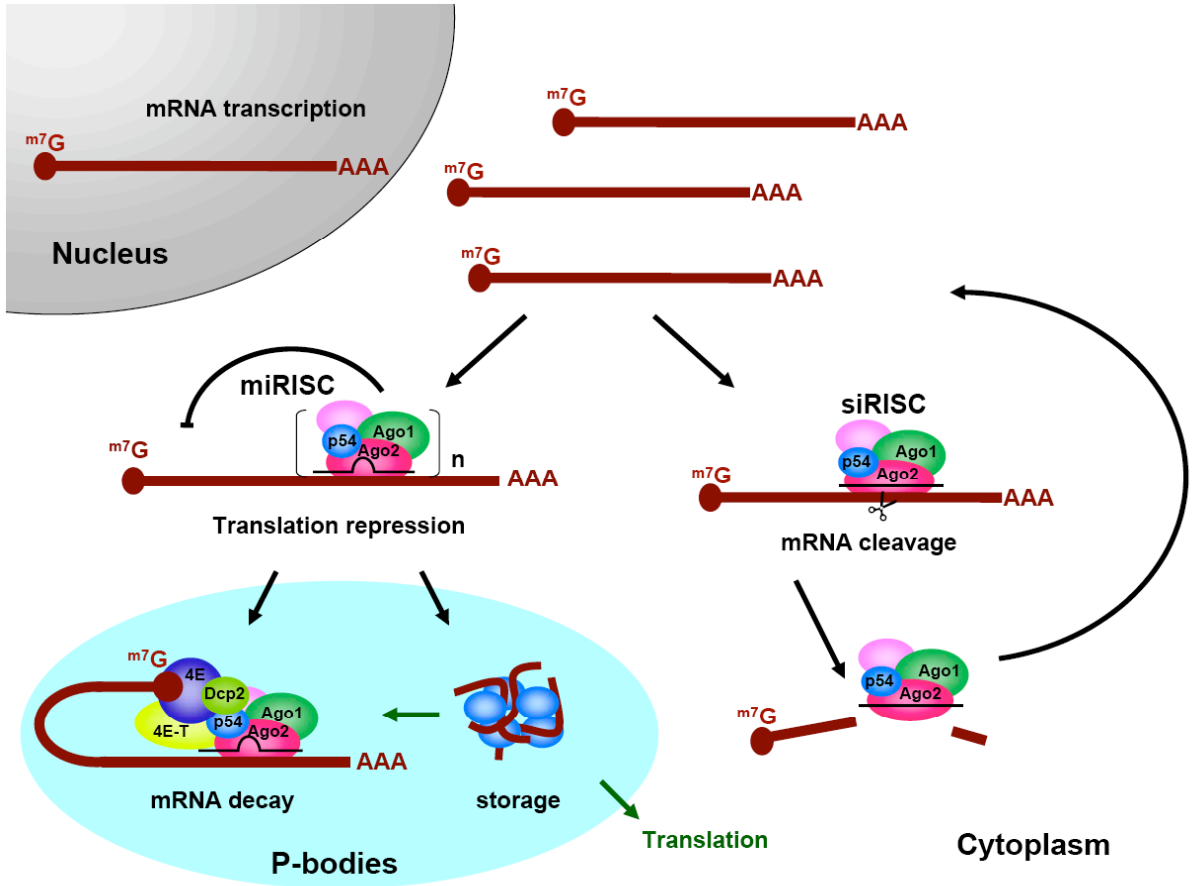
## MATERIALS AND METHODS

### Expression vectors

Ago1 and Ago2 expression vectors with N-terminal YFP- or CFP-epitope tags were generated by PCR amplification of *Ago*1 and *Ago*2 coding sequences from pMyc-Ago1 and pMyc-Ago2 followed by cloning into the *Xba*I and *EcoR*I sites of pEYFP-C1 and pECFP-C1 (BD Biosciences Palo Alto, CA). Expression vectors were kindly provided by four laboratories: pMyc-Ago1/2 (Dr. G. Hannon); pFlag-Ago-1/Ago2 (Dr. T. Tuschl), pGL3-control, pGL3-KRAS, and pGL3-NRAS (Dr. F. Slack), and pRL-TK-1p and pRL-TK-4B (Dr. P. Sharp).

Vectors for expressing YFP-tagged Lsm1, RCK/p54, eIF4E, and Dcp2 were generated through PCR amplification of their coding sequences from 293T cDNA followed by cloning into the *Bgl*II and *Sal*I sites of pEYFP-C1.

### Small interfering RNAs (siRNAs)

siRNAs against GFP, human Ago2, RCK/p54, Lsm1, and CDK9 mismatch were synthesized by Dharmacon (Dharmacon, Lafayette, CO) and 2'-OH deprotected according to the manufacturer's protocols. The sequences of siRNAs (passenger strand) for our experiments were:

GFP: 5'-GCAGCACGACUUCUUCAAGdTdT-3'; hAgo2: 5'-GCACGGAAGUCCAUCUGAAdTdT-3'

RCK/p54: 5'-GCAGAAACCCUAUGAGAUUUU-3'; CDK9mm: 5'-CCAAAGCUCUCCCC UAUAAdTdT-3'; Lsm1: 5'-GUGACAUCCUGCCACCUCACUU-3'

## Cell culture and transfection

HeLa cells were cultured in Dulbecco's minimal essential medium (DMEM) with 10% fetal bovine serum (FBS) at 37°C with 5% $CO_2$. Cells were transfected using Lipofectamine (Invitrogen, Carlsbad, CA) according to the manufacturer's protocol.

## Immunoprecipitation and immunoblotting

Total cell extracts were prepared by incubating cells in lysis buffer (20 mM HEPES, pH 7.9, 10 mM NaCl, 1 mM $MgCl_2$, 0.2 mM EDTA, 0.35% (v/v) Triton X-100, 1/100 (v/v) dilution in protease inhibitor cocktail) and centrifuging at 14000 rpm for 10 min at 4°C. Protein concentration was determined by Dc protein assay (Bio-Rad, Hercules, CA). To examine the RNA dependence of protein-protein interactions, total cell extracts (250 µg) were treated before immunoprecipitation with 0.2 µg/ul of RNase A for 20 min at room temperature. Myc-tagged proteins were precipitated by incubating overnight with polyclonal rabbit anti-myc antibodies directly conjugated to agarose beads (Santa Cruz Biotech, CA). Samples were washed 4 x in lysis buffer and eluted by boiling for 5 min at 100°C in SDS-PAGE sample loading buffer, separated by SDS-PAGE, and analyzed by

immunoblot. For immunoblotting, antibodies included monoclonal mouse anti-GFP (BD Biosciences), anti-eIF4E and anti-myc (Santa Cruz Biotech, CA), anti-Flag (Sigma); polyclonal rabbit anti-myc (Santa Cruz Biotech, CA), anti-DDX6 (RCK/p54; Bethyl Laboratories, Montgomery, TX); and polyclonal chicken anti-Lsm1 (GenWay Biotech, Inc., San Diego, CA).

To assess the ability of endogenous immunopurified miRISC to cleave target mRNA with perfect complementarity to *let*-7 miRNA, *in vitro* cleavage assays for *let*-7 miRISC were conducted. Aliquots (30 $\mu$l) of magnetic protein A beads (Dynal, Norway) were preincubated with rabbit IgG, anti-Ago2 or anti-RCK/p54 antibodies according to the manufacturer's protocol and incubated overnight at 4°C with 50 $\mu$g HeLa cytoplasmic extracts. Beads were then washed 3 x with Na-phosphate buffer (pH 8.0), 1x with lysis buffer, and resuspended in 30 $\mu$l of lysis buffer. Aliquots (10 $\mu$l) of these beads were used in each *let*-7 miRISC cleavage assay.

**Live cell imaging, fluorescence resonance energy transfer (FRET) and immunofluorescence**

HeLa cells were cultured in 35 mm dishes with glass coverslip bottoms (MatTek Corporation, Ashland, MA). Expression vectors for CFP- or YFP-tagged proteins were transfected into cells using Lipofectamine as described above. 24 h later, the live cells were monitored for CFP and YFP signals of the transiently expressed proteins. The signals were detected by a Leica confocal imaging

spectrophotometer system (TCS-SP2) attached to a Leica DMIRE inverted fluorescence microscope equipped with an argon laser, two HeNe lasers, an acousto-optic tunable filter (AOTF) to attenuate individual visible laser lines, and a tunable acousto-optical beam splitter (AOBS). A 63×, 1.32 NA oil-immersion objective was employed. For FRET studies, HeLa cells co-expressing CFP- and YFP-tagged proteins were fixed with 4% paraformaldehyde in PBS at room temperature for 20 min and washed 3 x with PBS. After the final wash, cells were visualized with a Leica confocal imaging system as described above. FRET experiments were performed by an acceptor photobleaching method as described (Bastiaens et al. 1996; Kenworthy and Edidin 1998; Chiu et al. 2005). FRET efficiencies were measured and images were analyzed using Leica confocal software. For immunofluorescence studies, cells transfected with myc-Ago2 were fixed with 4% paraformaldehyde in PBS at room temperature for 20 min and permeabilized with 0.25% (v/v) Triton X-100 for 5 min. Samples were washed 3 times with PBST (0.1% [v/v] Triton X-100 in PBS) and blocked for 30 min in PBST containing 2% (w/v) BSA. Primary and secondary antibodies were diluted in blocking solution during incubation. Secondary antibodies against rabbit IgG, mouse IgG, and chicken IgY were directly conjugated to Alexa Fluor dyes (Molecular Probes, Inc., Eugene, OR). After the final wash, samples were counterstained with Hoechst 33258 to visualize nuclei with a Leica confocal imaging system as described above.

**In vitro cleavage assay for siRISC and miRISC**

HeLa cells sequentially transfected with siRNAs against P-body components and EGFP were harvested 24 h after the second transfection. Cytoplasmic extracts of HeLa cells were prepared as described above and the protein concentration was determined by Dc protein assay (Bio-Rad). Target mRNAs were prepared and *in vitro* cleavage by GFP-siRISC and *let*-7-miRISC was assayed as described (Hutvagner et al. 2004; Meister et al. 2004a).

**Dual fluorescence assay**

A dual fluorescence assay was used to quantify the RNAi activity of siRNAs against GFP. To quantify RNAi effects, cell lysates were prepared from siRNA-treated cells 24 h post-transfection. Total cell lysate (150 µg in 200 µl of reporter lysis buffer) was measured using a Safire plate reader (TECAN). GFP fluorescence was detected in cell lysates by exciting at 488 nm and recording emissions from 504 to 514 nm. The spectrum peak at 509 nm represents the fluorescence intensity of GFP. RFP fluorescence was detected in the same cell lysates by exciting at 558 nm and recording emissions from 578 to 588 nm. The spectrum peak at 583 nm represents the fluorescence intensity of RFP. The fluorescence intensity ratio of target (GFP) to control (RFP) fluorophores was determined in the presence of siRNA duplexes and normalized to the emissions measured in mock-treated cells. Normalized ratios <1.0 indicated specific RNA interference.

## Incorporation of [$^{35}$S]methionine

HeLa cells cultured in 6-well plates were transfected with siRNAs against RCK/p54 or CDK9 mismatch as a scramble control. 24 h post-transfection, cells were incubated for 1 h in culture medium lacking methionine and cysteine, and metabolically labeled by incubating in culture medium containing 100 µCi/ml Tran$^{35}$S-label (MP Biomedicals, Irvine CA). At 0, 15, 30, 60, and 120 min after metabolic labeling, cells were washed twice and harvested in 300µl M-PER buffer (Pierce) with protease inhibitors (Sigma). For each experiment, two extra sets of siRNA-treated cells were trypsinized and counted for total cell numbers. Cell lysates (50 µl) were incubated with 10 µl of 100% TCA on ice for 30 min, and the protein precipitate was collected on GF/C filter paper (Whatman, Clifton, NJ), washed with 5 ml of 95% ethanol, and counted in scintillation fluid.

## Dual luciferase assay for *let*-7 miRNA-mediated gene silencing

A dual luciferase assay was used to quantify the effects of *let*-7- and RCK/p54-mediated gene silencing on human NRAS or KRAS 3' UTR. HeLa cells cultured in 6-well plates were co-transfected with 0.8 µg/well *Pp*-luc-expressing vectors (pGL3-control, pGL3-NRAS, or pGL3-KRAS) and with100 nM *let-7-2'-O*-Me inhibitor or 50 nM siRNA against RCK/p54. In all experiments, transfection efficiencies were normalized to those of cells co-transfected with the *Rr*-luc-expressing vector (pRL-TK; 0.1µg/well). Total cell extracts were prepared 48 h

post-transfection and dual luciferase assays (Promega Madison, WI) were

performed according to the manufacturer's protocol and quantified with a Victor2

multilabel counter (Perkin Elmer). The *Pp*-luc/*Rr*-luc signals were normalized to

those from pGL3-control-transfected cells, showing *let-7*-regulated gene silencing

of RAS 3'UTR.


**siRNA or miRNA luciferase reporter assays**

To analyze siRNA- or miRNA-mediated gene-silencing events, we chose

CXCR4 mRNA reporter system, in which siRNA- or miRNA-reporter constructs

harbor 1 x perfectly matched or 4 x bulged CXCR4 siRNA target sites,

respectively, in the 3'-UTR of *Renilla reniformis* luciferase (RL) mRNA (Doench

et al. 2003).  HeLa cells were co-transfected with siRNAs directed against P-

body proteins (RCK/p54, GW182, Lsm1, Ago2) and with siRNA or miRNA

reporters in the absence or presence of 25 nM CXCR4 siRNA. At 24 h post-

transfection, cells were harvested and RL activities were analyzed.  RL signals

were normalized to the GL signals from cells co-transfected with pGL3 plasmid

as control.

**SUPPLEMENTARY FIGURES**

**Figure III.S1 Subcellular localization of endogenous Ago2 in HeLa cells.**

HeLa cells were analyzed by immunofluorescence using antibodies against endogenous Ago2 (panel **a)** and Lsm1 (panel **b**), and stained with Hoechest 33258 to visualize the nucleus. The images were digitally merged to indicate co-localization of Ago2 and Lsm1 (panel **c**). Arrows point to P-bodies.
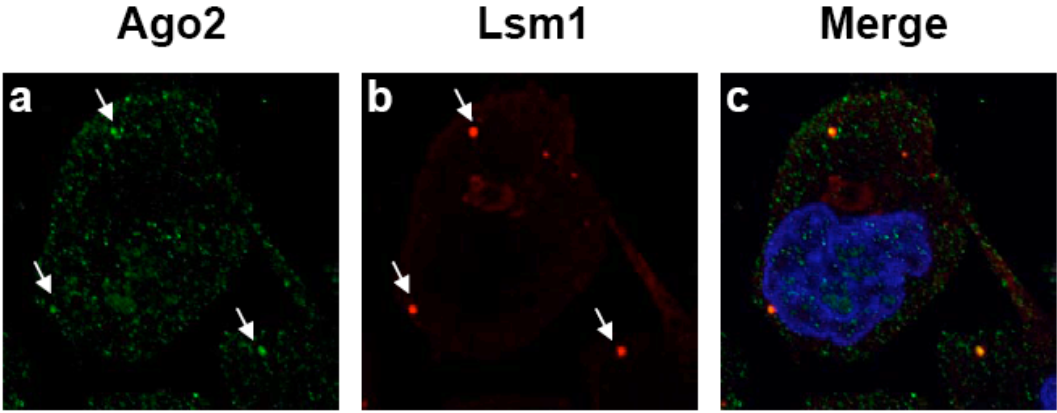
**Ago2**     **Lsm1**     **Merge**

**Figure III.S2  Specific depletion of RCK/p54 in HeLa cells by RNAi.  (A) Specific knockdown of RCK/p54 in HeLa cells.**  HeLa cells were transfected with 50 nM siRNA against RCK/p54, harvested at 24, 48, and 72 h post-transfection, and total cell extracts were prepared.  Analysis by immunoblot shows the specific knockdown of RCK/p54 protein without changing the protein levels of Lsm1 or Ago2.  **(B) Specific depletion of RCK/p54 mRNA after siRNA treatment**.  Total RNA samples (3 $\mu$g) from HeLa cells transfected with siRNA against RCK/p54 were reverse-transcribed and analyzed by quantitative PCR to quantify mRNA levels.  RCK/p54 mRNA levels were normalized to GAPDH mRNA and are presented relative to mock treatment.  Data are from two representative, independent experiments.

**A.**
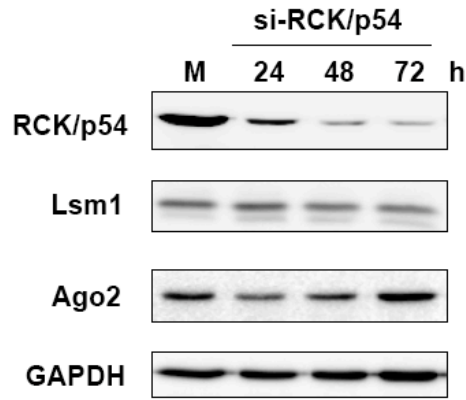


**B.**

**Figure III.S3 *Let*-7 inhibition does not affect RAS mRNA levels.** Total RNA

samples (3 $\mu$g) from HeLa cells transfected with 100 nM of *let*-7 2'-*O*-Me

oligonucleotides or 50 nM siRNA against RCK/p54 were reverse-transcribed and

analyzed by qPCR to quantify mRNA levels. RAS mRNA levels were normalized

to GAPDH mRNA and are presented relative to mock treatment. Data are from
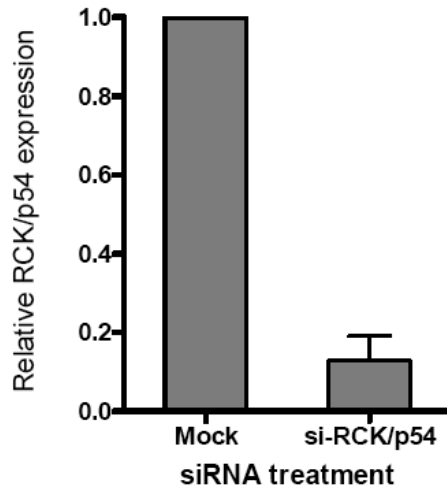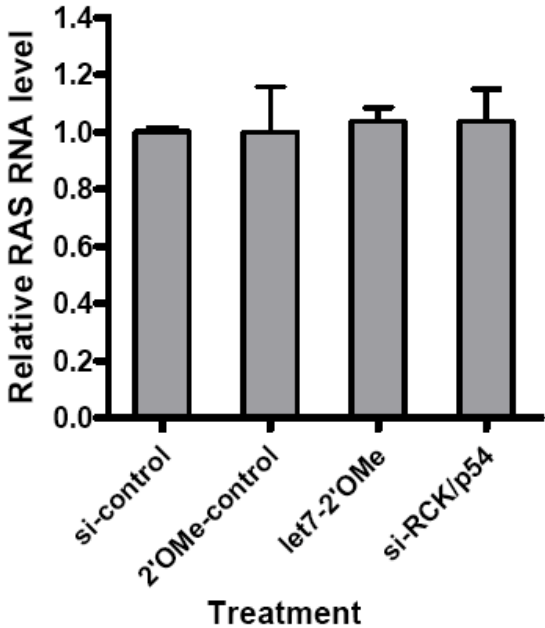
two representative, independent experiments.

# CHAPTER IV

# FUNCTIONAL ANALYSIS OF RCK/P54 IN GENERAL AND miRNA-MEDIATED TRANSLATION REPRESSION

*All figures in this chapter were produced by the author.

## ABSTRACT

MicroRNAs (miRNA), a class of ~22nt non-coding small RNAs, induce the gene silencing at post-transcriptional stage and repress the translation by imperfect base-pairing at the 3'UTR of the target mRNA. In human cells, several cellular factors have been identified to associate with miRNA complex and to modulate the function of miRNA. Our previous studies indicated that a human P-body protein, RCK/p54, is required for miRNA-mediated gene silencing. Here, we continued the study of RCK/p54 functions. By analyzing a series of YFP-tagged RCK/p54 mutants, we identified the motif required for P-body localization, interaction with Ago2, and/or facilitating the miRNA-mediated translation repression. In addition, we used rabbit reticulocyte lysate system to recapitulate the miRNA-mediated silencing in a cell-free system and confirmed the requirement of RCK/p54 in the miRNA pathway in vitro. Finally, analysis of Ago2 distribution in the polysome profiling in RCK/p54-depleted HeLa extracts, compared to that in normal cells, revealed that RCK/p54 facilitates miRISC by trapping it at translation initiation complex. Our data suggested that interaction of RCK/p54 with Ago2 is involved in the repression of translation initiation of miRNA function.

## Introduction

MicroRNAs (miRNAs) are a class of small (~22nt) non-coding regulatory RNAs that regulate gene expression at post-transcriptional level in metazoan and plants. Although miRNAs were discovered as recently as the past two decades, an increasing number of miRNAs have been identified in recent years and their functions have been widely studied in all model organisms. miRNAs have proven to be important for processes involved in developmental biology, cancer and viral pathologies, and the control of cell growth and differentiation.

In human cells, miRNAs are first generated by RNA polymerase II as a long RNA transcript, then processed into ~70-nt precursor miRNAs (pre-miRNA) by Drosha/DGCR8 complex, and then exported to cytoplasm. Following the exportation by Exportin-5 (Exp5), pre-miRNAs are further processed by Dicer and incorporated into Argonaute proteins with other co-factors to form the miRNA-induced silencing complex (miRISC). miRISC recognizes the 3'UTR of target mRNA and represses gene expression post-transcriptionally (reviewed in(Chu and Rana 2007)).

A general feature of the miRNA and target RNA interaction is imperfect base-pairing. Instead of perfect matches, miRNAs usually form several bulge structures with mismatches to the target sequence. Sequence specificity for target recognition is determined by the 5' region of guide miRNA strand at position 2-8nt, which called "seed sequence." Computational analysis of miRNAs and genome database predicts that more than 30% of human protein-coding

genes are regulated by miRNAs. However, most of the targets have not been validated yet by biochemical or genetic methods.

How does endogenous miRISC repress gene expression after it recognizes the 3'UTR of target mRNA? Recent studies provide evidence that miRISC functions in multiple ways, including repression of protein translation, accelerating mRNA degradation and sequestering mRNA to storage compartments. Several hypotheses have been proposed for the mechanism of translational repression by miRISC. These hypotheses include repression at initiation step, repression at post-initiation step, or destabilization of target mRNA. While miRISC may repress protein synthesis at either initiation or post-initiation steps, localization studies of Ago proteins, the key components of miRISC, in human cells have showed that they are concentrated at specific speckles known as mRNA-processing bodies (P-bodies) in the cytoplasm (Liu et al. 2005b; Sen and Blau 2005). P-bodies (also known as DCP or GW bodies) contain mRNAs that are not being translated and proteins involved in mRNA remodeling, decapping, translational repression, and 5' to 3' exonuclease activity (reviewed in (Eulalio et al. 2007a)). Localization of miRISC together with target mRNAs at P-bodies suggests that P-bodies also function in miRNA-mediated gene silencing as the place for target mRNA storage or decay.

Our previous data showed that one human P-body protein, RCK/p54, is involved in the miRNA-mediated pathway (Chu and Rana 2006). RCK/p54 is the human homolog of yeast Dhh1p, a member of the ATP-dependent DEAD box

helicase family. In human cells or in *Xenopus*, RCK/p54 (or Xp54, the *Xenopus* homolog of RCK/p54) interacts with the translation initiation factor eIF4E (Minshall and Standart 2004), and forms RNA-dependent oligomers, repressing the translation of mRNA (Minshall and Standart 2004). In yeast, Dhh1p interacts with the decapping and deadenylase complex and functions as a translational repressor by inhibiting production of the pre-initiation complex (Coller et al. 2001). Previously, we have shown that human RCK/p54 interacts with the argonaute proteins Ago1 and Ago2 in affinity-purified active siRISC or endogenous miRISC, facilitates formation of cytoplasmic P-bodies, and acts as a general repressor of translation(Chu and Rana 2006). Depletion of RCK/p54 did not significantly affect the RNAi function of RISC, but released general, miRNA-induced, and *let*-7-mediated translational repression of RAS protein, suggesting that RCK/p54 is one of the effector molecules in miRISC that represses translation (Chu and Rana 2006).

In this chapter, we report our recent study on RCK/p54 for its function in miRNA-mediated translation repression. Analysis of a series of YFP-tagged RCK/p54 mutants, we identified the motif required for P-body localization, interaction with Ago2, and/or facilitating the miRNA-mediated translation repression. In addition, we used rabbit reticulocyte lysate system to recapitulate miRNA-mediated silencing in a cell-free system and confirmed the requirement of RCK/p54 in the miRNA pathway. Finally, analysis of Ago2 distribution in polysome profiling in RCK-depleted HeLa extracts, compared to that in normal

cells, revealed that RCK/p54 facilitates miRISC by trapping it at translation initiation stage.

## Results

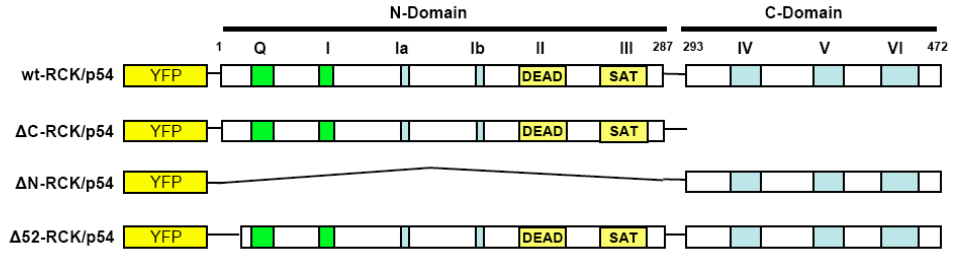### Construction of YFP-RCK/p54 expression mutant clones

To define the motif of RCK/p54 capable of interacting with Ago2 and mediating P-body localization, we firstly generated a YFP-tagged RCK/p54 silencing mutant, which is resistant to siRNA against endogenous RCK/p54 (Fig IV.1A). After that, we engineered a series of YFP-tagged RCK/p54 mutants with deletions or point mutations at each conserved functional motif (Fig IV.1B and IV.1C). In all cases, the mutants retained the siRNA-resistant sequence. Deletion mutants include Δ52-RCK/p54, which lacks the 1-52 amino acid at N-terminal, ΔN-RCK/p54, with a deletion at N-terminal 1-292 amino acid residues, and ΔC-RCK/p54, which contains the N-terminal only. Schematic of the YFP-tagged RCK/p54 point mutants is shown in Fig IV.1C. To confirm that the expression of all those point mutants are not affect by the siRNA that targets endogenous RCK/p54, HeLa cells were co-transfected with various YFP-RCK/p54 constructs and siRNAs which are perfectly match or mis-match to the wild type RCK sequence. 24 h post transfection, HeLa cell extracts were prepared and the total cell extracts were analyzed by immunoblot with antibodies against YFP, GAPDH, and RCK/p54. Our results showed that RCK/p54 siRNA specifically depleted the endogenous RCK/p54 and the YFP-RCK/p54 with wild type sequence, but not the silencing mutant and all other mutants (Fig IV.1D).

**Figure IV.1. Constructions of YFP-RCK/p54 mutants.** (A) Schematic diagrams the siRNA-resistant RCK/p54 sequence. siRNA resistant YFP-RCK/p54 silence mutant was generated from siRNA sensitive (wild-type) construct by site-directed mutagenesis. (B) Schematic of YFP-RCK/p54 deletion mutants. (C) Schematic of YFP-RCK/p54 mutants with specific point mutations at various conserved domain.

Fig 1
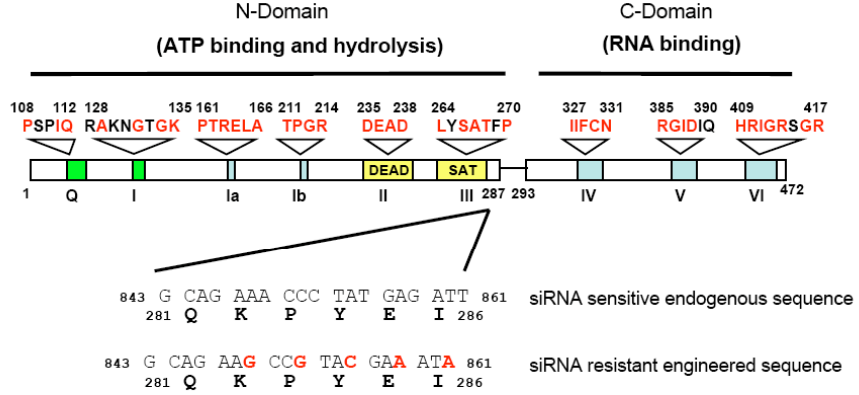
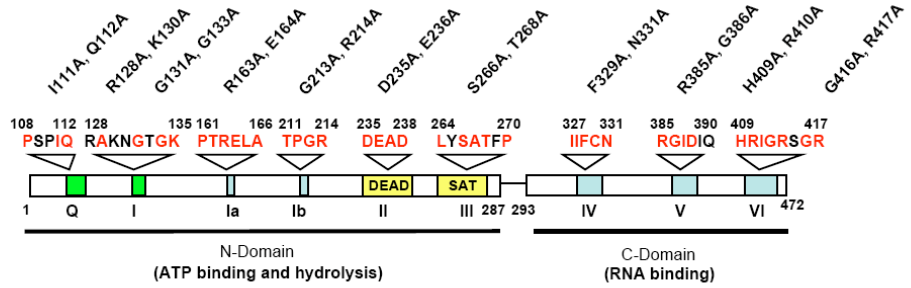**Figure IV.1 (Continued). Constructions of YFP-RCK/p54 mutants.** (D) Expression of siRNA-resistant YFP-RCK/p54 mutants in HeLa cells. HeLa cells co-transfected with mis-matched siRCK (-) or prefect matched siRCK (+) and various YFP-RCK mutants are harvested 24 h post transfection. Expression of YFP-tagged RCK mutants and endogenous RCK were analyzed by immunoblot using anti-GFP and anti-RCK antibodies.

**Fig 1**

**D**
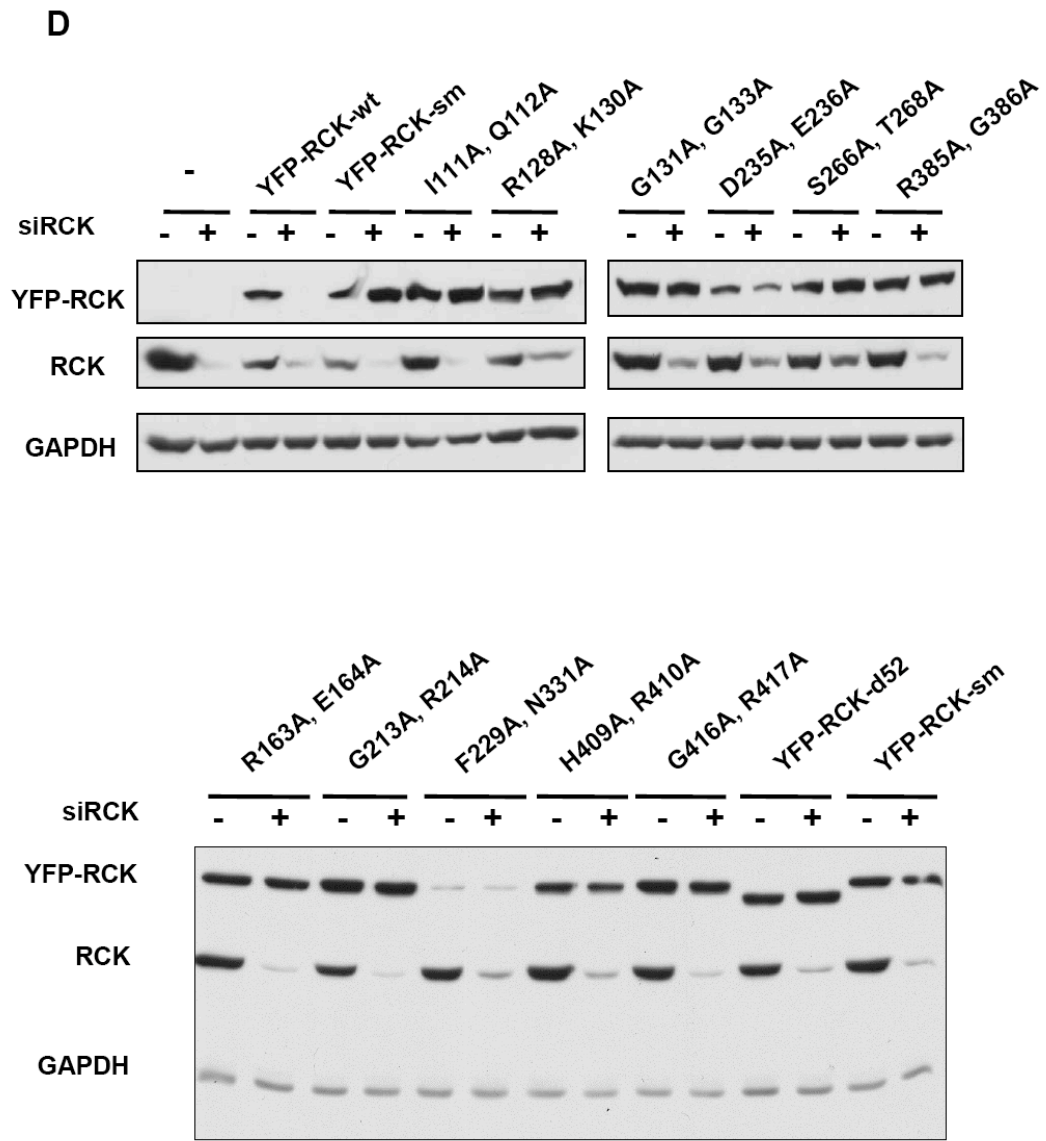
**The C-terminal of RCK/p54 is required for the P-body localization and Ago2 interaction.**

To determine which motif is required for the P-body localization of RCK/p54, we analyzed the subcellular localization of YFP-RCK/p54 deletion mutants by imaging the YFP fluorescence with confocal microscopy. HeLa cells transfected with various RCK/p54 truncated mutants were fixed at 24 h posttransfection and followed by the Hoescht staining as the marker for nucleus (Fig IV.2A). Our data showed that deletion at the N-terminal 52aa does not affect the localization of RCK/p54 to P-bodies (Fig IV.2A, panels b and f). Deletion of the whole N-terminal domain (aa 1-292) increases the nuclear localization of RCK/p54 while the cytoplasmic RCK/p54 still localizes to P-bodies (Fig IV.2A, panels d and h). Interestingly, the C-terminal deletion mutant of RCK/p54 is diffused through out the cytoplasm, suggesting that the C-terminal domain is important for the RCK/p54 localization (Fig IV.2A, panels c and d).

To examine if the diffusion of C-terminal deletion mutant affects the localization of endogenous Ago2, P-bodies were visualized by immunostaining using antibody against endogenous Ago2 (Fig IV.S1). Our results showed the wild type, as well as the N-terminal-deleted RCK/p54 co-localized with Ago2 in the cytoplasm (Fig IV.S1, panels a, c, d, f). The C-terminal-deleted RCK/p54 did not localize to P-bodies (Fig IV.S1 panel b), whereas endogenous Ago2 are detected at P-bodies (Fig IV.S1 panel e). This result suggested that with the

deletion of C-terminal domain, RCK/p54 may lose not only P-body localization but also its interaction with Ago2.

While the N-terminal-deleted RCK/p54 mutant still localized to P-bodies, the number of YFP-positive P-bodies is significantly less than that in cells expressing wt or Δ52-RCK/p54. To quantify the difference between these mutants, we calculate the average number of P-bodies in one cell that is expression YFP-RCK/p54-wt or mutants (FigIV.2B). In cells overexpressing wt-RCK/p54 or Δ52-RCK/p54, the average RCK-positive P-body (blue bars) can be as many as 12-14 per cell. We also calculated the endogenous Ago2-localized P-body numbers in the same cells (red bars) and found the number of Ago2-positive P-bodies is much less than RCK-positive ones (~4-6 per cell). In the cells that overexpress ΔC-RCK/p54, which does not localize to P-bodies, we still observed the Ago2-positive P-bodies and the average number of P-bodies was close to that in HeLa cells overexpressing wt or mutant RCK/p54. Interestingly, in the cells overexpressing ΔN-RCK/p54 mutants, the YFP-positive P-body number is almost the same as the Ago2-positive P-bodies, although a portion of ΔN-RCK/p54 was trapped in the nucleus. These results suggested that overexpression of wt-RCK/p54 or Δ52-RCK/p54 increases P-body numbers but not all overexpressed RCK/p54 interacts with RNAi machinery. To examine if the overexpression of wt-RCK/p54 also increases the P-body size, as well as the P-body number, we measured the average diameter of each YFP-positive P-body

**Figure IV.2**. **C-terminal deleted YFP-RCK/p54 mutants does not localize to P-bodies in HeLa cells.** (A). Subcellular localization of YFP-RCK/p54 truncated mutants. HeLa cells were transfected with 300ng of wt-RCK/p54 (a, e), ΔN-RCK/p54 (b, f), ΔN-RCK/p54 (c, g), or Δ52-RCK/p54 (d, h) and visualized by imaging of YFP fluorescence 24 h post-transfection. (B). Quantitative analysis of YFP-RCK/p54 and Ago2-localized P-bodies. The average numbers of YFP-RCK/p54(+) and Ago2(+) P-bodies per cell were calculated by analyzing the YFP fluorescence and visualized by immunostaining (anti-Ago2) (C). Quantitative analysis of P-body sizes in HeLa cells expressing various YFP-RCK/p54 truncated mutants. The average diameter of P-body was measured by Leica confocal microscope software.

**Fig 2**

**A**



| wt-RCK/p54 | Δ52-RCK/p54 | ΔC-RCK/p54 | ΔN-RCK/p54 |
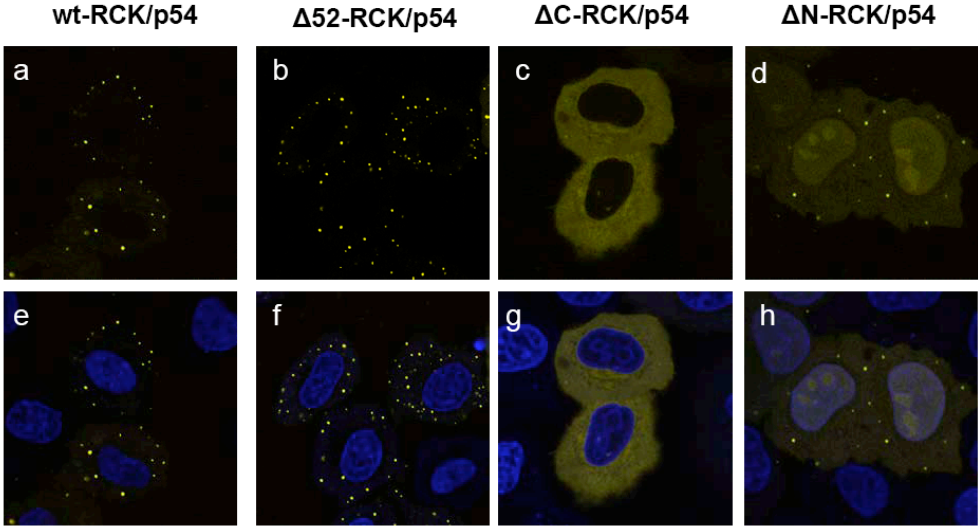
**B**
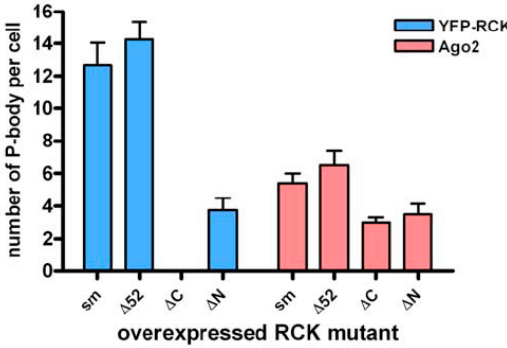


**C**
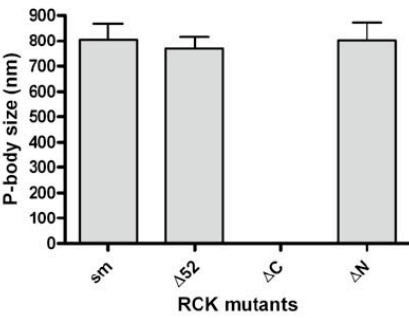
in HeLa cells expressing YFP-RCK/p54 constructs (Fig IV.2C). The average P-body size is similar for each YFP-RCK/p54 mutant or wild type, suggesting that the N-terminal domain only affects the number of RCK/p54-positive P-bodies, not the size of P-bodies.

**Motif II (DEAD box), III (SAT box), V and VI are important for RCK/p54 localization in P-bodies.**

We further examined the subcellular localization of all the engineered RCK/p54 point mutants to zoom in the possible important motif for the RCK/p54 function in translation repression. All the point mutants were expressed in HeLa cells and visualized as described above. Fig IV.3 summarizes the images of each mutant. As compared to the silencing mutant (sm, Fig IV.3A, panel a), we observed significant change in RCK/p54 localization in the cells expressing D235A, S266A, R385A, and H409A mutant. Although the YFP signals of these four mutants are predominately dispersed throughout cytoplasm, we can still detect small and fewer cytoplasmic foci at where the YFP-RCK/p54 mutants are concentrated. To ascertain whether the mutations at these motifs affect the P-body localization of RCK/p54 protein, we quantified the number of YFP-positive and Ago2-positive P-bodies in the cells expressing different point mutant (Fig IV.3B). Our result showed that mutations in the DEAD box motif (D235A, E236A), SAT (S266A, T268A), motif V (R385A, G386A), and motif VI (H409A, R410A)

**Figure IV.3. Motif II (DEAD box), motif III (SAT box), motif V and VI are important for RCK/p54 localization in P-body.** (A). Subcellular localization of YFP-RCK/p54 mutants. HeLa cells transfected with YFP-RCK/p54 constructs containing point mutations at different conserved motif were fixed 24 h post transfection. Localization of RCK/p54 mutants was visualized by imaging the YFP fluorescence. (B). Quantitative analysis of average P-body numbers in HeLa cells expression YFP-RCK/p54 mutants. (C). Average size of P-bodies expressing YFP-RCK/p54 mutants. The diameter of each P-body was measured by Leica confocal software.

**Fig 3**

**A**

| RCK-sm | I111A, Q112A | R128A, K130A | G131A, G133A |
|---|---|---|---|



| R163A, E164A | G213A, R214A | D235A, E236A | S266A, T268A |
|---|---|---|---|

| F329A, N331A | R385A, G386A | H409A, R410A | G416A, R417A |
|---|---|---|---|

**Fig 3**

**B**



**C**



sm:YFP-RCKsm
m1: I111A, Q112A
m2: R128A, K130A
m3: G131A, G133A
m4: R163A, E164A
m5: G213A, R214A
m6: D235A, E236A
m7: S266A, T268A
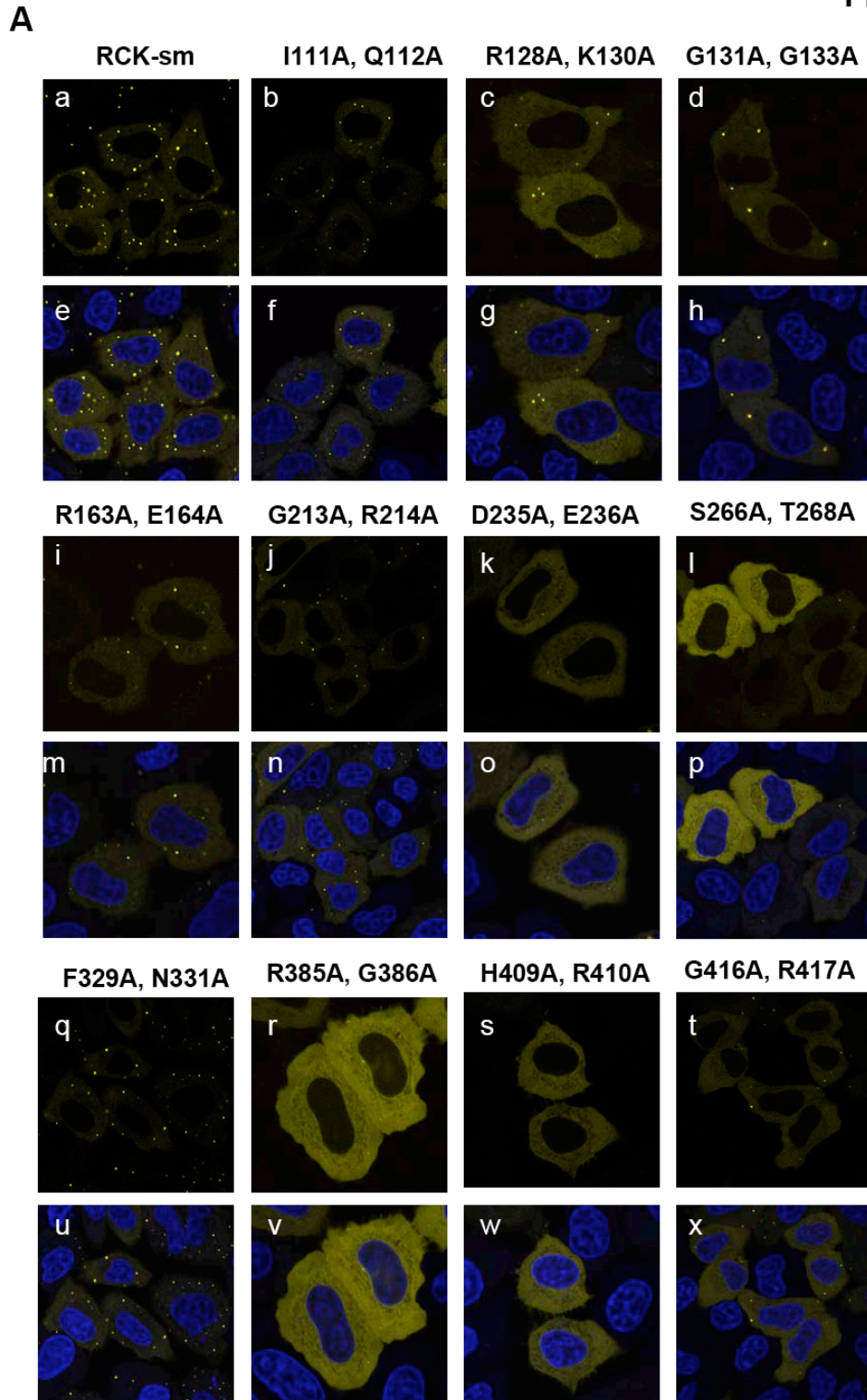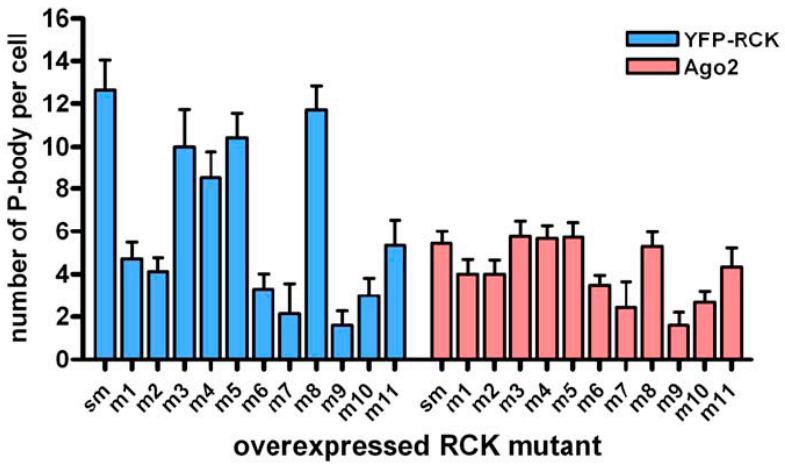m8: F329A, N331A
m9: R385A, G386A
m10: H409A, R410A
m11: G416A, R417A
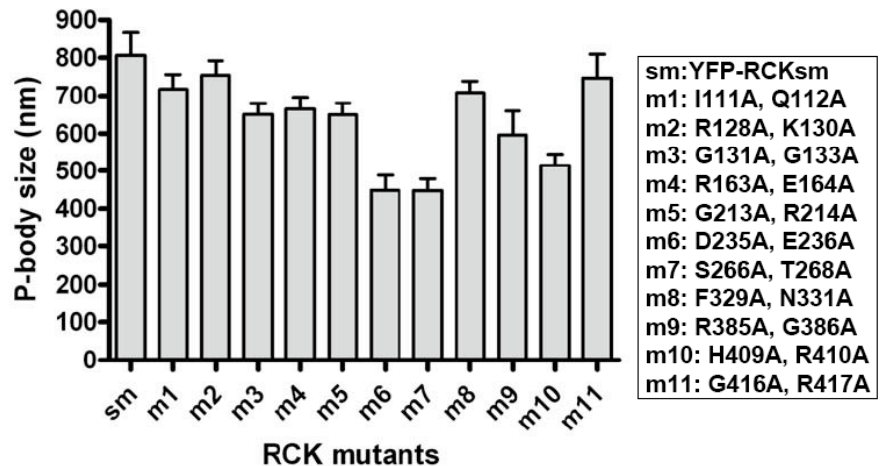
affect the localization of RCK/p54, reduce the number of P-bodies, and reduce the size of P-bodies (Fig IV.3C).

**The C-terminal of RCK/p54 determines the interaction of RCK/p54 and Ago2**

To examine which domain mediates the interaction of RCK/p54 with Ago2, YFP-RCK/p54 deletion mutants were co-expressed in HeLa cells with myc-tagged Ago2 and immunopurified using anti-myc antibodies. The protein composition of isolated complexes was analyzed by immunoblot using antibodies against GFP or myc. When total cell extracts (TCE) were analyzed to determine the protein expression efficiencies of the vectors used in these experiments (TCE panel in Fig IV.4A), all YFP- and myc-tagged proteins were efficiently expressed. Analysis of immunopurified complexes revealed that wt, ΔN, and Δ52-RCK/p54 formed complexes with Ago2 (Myc-IP panel, Fig IV.1A). Interestingly, the ΔC-RCK/p54 mutant did not co-purify with Ago2, which is consistent with the previous localization data.

To confirm the specific motif that mediates the interaction of RCK/p54 with Ago2, YFP-RCK/p54 point mutants were co-expressed with myc-Ago2 in HeLa cells and the interaction between RCK/p54 mutants and Ago2 were analyzed by immunopurification and immunoblot (Fig IV.4B). Our immunoblot data indicated that mutations at C-terminal motives IV, V, VI, and motif SAT affect the interaction of RCK/p54 with Ago2, the key component of RNAi

**Figure IV.4. RCK/p54 interacts with Ago2 via C-terminal domain.** (A). Immunoprecipitation and immunoblot analysis of RCK/p54 truncated mutants. Total cell extracts from HeLa cells co-expressing myc-Ago2 and YFP-wt-RCK/p54, YFP-ΔN-RCK/p54, YFP-ΔC-RCK/p54, or YFP-Δ52-RCK/p54 were used for immunoprecipitation (IP). Total cell extract (TCE) and anti-myc IPs were analyzed by immunoblot using anti-GFP and anti-myc antibodies. (B). Immunoprecipitation and immunoblot analysis of RCK/p54 truncated mutants. Total cell extracts from HeLa cells co-expressing myc-Ago2 and YFP- RCK/p54 mutants were prepared and followed by immunoprecipitation (IP). TCE and anti-myc IPs were analyzed by immunoblot as described previously.

**Fig 4**

**A**



myc-Ago2

YFP-RCK

|  | TCE | | | | Myc-IPed | | | |
|--|-----|--|--|--|----------|--|--|--|
|  | ΔC | ΔN | Δ52 | wt | ΔC | ΔN | Δ52 | wt |

**B**

myc-Ago2 + YFP-RCK mutants

1  2  3  4  5  6  7  8  9  10  11  12

TCE:
myc-Ago2

YFP-RCK

Myc-IP:
myc-Ago2

YFP-RCK

1: sm
2: I111A, Q112A
3: R128A, K130A
4: G131A, G133A
5: R163A, E164A
6: G213A, R214A
7: D235A, E236A
8: S266A, T268A
9: F329A, N331A
10: R385A, G386A
11: H409A, R410A
12: G416A, R417A
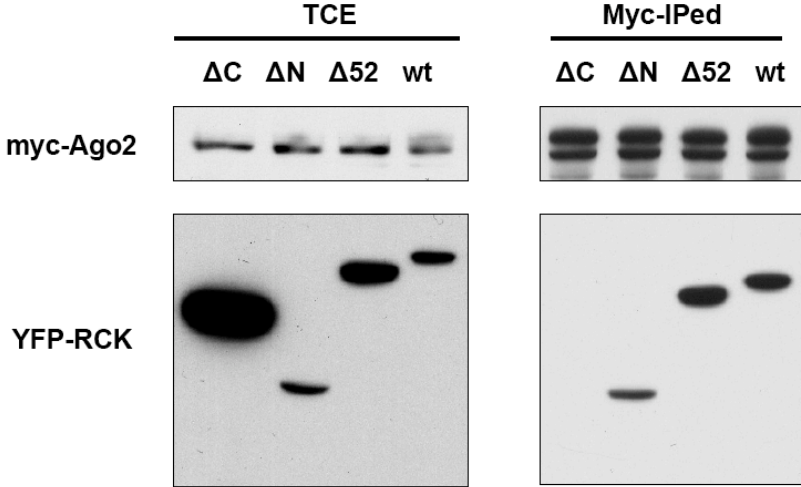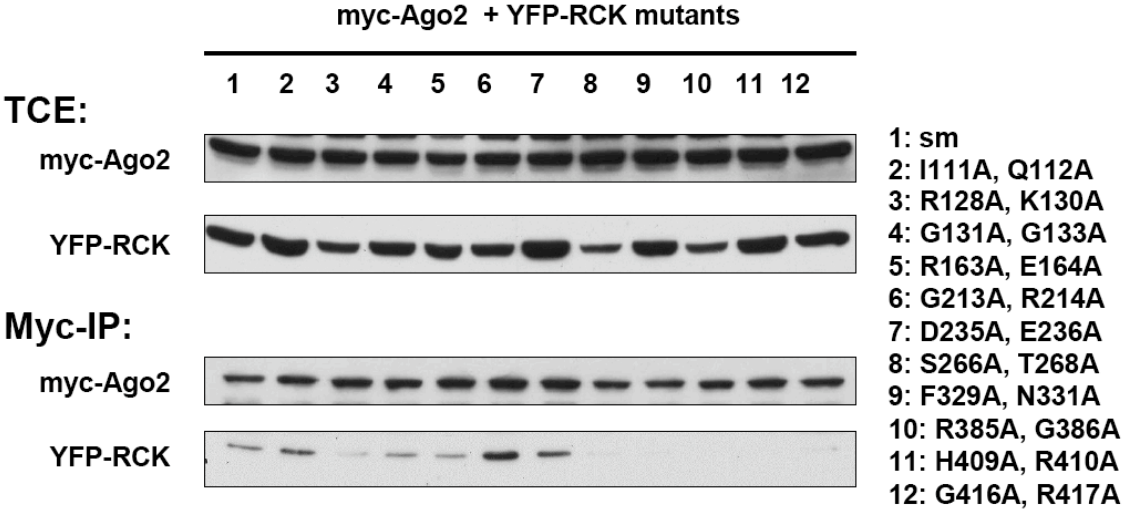
machinery (Fig IV.4B, lane 8-12). This result has also been observed in the immunopurification using HA antibody when YFP-RCK/p54 mutants were co-expressed with HA-tagged Ago2 in HeLa cells (Fig IV.S2).

**DEAD box motif and motif VI are important for the RCK/p54 function in miRNA-mediated translation repression**

Our previous data has shown that RCK/p54 is involved in the miRNA-mediated translation repression. To determine whether the RCK/p54 mutants are deficient for the miRNA-mediated gene silencing, we performed a dual luciferase reporter assay for miRNA function in RCK/p54 depleted cells expressing various exogenous RCK/p54 mutants. The experimental design is outlined in Fig IV.5A. In brief, HeLa cells were co-transfected with perfect matched siRCK or mismatched siRCK and YFP-RCK-wt or mutants. Endogenous RCK/p54 was depleted using siRCKpm while exogenous siRNA-resistant RCK/p54 was expressed in HeLa cells. At 24 h post transfection, HeLa cells were subsequently transfected with miRNA-reporter constructs harboring 4 x bulged CXCR4 siRNA target sites in the 3'-UTR of *Renilla reniformis* luciferase (RL) mRNA, in the absence or presence of 25 nM CXCR4 siRNA. In this system, bulged-containing sequences are targets for translation suppression by miRISC. At 24 h post-transfection, cells were harvested and RL activities were analyzed. RL signals were normalized to GL signals from cells co-transfected with pGL3 plasmid as control. Depletion of RCK/p54 without adding any exogenous RCK/p54

(siRCKpm in columns (-) ) released miRNA-mediated gene suppression to ~1.6 fold in comparison with the control (siRCKmm) (Fig IV.5B). A similar result was observed when cells were co-transfected with wt-RCK/p54. However, the release of translation repression by depleting endogenous RCK/p54 was restored in the cells expressing silencing mutant of RCK/p54, which is resistant to siRCK, suggesting that the YFP-RCK/p54sm compensated the translation repression activity of endogenous RCK/p54 in RCK/p54-depleted cells (Fig IV.5B, columns YFP-RCK-sm).

We next tested the series of YFP-RCK/p54 deletion and point mutants in the same experiments. In contrast to the effect of RCK/p54 silencing mutant that restored the miRNA-mediated translation repression, overexpression of C-terminal deletion mutant, DEAD box (D235A), or motif VI (H409A) mutant did not rescue translation repression in RCK-depleted cell. This result indicated that the C-terminal domain, DEAD box and motif VI are critical for the RCK/p54 functions in miRNA-mediated translation repression.

**Figure IV.5. DEAD motif and motif VI are important for the RCK/p54 function in miRNA-mediated translation repression.** (A). Experimental outline to test the function of exogenous RCK mutants. On Day 1, HeLa cells were transfected with perfectly matched siRCK (siRCKpm) or mismatched siRCK (siRCKmm) to deplete the endogenous RCK/p54 and also co-transfected with YFP-RCK mutants to express the engineered exogenous RCK mutants. 24 h post the first transfection, HeLa cells were co-transfected with siCXCR4 and pRL-TK-4XB for the functional assay (dual luciferase assay) of miRNA pathway. (B). Exogenous YFP-smRCK/p54 restores the release of translation repression by silencing RCK/p54 in dual luciferase reporter system, while C-terminal truncated, DEAD motif, or motif VI does not. *R. reniformis* luciferase (RL) activities were measured 24 h after the second transfection and normalized to firefly luciferase (FL) activity as a control. Release of gene repression by siRNA or miRNA is presented as the fold induction of RL compared to FL activity.

**Fig 5**

**A**

HeLa cell transfected with
siRCKpm or siRCKmm
+
YFP-RCKwt or YFP-RCK
mutants

Day1

| Depletion of |
| endogenous RCK/p54 |
| Expression of |
| exogenous RCK/p54 |
| mutants |

↓

Transfected with siCXCR4
and pRL-TK-4XB reporter

Day2

| miRISC reporter assay |

↓

Dual luciferase assay

Day3
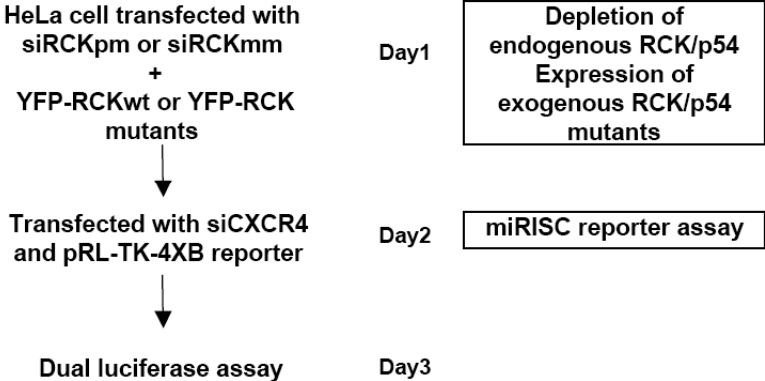
**B**
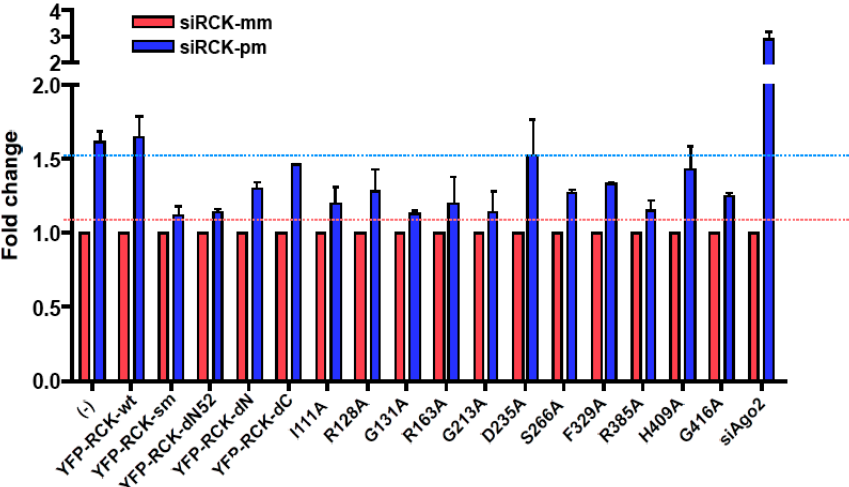
**Recapitulation of miRNA-mediated translation repression in a cell-free system**

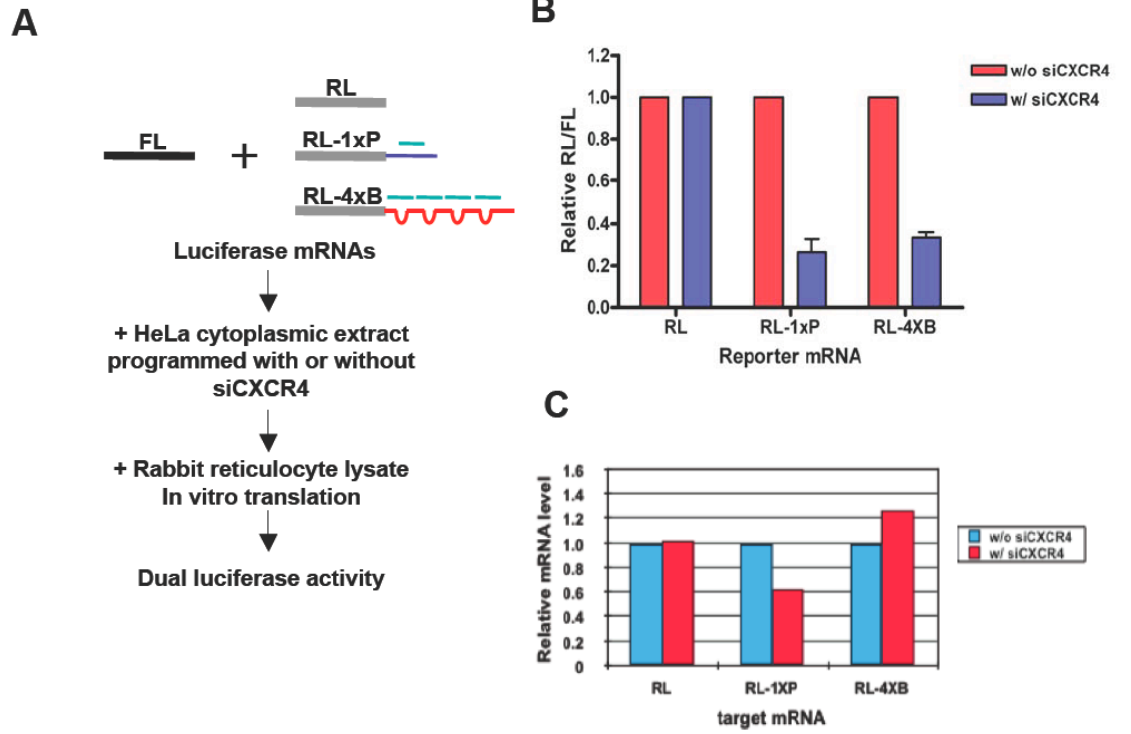To further study the mechanism of RCK/p54 function in miRNA-mediated translation repression, we developed a cell-free system using rabbit reticuloyte lysate to recapitulate the translation repression by miRNA. Target mRNAs, which harbor 1 x perfectly matched or 4 x bulged CXCR4 siRNA target sites in the 3'-UTR of *Renilla reniformis* luciferase (RL), and the control firefly luciferase (FL) mRNA are *in vitro* transcribed, 5' capped and poly-adenylated (see Material and Methods). The *in vitro* mRNA translation assay was carried out with nuclease-treated rabbit reticulocyte lysate (RRL, Promega). HeLa cytoplasmic extract primed with or without siCXCR4 was incubate with reporter mRNA (RL-1xP, or RL-4xB) and control mRNA (FL) at 37˚C for 20min before in vitro translation. As a control experiment, we use RL mRNA without siCXCR4 sites. After that, RRL translation mixture with RNase inhibitor (RNasin, Promega) was added into the reaction and incubated at 30˚C for 90min according to the manufacturer's protocol. The effect of translation repression regulated by miRNA was analyzed by comparing the relative luciferase protein levels in different treatments (Fig IV.6A). Relative RL/FL was calculated by measuring the luciferase activities for both RL and FL using Dual-Luciferase Reporter Assay System and normalized to the value of control RL without target sites. The *in vitro* translation results showed that by adding the HeLa extracts primed with siCXCR4, the levels of target

**Figure IV.6. Recapitulation of miRNA-mediated translation repression in a cell-free system.** (A). Experimental outline of *in vitro* translation assay for siRNA or miRNA-mediated gene silencing*. In vitro* transcribed firefly luciferase (FL) mRNA and *R. reniformis* luciferase (RL) mRNAs harboring one perfectly matched or four bulged siCXCR4 target sites were pre-incubated with HeLa extracts programmed with siCXCR4 at 37°C for 20 min and followed by in vitro translation with rabbit reticulocyte lysate (RRL) at 30°C for 90 min.  (B). *In vitro* silencing effects by siRNA or miRNA from programmed HeLa extracts. HeLa extracts programmed with or without siCXCR4 are pre-incubate with target mRNA before *in vitro* translation by RRL. After the *in vitro* translation, RNAi and miRNA-mediated translation repression efficiencies were analyzed by dual luciferase assay (see Materials and Methods). To quantify the effect of RNAi and miRNA, the ratio of RL/FL signals was normalized to that observed in the absence of siCXCR4. Normalized ratios <1.0 indicates specific gene silencing induced by RNAi or miRNA. (C). RT-qPCR analysis showed miRISC does not induce the decay of target mRNA.

**Fig 6**

**A**

FL  +  RL

RL-1xP

RL-4xB

Luciferase mRNAs

↓

+ HeLa cytoplasmic extract
programmed with or without
siCXCR4

↓

+ Rabbit reticulocyte lysate
In vitro translation

↓

Dual luciferase activity

**B**



**C**

proteins in siRNA or miRNA (RL-1XP or RL-4XB, respectively) reporter were reduced as compared to that with control HeLa extract not primed with siCXCR4 (Fig IV.6B). To confirm that these two reporter mRNAs represent the function of siRNA or miRNA, we compared target mRNA levels before and after adding cell extracts by quantitative RT-PCR. The relative mRNA results corroborate that target mRNA was depleted in siRNA induced silencing (RL-1XP), while the level of miRNA reporter mRNA remained the same in the miRNA-mediated translation repression (Fig IV.6C).

**Depletion of RCK/p54 releases miRNA-mediated translation repression *in vitro*.**

We next examined whether the function of RCK/p54 can be reproduced by using this cell-free system. Experimental design is outlined in Fig IV.7A. HeLa cells transfected with perfect matched or mismatched siRNAs against RCK/p54 are co-transfected with YFP, YFP-RCKsm, or YFP-RCKwt. 24 h post transfection, HeLa cells are primed with siCXCR4 to generate RISC complexes against 3'UTR region of target genes (RL-1xP or RL-4xB). HeLa cytoplasmic extracts were prepared at 24 h post second transfection for the following assay. The depletion of endogenous RCK/p54 and the expression of YFP-RCK in HeLa extracts were analyzed by immunoblot (Fig IV.7B). *In vitro* translation assay was carried out as described previousely. The RL⁄FL signals for RL-1xP and RL-4XB were normalized to those from *Renilla*

**Figure IV.7. RCK/p54 is required for miRNA-mediated translation repression in a cell-free system.** (A).Experimental outline for RCK functional assay in a cell-free translation system. (B). Specific depletion of wild type RCK/p54 in HeLa cells without affecting the expression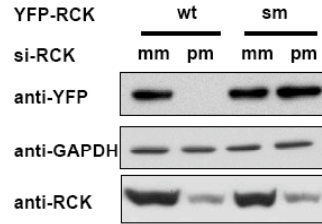 of siRNA-resistant RCK/p54 silencing mutant (YFP-RCKsm). HeLa cells transfected with two YFP-RCK constructs (wt or sm) are co-transfected with siRNA against wild type RCK sequence. 24 h post transfection, HeLa cell extracts were prepared and the TCE were analyzed by immunoblot with antibodies against YFP, GAPDH, and RCK. (C). Depletion of RCK reduces the translation repression *in vitro*, while the RCK-sm can restore translation repression when endogenous RCK is depleted. siCXCR4-programmed HeLa extracts were prepared from the cells pre-treated with siRCKpm or siRCKmm to deplete the endogenous RCK/p54. To test if overexpression of RCK/p54 can induce the translation repression, wild type YFP-RCK/p54 (YFP-RCKwt) or siRNA resistant silence mutant YFP-RCK/p54 (YFP-RCKsm) was co-transfected with siRCK into HeLa cells. 24 h post the first transfection, HeLa cells were transfected with siCXCR4 to program RISC. Cytoplasmic lysates were prepared at 24 h post the second transfection from HeLa cells overexpressing different constructs. Method to analysis the effects of siRNA and miRNA in the in vitro dual luciferase assay has been described above.

**Fig 7**

**A**

HeLa cell transfected with
siRCKpm or siRCKmm
**+**
YFP-RCKwt or YFP-RCKsm

↓

Programmed with siCXCR4

↓

Make cytoplasmic extract

↓

Add into in vitro translation reaction
(RRL and luciferase mRNAs harboring
1XP or 4XB target sites at 3'UTR)
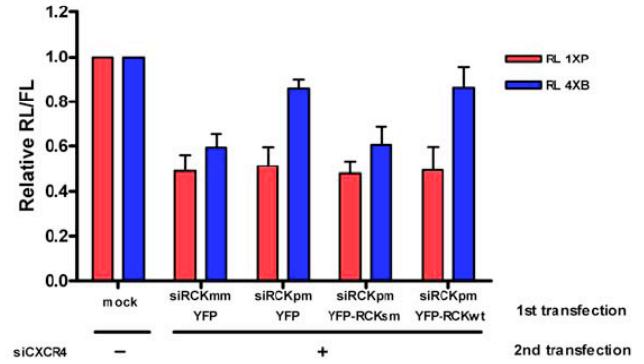
↓

Read dual luciferase activity
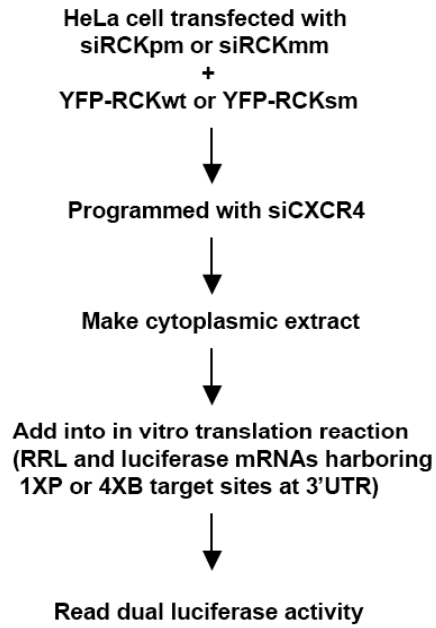
**B**



**C**

luciferase without 3' UTR modification (RL), indicating gene silencing effects controlled by siRNA or miRNA at 3′ UTR of target genes.

In the assays for siRNA reporter system (Fig IV.7C, red bars), depletion of endogenous RCK/p54 did not release the siRNA-mediated gene silencing. However, RCK/p54 depletion significantly released the miRNA-mediated gene silencing (Fig IV.7C, blue bars, siRCKmm vs siRCKpm). The miRNA-mediated translation repression was restored in RCK/p54-depleted cells with the expression of siRCK-resistant YFP-RCK/p54 silencing mutant (YFP-RCKsm). Our results revealed that the miRNA-mediated translation repression specifically requires RCK/p54.

**Depletion of RCK/p54 shifts the endogenous Ago2 distribution in the polysome**

We next performed polysome profiling experiments to test whether depletion of RCK/p54 significantly changes the distribution of RISC and its associated proteins. HeLa cells transfected with siRCKmm or siRCKpm were harvested and the cytoplasmic extracts were prepared in the presence of cyclohexamine, followed by ultracentrifugation in a 15% to 50% sucrose gradient (see Materials and Methods). The gradient was then separated into 20 fractions and the proteins in each fraction are analyzed by immunoblot using anti-Ago2 and anti-RCK/p54 antibodies. In the control experiment, in which HeLa cells were

transfected with siRCKmm, Ago2 is predominately trapped in the low molecular weight fractions, which may be comprised of the translation initiation complex (Fig IV.8A). Interestingly, depletion of RCK/p54 induced Ago2 distribution in the polysome fractions (Fig IV.8B). This result suggested that the function of RCK/p54, together with Ago2 in RISC, is to block the translation of target mRNA at the initiation stage. Depletion of RCK/p54 releases the Ago2 association with initiation complex and allows the translation of target mRNA, even though miRISCs still bind on target mRNA.

**Figure IV.8. Depletion of RCK/p54 shifts the Ago2 distribution from monosome fractions to polysome fractions.** (A) Distribution of Ago2 in polysome profile from HeLa cells transfected with mismatched siRCK (siRCKmm). 10 mg of HeLa cytoplasmic extract was used to analyze the polysome profile (see Material and Methods). One third of the total protein in each fraction was analyzed by immunoblot using anti-Ago2 and anti-RCK/p54 antibodies. The majority of Ago2 was detected in the monosome fractions. TCE lane represents 50ug of TCE as the control. (B) Polysome distribution of Ago2 in RCK-depleted cells.

**Fig 8**



A

50%                                                    15%

anti-Ago2

anti-RCK

50ug TCE

B

50%                                                    15%

anti-Ago2

anti-RCK

50ug TCE
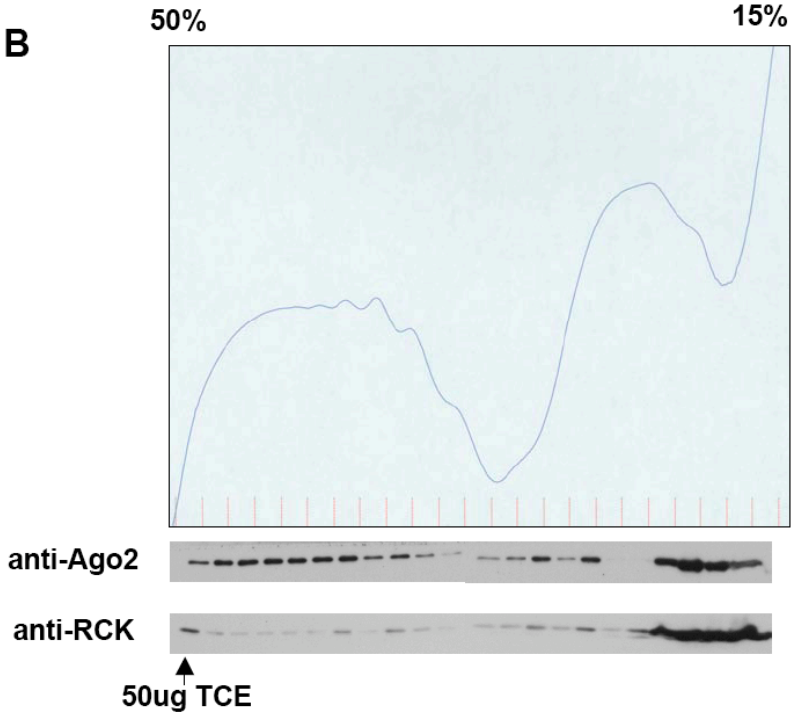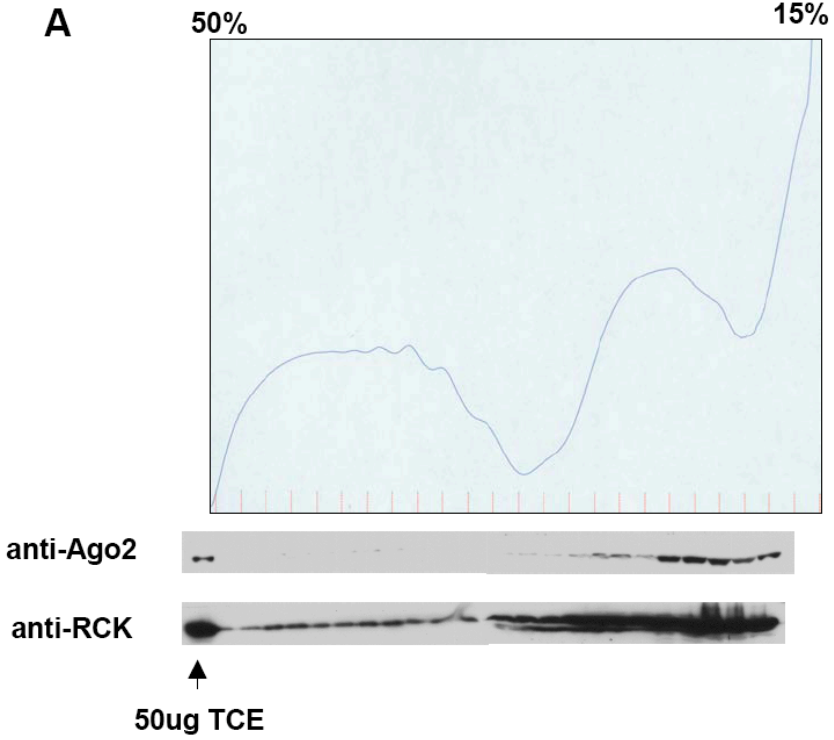
**DISCUSSION**

In this study, we have investigated the functional motifs for RCK/p54 regulation of translation repression. By systematically analyzing RCK/p54 deletion and point mutants, we showed that deletion of C-terminal domain, as well as mutations at the DEAD, SAT, V and VI motifs, abolished the P-body localization role of RCK/p54. We performed immunoprecipitation experiments to show that the C-terminal domain of RCK/p54 is involved in the interaction with Ago2. We also developed a cell-free system to recapitulate miRNA-mediated silencing in vitro and confirmed the requirement of RCK/p54 in the miRNA pathway. Additionally, we performed polysome profiling experiments to analyze the protein components in polysome fractions from RCK/p54-depleted cells. Our results showed that depletion of endogenous RCK/p54 induced the shift of Ago2 distribution from initiation complex to polysome. These data suggested that RCK/p54 facilitates the miRNA-mediated gene silencing at translation initiation stage.

RCK/p54 is a member of a highly conserved DEAD-box protein family and its homologues have been identified in yeast, Drosophila, and worms (Weston and Sommerville 2006). Sequence analysis of DEAD-box proteins indicates that they contain eight to nine conserved motifs (Fig IV.1A) (Weston and Sommerville 2006). Crystal studies on the yeast homologue of RCK/p54, Dhh1p, and the N-terminal core domain of human RCK/p54 revealed that motif II (DEAD) and motif

II (SAT) are important for the ATP binding, whereas motifs I, V, and VI contribute to form a positively charged patch on the surface of protein as a conserved RNA-binding pocket (Cheng et al. 2005; Matsui et al. 2006).

Our subcellular localization data showed that DEAD-box, SAT and motifs V and VI are important for the RCK/p54 localization at P-body (Fig IV.2, Fig IV.3). Since the P-body is the place where mRNAs undergo decapping and decay, we therefore hypothesized that these domains are required for the downstream function of RCK/p54 in mRNA processing at P-body, and the phenomena requires RNA association with RCK/p54. Interestingly, the N-terminal deletion mutant that localizes to the nucleus, provides evidence that the N-terminal contains a nuclear export signal as suggested in the Xenopus Xp54 (Weston and Sommerville 2006), and that RCK/p54 may shuttle between nucleus and cytoplasm for its physiological function.

Since we have shown that RCK/p54 directly interacts with Ago2 in RISC, the second question we wanted to ask is whether mutations in the conserved region of RCK/p54 will abolish its interaction with RISC. We determined the Ago2-interacting domain of RCK/p54 by immunoprecipitation of myc-Ago2. The C-terminal deletion mutant cannot be co-purified with Ago2, suggesting that Ago2 interacts with the C-terminal domain of RCK/p54. However, unlike the subcellular localization results in which C-terminal mutants localized to P-bodies, all the C-terminal point mutants and DEAD motif mutant lost the association with Ago2. This result suggested that the C-terminal is required for this interaction. We

hypothesize that the mutations at any conserved motif in the C-terminal region that we have studied may induce the conformational change of the RCK/p54 protein, resulting in the loss of RISC interaction. However, the specific Ago2 interacting motif located in the C-terminal of RCK/p54 is still not well defined.

The reporter assay for miRISC activity in cells expressing RCK/p54 mutants has provided us more details about the function for each motif of RCK/p54. Consistent with our previous results, depletion of endogenous RCK/p54 inhibits the miRNA-mediated translation repression to ~1.6 fold (Chu and Rana 2006). Based on this phenomenon, we overexpressed each RCK/p54 mutant in RCK-depleted cells to determine which mutants failed to restore the translation repression. Our data clearly showed the C-terminal and DEAD motif are important for facilitating the RISC function (Fig IV.5B), suggested that the function of RCK/p54, together with the P-body localization feature, may require ATP binding for the helicase activity.

To dissect the mechanism of RCK/p54 function in miRNA-mediated translation repression, a biochemical approach using cell-free system is necessary and can provide us more details about how RCK/p54 and miRISC function. We therefore established an *in vitro* translation assay for the miRNA reporter system to recapitulate the phenomena of gene silencing. Using the dual luciferase reporter assay that is similar to the well-established *in vivo* dual luciferase assay, we successfully reproduced the RISC-mediated gene silencing in the combination of RRL and HeLa cell extract primed with siRNA (Fig IV.6).

We further test the RCK/p54 function in the cell-free system and confirmed our previous founding that RCK/p54 is indeed required in the miRNA-mediated gene silencing (Fig IV.7).

How does miRNA function in post-transciptional silencing? Recently, three hypotheses have been proposed based on the evidences from different studies. One of the explanations is that the miRNA regulate the translation of target mRNA at the initiation stage. The supporting evidence includes: (1). Studies of human cells where translation initiation was inhibited by endogenous let-7 miRNA or by Ago2 tethered at the 3'UTR of reporter mRNA showed that cap-independent translation by IRES resists miRNA-mediated gene silencing (Pillai et al. 2005). (2). The m7Gppp-cap and poly(A) tail of target mRNA are required for the miRNA-mediated repression in the cell-free systems, suggesting that miRNA mediates the inhibition of translation initiation (Wang et al. 2006; Mathonnet et al. 2007; Thermann and Hentze 2007; Wakiyama et al. 2007). (3). Ago2 contains a cap-binding motif (MC) which is similar to that of eIF4E, a translation initiation factor. Mutations in the MC domain of Ago2 abolish the cap-binding ability of Ago2 as well as its function in translation repression (Kiriakidou et al. 2007).

Our results of Ago2 association with polysomes in the RCK/p54-depleted cells revealed an agreement to that RCK/p54 mediated the miRNA-induced silencing at the initiation stage. In cells that express RCK/p54 normally, the interaction of RCK with Ago2 occurs in the low molecular weight fractions, suggesting that the majority of Ago2, along with the target mRNAs that are bound

by RISC, are trapped at the initiation complex and cannot continue the translation. Depletion of RCK/p54 resulted in the distribution of Ago2 in translating mRNA complexes (polysome fractions), suggesting that RCK/p54 facilitates miRISC residence at the initiation step, when miRNA recognize the target mRNA. Since RCK/p54 has been shown to interact with eIF4E, a cap-binding protein, we hypothesized that interaction RCK/p54 with Ago2 can ensure that Ago2 interacts with the 5'cap structure of target mRNA and prevents translation at the initiation stage. This hypothesis needs to be explored further by more experiments such as Northern blot analysis of miRNA and its coupled target mRNA in the polysome profiles of RCK/p54-depleted cells, or by using the RCK/p54 mutant constructs to provide details of this mechanism in follow up studies.

## Materials and Methods

### Construction of YFP-RCK/p54 silenced mutant

siRNA-resistant YFP-RCK/p54 mutant was generated through site-directed mutagenesis by a two-step PCR amplification of coding sequence and followed by cloning into the BglII and SalI sites of pEYFP-C1.

The sequences of PCR primers for siRNA-resistant silencing mutant are: FW: 5'-CCCATTTGCAGAAGCCGTACGAAATTAACCTGATGGAGGAAC-3'; RV: 5'-GTTCCTCCATCAGGTTAATTTCGTACGGCTTCTGCAAATGGG-3'. The sequences of PCR primers for deletion and point mutants are list in Appendix Table 1.

### Preparation of in vitro transcripts

pRL-TK reporter vector (RL) was linearized with HindIII and XbaI. pRL-TK reporter vectors harboring one perfect matched siCXCR4 site (RL-1xP) or four bulged siCXCR4 sites (RL-4XB) were linearized with HindIII and ApaI to generate the template for T7 transcription. Control reporter DNA encoding firefly luciferase (FL) with T7 promoter was generated by PCR using pGL3 vector as the template. Large scale of RL, RL-1xP, RL-4XB and FL mRNAs were transcribed in vitro and capped by T7 mMESSAGE mMACHINE™ transcription kit (Ambion), followed by polyadenylation using Poly(A) tailing kit (Ambion) and finally purified with a MEGAclear kit (Ambion).

**Transfection and preparation of HeLa cytoplasmic extract**

HeLa cells plated on the 100mm tissue culture dishes are co-transfected with siRNAs against RCK/p54 (perfect-matched or mismatched) and the expression constructs encoding RCK/p54 wild type (YFP-RCKwt) or silenced mutant (YFP-RCKsm). 24 hr post transfection, HeLa cells are transfected again with the siRNA against CXCR4. HeLa cytoplasmic extract were harvested at 24 h after the second transfecton by the method as described previously.

**Cell-free RISC activity assay**

The *in vitro* mRNA translation assay was carried out with nuclease-treated rabbit reticulocyte lysate (RRL, Promega). 60ug HeLa cytoplasmic extract primed with or without siCXCR4 was incubate with 0.8 ug reporter mRNA (RL, RL-1xP, and RL-4xB) and 0.5ug control mRNA (FL) at 37°C for 20min before in vitro translation. After that, 17ul RRL translation mixture 0.5ul of amino acid mix and 0.5ul RNase inhibitor (RNasin, Promega) was added into the reaction and incubated at 30°C for 90min according to the manufacturer's protocol. The effect of translation repression regulated by miRNA was analyzed by comparing the relative luciferase protein levels in different treatments. Relative RL/FL was calculated by measuring the luciferase activities for both RL and FL using Dual-Luciferase Reporter Assay System (Promega).

**Figure IV.S1 C-terminal deleted RCK/p54 does not localize to P-body while the endogenous Ago2 still localizes P-bodies.** Subcellular localization of YFP-RCK/p54 mutants. HeLa cells transfected with YFP-RCK/p54 constructs containing point mutations at different conserved motif were fixed 24 h post transfection. Localization of RCK/p54 mutants was visualized by imaging the YFP fluorescence, and the localization of endogenous Ago2 was detected by the immunofluorescence staining by using anti-Ago2 antibody (Wako).

**Fig S1**
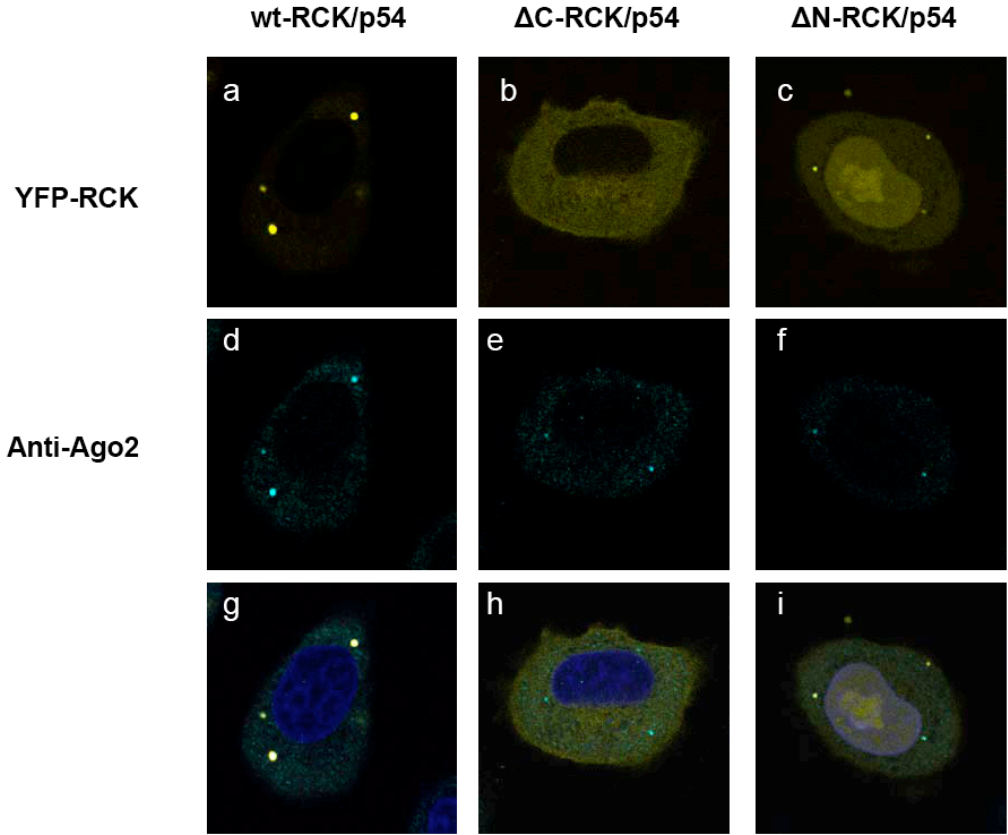
**Figure IV.S2 C-terminal and DEAD-motif of RCK/p54 are required for the interaction with Ago2.** Immunoprecipitation and immunoblot analysis of RCK/p54 truncated mutants. Total cell extracts from HeLa cells co-expressing HA-Ago2 and YFP-RCK/p54 mutants were prepared and followed by immunoprecipitation (IP). TCE and anti-HA IPs were analyzed by immunoblot as described previously.

# Fig S2



```
      0   1   2   3   4   5   6   7   8   9  10  11  12
```

HA-Ago2

YFP-RCK                                                    TCE

HA-Ago2                                                    HA-IPed
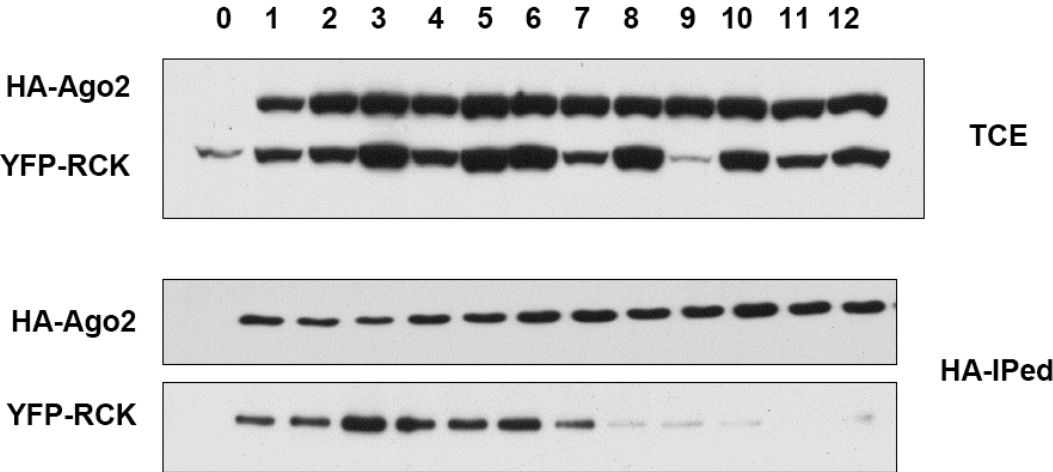
YFP-RCK

0: YFP-RCKsm + HA vector
1: sm
2: I111A, Q112A
3: R128A, K130A
4: G131A, G133A
5: R163A, E164A
6: G213A, R214A                    + HA-Ago2
7: D235A, E236A
8: S266A, T268A
9: F329A, N331A
10: R385A, G386A
11: H409A, R410A
12: G416A, R417A

# REFERENCES

Akao, Y., O. Marukawa, et al. (1995). "The rck/p54 candidate proto-oncogene product is a 54-kilodalton D-E-A-D box protein differentially expressed in human and mouse tissues." Cancer Res **55**(15): 3444-9.

Amarzguioui, M., T. Holen, et al. (2003). "Tolerance for mutations and chemical modifications in a siRNA." Nucleic Acids Res **31**(2): 589-95.

Amarzguioui, M. and H. Prydz (2004). "An algorithm for selection of functional siRNA sequences." Biochem Biophys Res Commun **316**(4): 1050-8.

Ambros, V. (2004). "The functions of animal microRNAs." Nature **431**(7006): 350-5.

Ameres, S. L., J. Martinez, et al. (2007). "Molecular Basis for Target RNA Recognition and Cleavage by Human RISC." Cell **130**(1): 101-12.

Andrei, M. A., D. Ingelfinger, et al. (2005). "A role for eIF4E and eIF4E-transporter in targeting mRNPs to mammalian processing bodies." Rna **11**(5): 717-27.

Aravin, A. A., N. M. Naumova, et al. (2001). "Double-stranded RNA-mediated silencing of genomic tandem repeats and transposable elements in the D. melanogaster germline." Curr Biol **11**(13): 1017-27.

Aravin, A. A., R. Sachidanandam, et al. (2007). "Developmentally regulated piRNA clusters implicate MILI in transposon control." Science **316**(5825): 744-7.

Bagga, S., J. Bracht, et al. (2005). "Regulation by let-7 and lin-4 miRNAs results in target mRNA degradation." Cell **122**(4): 553-63.

Bartel, D. P. (2004). "MicroRNAs: genomics, biogenesis, mechanism, and function." Cell **116**(2): 281-97.

Bastiaens, P. I., I. V. Majoul, et al. (1996). "Imaging the intracellular trafficking and state of the AB5 quaternary structure of cholera toxin." Embo J **15**(16): 4246-53.

Baulcombe, D. (2004). "RNA silencing in plants." Nature **431**(7006): 356-63.

Behm-Ansmant, I., J. Rehwinkel, et al. (2006). "mRNA degradation by miRNAs and GW182 requires both CCR4:NOT deadenylase and DCP1:DCP2 decapping complexes." Genes Dev **20**(14): 1885-98.

Bernstein, E., A. A. Caudy, et al. (2001). "Role for a bidentate ribonuclease in the initiation step of RNA interference." Nature **409**(6818): 363-6.

Bhattacharyya, S. N., R. Habermacher, et al. (2006). "Relief of microRNA-mediated translational repression in human cells subjected to stress." Cell **125**(6): 1111-24.

Birmingham, A., E. Anderson, et al. (2007). "A protocol for designing siRNAs with high functionality and specificity." Nat Protoc **2**(9): 2068-78.

Bohnsack, M. T., K. Czaplinski, et al. (2004). "Exportin 5 is a RanGTP-dependent dsRNA-binding protein that mediates nuclear export of pre-miRNAs." Rna **10**(2): 185-91.

Bohnsack, M. T., K. Regener, et al. (2002). "Exp5 exports eEF1A via tRNA from nuclei and synergizes with other transport pathways to confine translation to the cytoplasm." Embo J **21**(22): 6205-15.

Braasch, D. A., S. Jensen, et al. (2003). "RNA interference in mammalian cells by chemically-modified RNA." Biochemistry **42**(26): 7967-75.

Brennecke, J., A. A. Aravin, et al. (2007). "Discrete small RNA-generating loci as master regulators of transposon activity in Drosophila." Cell **128**(6): 1089-103.

Brennecke, J., A. Stark, et al. (2005). "Principles of microRNA-target recognition." PLoS Biol **3**(3): e85.

Brown, K. M., C. Y. Chu, et al. (2005). "Target accessibility dictates the potency of human RISC." Nat Struct Mol Biol **12**(5): 469-70.

Carmell, M. A., A. Girard, et al. (2007). "MIWI2 is essential for spermatogenesis and repression of transposons in the mouse male germline." Dev Cell **12**(4): 503-14.

Carmell, M. A. and G. J. Hannon (2004). "RNase III enzymes and the initiation of gene silencing." Nat Struct Mol Biol **11**(3): 214-8.

Carrington, J. C. (2005). "Small RNAs and Arabidopsis. A fast forward look." Plant Physiol **138**(2): 565-6.

Caudy, A. A., M. Myers, et al. (2002). "Fragile X-related protein and VIG associate with the RNA interference machinery." Genes Dev **16**(19): 2491-6.

Chendrimada, T. P., K. J. Finn, et al. (2007). "MicroRNA silencing through RISC recruitment of eIF6." Nature.

Chendrimada, T. P., R. I. Gregory, et al. (2005). "TRBP recruits the Dicer complex to Ago2 for microRNA processing and gene silencing." Nature **436**(7051): 740-4.

Cheng, Z., J. Coller, et al. (2005). "Crystal structure and functional analysis of DEAD-box protein Dhh1p." RNA **11**(8): 1258-70.

Chiu, Y.-L. and T. M. Rana (2002a). "RNAi in human cells: basic structural and functional features of small interfering RNA." Molecular Cell **10**: 549-561.

Chiu, Y. L., C. U. Dinesh, et al. (2005). "Dissecting RNA-interference pathway with small molecules." Chem Biol **12**(6): 643-8.

Chiu, Y. L. and T. M. Rana (2002b). "RNAi in human cells: basic structural and functional features of small interfering RNA." Mol Cell **10**(3): 549-61.

Chiu, Y. L. and T. M. Rana (2003). "siRNA function in RNAi: a chemical modification analysis." Rna **9**(9): 1034-48.

Chu, C. Y. and T. M. Rana (2006). "Translation repression in human cells by microRNA-induced gene silencing requires RCK/p54." PLoS Biol **4**(7): e210.

Chu, C. Y. and T. M. Rana (2007). "Small RNAs: regulators and guardians of the genome." J Cell Physiol **213**(2): 412-9.

Chung, W. J., K. Okamura, et al. (2008). "Endogenous RNA interference provides a somatic defense against Drosophila transposons." <u>Curr Biol</u> **18**(11): 795-802.

Clegg, R. M. (2002). "FRET tells us about proximities, distances, orientations and dynamic properties." <u>J Biotechnol.</u> **82**(3): 177-9.

Coller, J. and R. Parker (2004). "Eukaryotic mRNA decapping." <u>Annu Rev Biochem</u> **73**: 861-90.

Coller, J. and R. Parker (2005). "General translational repression by activators of mRNA decapping." <u>Cell</u> **122**(6): 875-86.

Coller, J. M., M. Tucker, et al. (2001). "The DEAD box helicase, Dhh1p, functions in mRNA decapping and interacts with both the decapping and deadenylase complexes." <u>Rna</u> **7**(12): 1717-27.

Cougot, N., S. Babajko, et al. (2004). "Cytoplasmic foci are sites of mRNA decay in human cells." <u>J Cell Biol</u> **165**(1): 31-40.

Cox, D. N., A. Chao, et al. (1998). "A novel class of evolutionarily conserved genes defined by piwi are essential for stem cell self-renewal." <u>Genes Dev</u> **12**(23): 3715-27.

Czauderna, F., M. Fechtner, et al. (2003). "Structural variations and stabilising modifications of synthetic siRNAs in mammalian cells." <u>Nucleic Acids Res</u> **31**(11): 2705-16.

Czech, B., C. D. Malone, et al. (2008). "An endogenous small interfering RNA pathway in Drosophila." <u>Nature</u> **453**(7196): 798-802.

Deng, W. and H. Lin (2002). "miwi, a murine homolog of piwi, encodes a cytoplasmic protein essential for spermatogenesis." Dev Cell **2**(6): 819-30.

Ding, L., A. Spencer, et al. (2005). "The developmental timing regulator AIN-1 interacts with miRISCs and may target the argonaute protein ALG-1 to cytoplasmic P bodies in C. elegans." Mol Cell **19**(4): 437-47.

Doench, J. G., C. P. Petersen, et al. (2003). "siRNAs can function as miRNAs." Genes Dev **17**(4): 438-42.

Doench, J. G. and P. A. Sharp (2004). "Specificity of microRNA target selection in translational repression." Genes Dev **18**(5): 504-11.

Elbashir, S. M., J. Harborth, et al. (2001a). "Duplexes of 21-nucleotide RNAs mediate RNA interference in cultured mammalian cells." Nature **411**(6836): 494-8.

Elbashir, S. M., W. Lendeckel, et al. (2001b). "RNA interference is mediated by 21- and 22-nucleotide RNAs." Genes Dev **15**(2): 188-200.

Elbashir, S. M., J. Martinez, et al. (2001c). "Functional anatomy of siRNAs for mediating efficient RNAi in Drosophila melanogaster embryo lysate." Embo J **20**(23): 6877-88.

Enright, A. J., B. John, et al. (2003). "MicroRNA targets in Drosophila." Genome Biol **5**(1): R1.

Eulalio, A., I. Behm-Ansmant, et al. (2007a). "P bodies: at the crossroads of post-transcriptional pathways." Nat Rev Mol Cell Biol **8**(1): 9-22.

Eulalio, A., I. Behm-Ansmant, et al. (2007b). "P-body formation is a consequence, not the cause, of RNA-mediated gene silencing." Mol Cell Biol **27**(11): 3970-81.

Ferraiuolo, M. A., S. Basak, et al. (2005). "A role for the eIF4E-binding protein 4E-T in P-body formation and mRNA decay." J Cell Biol **170**(6): 913-24.

Ferraiuolo, M. A., C. S. Lee, et al. (2004). "A nuclear translation-like factor eIF4AIII is recruited to the mRNA during splicing and functions in nonsense-mediated decay." Proc Natl Acad Sci U S A **101**(12): 4118-23.

Filipowicz, W. (2005). "RNAi: the nuts and bolts of the RISC machine." Cell **122**(1): 17-20.

Fire, A., S. Xu, et al. (1998). "Potent and specific genetic interference by double-stranded RNA in Caenorhabditis elegans." Nature **391**(6669): 806-11.

Förstemann, K., M. D. Horwich, et al. (2007). "Drosophila microRNAs Are Sorted into Functionally Distinct Argonaute Complexes after Production by Dicer-1." Cell **130**(2): 287-97.

Forstemann, K., Y. Tomari, et al. (2005). "Normal microRNA maturation and germ-line stem cell maintenance requires Loquacious, a double-stranded RNA-binding domain protein." PLoS Biol **3**(7): e236.

Gebauer, F. and M. W. Hentze (2004). "Molecular mechanisms of translational control." Nat Rev Mol Cell Biol **5**(10): 827-35.

Ghildiyal, M., H. Seitz, et al. (2008). "Endogenous siRNAs derived from transposons and mRNAs in Drosophila somatic cells." Science **320**(5879): 1077-81.

Golden, D. E., V. R. Gerbasi, et al. (2008). "An inside job for siRNAs." Mol Cell **31**(3): 309-12.

Gregory, R. I., T. P. Chendrimada, et al. (2005). "Human RISC Couples MicroRNA Biogenesis and Posttranscriptional Gene Silencing." Cell **123**(4): 631-40.

Grimson, A., K. K. Farh, et al. (2007). "MicroRNA targeting specificity in mammals: determinants beyond seed pairing." Mol Cell **27**(1): 91-105.

Grun, D., Y. L. Wang, et al. (2005). "microRNA target predictions across seven Drosophila species and comparison to mammalian targets." PLoS Comput Biol **1**(1): e13.

Gunawardane, L. S., K. Saito, et al. (2007). "A slicer-mediated mechanism for repeat-associated siRNA 5' end formation in Drosophila." Science **315**(5818): 1587-90.

Haase, A. D., L. Jaskiewicz, et al. (2005). "TRBP, a regulator of cellular PKR and HIV-1 virus expression, interacts with Dicer and functions in RNA silencing." EMBO Rep **6**(10): 961-7.

Haley, B. and P. D. Zamore (2004). "Kinetic analysis of the RNAi enzyme complex." Nat Struct Mol Biol **11**(7): 599-606.

Hamilton, A., O. Voinnet, et al. (2002). "Two classes of short interfering RNA in RNA silencing." Embo J **21**(17): 4671-9.

Hammond, S. M., S. Boettcher, et al. (2001). "Argonaute2, a link between genetic and biochemical analyses of RNAi." Science **293**(5532): 1146-50.

Hartig, J. V., Y. Tomari, et al. (2007). "piRNAs--the ancient hunters of genome invaders." Genes Dev **21**(14): 1707-13.

Hashimoto, K., Y. Nakagawa, et al. (2001). "Co-overexpression of DEAD box protein rck/p54 and c-myc protein in human colorectal adenomas and the relevance of their expression in cultured cell lines." Carcinogenesis **22**(12): 1965-70.

He, L. and G. J. Hannon (2004). "MicroRNAs: small RNAs with a big role in gene regulation." Nat Rev Genet **5**(7): 522-31.

He, L., J. M. Thomson, et al. (2005). "A microRNA polycistron as a potential human oncogene." Nature **435**(7043): 828-33.

Holcik, M. and N. Sonenberg (2005). "Translational control in stress and apoptosis." Nat Rev Mol Cell Biol **6**(4): 318-27.

Horwich, M. D., C. Li, et al. (2007). "The Drosophila RNA Methyltransferase, DmHen1, Modifies Germline piRNAs and Single-Stranded siRNAs in RISC." Curr Biol **17**(14): 1265-72.

Houwing, S., L. M. Kamminga, et al. (2007). "A role for Piwi and piRNAs in germ cell maintenance and transposon silencing in Zebrafish." Cell **129**(1): 69-82.

Humphreys, D. T., B. J. Westman, et al. (2005). "MicroRNAs control translation initiation by inhibiting eukaryotic initiation factor 4E/cap and poly(A) tail function." Proc Natl Acad Sci U S A.

Hutvagner, G., M. J. Simard, et al. (2004). "Sequence-specific inhibition of small RNA function." PLoS Biol 2(4): E98.

Hutvagner, G. and P. D. Zamore (2002). "A microRNA in a multiple-turnover RNAi enzyme complex." Science 297(5589): 2056-60.

Jackson, A. L., S. R. Bartz, et al. (2003). "Expression profiling reveals off-target gene regulation by RNAi." Nat Biotechnol 21(6): 635-7.

Jackson, A. L., J. Burchard, et al. (2006). "Position-specific chemical modification of siRNAs reduces "off-target" transcript silencing." Rna 12(7): 1197-205.

Jakymiw, A., S. Lian, et al. (2005). "Disruption of GW bodies impairs mammalian RNA interference." Nat Cell Biol 7(12): 1267-74.

John, B., A. J. Enright, et al. (2004). "Human MicroRNA targets." PLoS Biol 2(11): e363.

Johnson, S. M., H. Grosshans, et al. (2005). "RAS is regulated by the let-7 microRNA family." Cell 120(5): 635-47.

Kawamura, Y., K. Saito, et al. (2008). "Drosophila endogenous small RNAs bind to Argonaute 2 in somatic cells." Nature 453(7196): 793-7.

Kenworthy, A. K. and M. Edidin (1998). "Distribution of a glycosylphosphatidylinositol-anchored protein at the apical surface of

MDCK cells examined at a resolution of <100 A using imaging fluorescence resonance energy transfer." J Cell Biol **142**(1): 69-84.

Khvorova, A., A. Reynolds, et al. (2003). "Functional siRNAs and miRNAs exhibit strand bias." Cell **115**(2): 209-16.

Kim, D. H., M. A. Behlke, et al. (2005). "Synthetic dsRNA Dicer substrates enhance RNAi potency and efficacy." Nat Biotechnol **23**(2): 222-6.

Kim, V. N. (2005). "MicroRNA biogenesis: coordinated cropping and dicing." Nat Rev Mol Cell Biol **6**(5): 376-85.

Kiriakidou, M., P. T. Nelson, et al. (2004). "A combined computational-experimental approach predicts human microRNA targets." Genes Dev **18**(10): 1165-78.

Kiriakidou, M., G. S. Tan, et al. (2007). "An mRNA m(7)G Cap Binding-like Motif within Human Ago2 Represses Translation." Cell **129**(6): 1141-51.

Kirino, Y. and Z. Mourelatos (2007). "Mouse Piwi-interacting RNAs are 2'-O-methylated at their 3' termini." Nat Struct Mol Biol **14**(4): 347-8.

Krek, A., D. Grun, et al. (2005). "Combinatorial microRNA target predictions." Nat Genet **37**(5): 495-500.

Kuramochi-Miyagawa, S., T. Kimura, et al. (2004). "Mili, a mammalian member of piwi family gene, is essential for spermatogenesis." Development **131**(4): 839-49.

Kuramochi-Miyagawa, S., T. Kimura, et al. (2001). "Two mouse piwi-related genes: miwi and mili." Mech Dev **108**(1-2): 121-33.

Ladomery, M., E. Wade, et al. (1997). "Xp54, the Xenopus homologue of human RNA helicase p54, is an integral component of stored mRNP particles in oocytes." Nucleic Acids Res **25**(5): 965-73.

Lall, S., D. Grun, et al. (2006). "A genome-wide map of conserved microRNA targets in C. elegans." Curr Biol **16**(5): 460-71.

Lee, R. C., R. L. Feinbaum, et al. (1993). "The C. elegans heterochronic gene lin-4 encodes small RNAs with antisense complementarity to lin-14." Cell **75**(5): 843-54.

Lee, Y., I. Hur, et al. (2006). "The role of PACT in the RNA silencing pathway." Embo J **25**(3): 522-32.

Lee, Y. S., K. Nakahara, et al. (2004). "Distinct roles for Drosophila Dicer-1 and Dicer-2 in the siRNA/miRNA silencing pathways." Cell **117**(1): 69-81.

Lewis, B. P., C. B. Burge, et al. (2005). "Conserved seed pairing, often flanked by adenosines, indicates that thousands of human genes are microRNA targets." Cell **120**(1): 15-20.

Lewis, B. P., I. H. Shih, et al. (2003). "Prediction of mammalian microRNA targets." Cell **115**(7): 787-98.

Liu, J., M. A. Carmell, et al. (2004). "Argonaute2 is the catalytic engine of mammalian RNAi." Science **305**(5689): 1437-41.

Liu, J., F. V. Rivas, et al. (2005a). "A role for the P-body component GW182 in microRNA function." Nat Cell Biol **7**(12): 1261-6.

Liu, J., M. A. Valencia-Sanchez, et al. (2005b). "MicroRNA-dependent
    localization of targeted mRNAs to mammalian P-bodies." <u>Nat Cell Biol</u>
    **7**(7): 719-23.

Lu, J., G. Getz, et al. (2005). "MicroRNA expression profiles classify human
    cancers." <u>Nature</u> **435**(7043): 834-8.

Lund, E., S. Guttinger, et al. (2004). "Nuclear export of microRNA precursors."
    <u>Science</u> **303**(5654): 95-8.

Ma, J. B., Y. R. Yuan, et al. (2005). "Structural basis for 5'-end-specific
    recognition of guide RNA by the A. fulgidus Piwi protein." <u>Nature</u>
    **434**(7033): 666-70.

Maroney, P. A., Y. Yu, et al. (2006). "Evidence that microRNAs are associated
    with translating messenger RNAs in human cells." <u>Nat Struct Mol Biol</u>
    **13**(12): 1102-7.

Martinez, J. and T. Tuschl (2004). "RISC is a 5' phosphomonoester-producing
    RNA endonuclease." <u>Genes Dev</u> **18**(9): 975-80.

Mathonnet, G., M. R. Fabian, et al. (2007). "MicroRNA Inhibition of Translation
    Initiation in Vitro by Targeting the Cap-Binding Complex eIF4F " <u>Science</u>.

Matranga, C., Y. Tomari, et al. (2005). "Passenger-strand cleavage facilitates
    assembly of siRNA into Ago2-containing RNAi enzyme complexes." <u>Cell</u>
    **123**(4): 607-20.

Matsui, T., K. Hogetsu, et al. (2006). "Structural insight of human DEAD-box protein rck/p54 into its substrate recognition with conformational changes." Genes Cells **11**(4): 439-52.

Meister, G., M. Landthaler, et al. (2004a). "Sequence-specific inhibition of microRNA- and siRNA-induced RNA silencing." Rna **10**(3): 544-50.

Meister, G., M. Landthaler, et al. (2004b). "Human Argonaute2 Mediates RNA Cleavage Targeted by miRNAs and siRNAs." Mol Cell **15**(2): 185-97.

Meister, G. and T. Tuschl (2004). "Mechanisms of gene silencing by double-stranded RNA." Nature **431**(7006): 343-9.

Mello, C. C. and D. Conte (2004). "Revealing the world of RNA interference." Nature **431**(7006): 338-42.

Minshall, N. and N. Standart (2004). "The active form of Xp54 RNA helicase in translational repression is an RNA-mediated oligomer." Nucleic Acids Res **32**(4): 1325-34.

Minshall, N., G. Thom, et al. (2001). "A conserved role of a DEAD box helicase in mRNA masking." Rna **7**(12): 1728-42.

Miyaji, K., Y. Nakagawa, et al. (2003). "Overexpression of a DEAD box/RNA helicase protein, rck/p54, in human hepatocytes from patients with hepatitis C virus-related chronic hepatitis and its implication in hepatocellular carcinogenesis." J Viral Hepat **10**(4): 241-8.

Miyawaki, A. and R. Y. Tsien (2000). "Monitoring protein conformations and interactions by fluorescence resonance energy transfer between mutants of green fluorescent protein." Methods Enzymol **327**: 472-500.

Mochizuki, K., N. A. Fine, et al. (2002). "Analysis of a piwi-related gene implicates small RNAs in genome rearrangement in tetrahymena." Cell **110**(6): 689-99.

Morrissey, D. V., J. A. Lockridge, et al. (2005). "Potent and persistent in vivo anti-HBV activity of chemically modified siRNAs." Nat Biotechnol **23**(8): 1002-7.

Nakagawa, Y., H. Morikawa, et al. (1999). "Overexpression of rck/p54, a DEAD box protein, in human colorectal tumours." Br J Cancer **80**(5-6): 914-7.

Nakamura, A., R. Amikura, et al. (2001). "Me31B silences translation of oocyte-localizing RNAs through the formation of cytoplasmic RNP complex during Drosophila oogenesis." Development **128**(17): 3233-42.

Nottrott, S., M. J. Simard, et al. (2006). "Human let-7a miRNA blocks protein production on actively translating polyribosomes." Nat Struct Mol Biol **13**(12): 1108-14.

O'Donnell, K. A. and J. D. Boeke (2007). "Mighty Piwis defend the germline against genome intruders." Cell **129**(1): 37-44.

Ohara, T., Y. Sakaguchi, et al. (2007). "The 3' termini of mouse Piwi-interacting RNAs are 2'-O-methylated." Nat Struct Mol Biol **14**(4): 349-50.

Okamura, K., S. Balla, et al. (2008a). "Two distinct mechanisms generate endogenous siRNAs from bidirectional transcription in Drosophila melanogaster." Nat Struct Mol Biol **15**(6): 581-90.

Okamura, K., W. J. Chung, et al. (2008b). "The Drosophila hairpin RNA pathway generates endogenous short interfering RNAs." Nature **453**(7196): 803-6.

Okamura, K., J. W. Hagen, et al. (2007). "The Mirtron Pathway Generates microRNA-Class Regulatory RNAs in Drosophila." Cell **130**(1): 89-100.

Okamura, K., A. Ishizuka, et al. (2004). "Distinct roles for Argonaute proteins in small RNA-directed RNA cleavage pathways." Genes Dev **18**(14): 1655-66.

Okamura, K. and E. C. Lai (2008). "Endogenous small interfering RNAs in animals." Nat Rev Mol Cell Biol **9**(9): 673-8.

Olsen, P. H. and V. Ambros (1999). "The lin-4 regulatory RNA controls developmental timing in Caenorhabditis elegans by blocking LIN-14 protein synthesis after the initiation of translation." Dev Biol **216**(2): 671-80.

Pane, A., K. Wehr, et al. (2007). "zucchini and squash encode two putative nucleases required for rasiRNA production in the Drosophila germline." Dev Cell **12**(6): 851-62.

Patterson, G. H., D. W. Piston, et al. (2000). "Forster distances between green fluorescent protein pairs." Anal Biochem **284**(2): 438-40.

Peragine, A., M. Yoshikawa, et al. (2004). "SGS3 and SGS2/SDE1/RDR6 are required for juvenile development and the production of trans-acting siRNAs in Arabidopsis." Genes Dev **18**(19): 2368-79.

Petersen, C. P., M. E. Bordeleau, et al. (2006). "Short RNAs repress translation after initiation in mammalian cells." Mol Cell **21**(4): 533-42.

Pillai, R. S., S. N. Bhattacharyya, et al. (2005). "Inhibition of translational initiation by Let-7 MicroRNA in human cells." Science **309**(5740): 1573-6.

Poy, M. N., L. Eliasson, et al. (2004). "A pancreatic islet-specific microRNA regulates insulin secretion." Nature **432**(7014): 226-30.

Prakash, T. P., C. R. Allerson, et al. (2005). "Positional effect of chemical modifications on short interference RNA activity in mammalian cells." J Med Chem **48**(13): 4247-53.

Rana, T. M. (2007). "Illuminating the silence: understanding the structure and function of small RNAs." Nat Rev Mol Cell Biol **8**(1): 23-36.

Rand, T. A., S. Petersen, et al. (2005). "Argonaute2 cleaves the anti-guide strand of siRNA during RISC activation." Cell **123**(4): 621-9.

Rehmsmeier, M., P. Steffen, et al. (2004). "Fast and effective prediction of microRNA/target duplexes." Rna **10**(10): 1507-17.

Rehwinkel, J., I. Behm-Ansmant, et al. (2005). "A crucial role for GW182 and the DCP1:DCP2 decapping complex in miRNA-mediated gene silencing." Rna **11**(11): 1640-7.

Reynolds, A., D. Leake, et al. (2004). "Rational siRNA design for RNA interference." Nat Biotechnol **22**(3): 326-30.

Rivas, F. V., N. H. Tolia, et al. (2005). "Purified Argonaute2 and an siRNA form recombinant human RISC." Nat Struct Mol Biol **12**(4): 340-9.

Robb, G. B. and T. M. Rana (2007). "RNA helicase A interacts with RISC in human cells and functions in RISC loading." Mol Cell **26**(4): 523-37.

Ruby, J. G., C. H. Jan, et al. (2007). "Intronic microRNA precursors that bypass Drosha processing." Nature **448**(7149): 83-6.

Rusinov, V., V. Baev, et al. (2005). "MicroInspector: a web tool for detection of miRNA binding sites in an RNA sequence." Nucleic Acids Res **33**(Web Server issue): W696-700.

Saetrom, O., O. Snove, Jr., et al. (2005). "Weighted sequence motifs as an improved seeding step in microRNA target prediction algorithms." Rna **11**(7): 995-1003.

Saito, K., A. Ishizuka, et al. (2005). "Processing of pre-microRNAs by the Dicer-1-Loquacious complex in Drosophila cells." PLoS Biol **3**(7): e235.

Saito, K., K. M. Nishida, et al. (2006). "Specific association of Piwi with rasiRNAs derived from retrotransposon and heterochromatic regions in the Drosophila genome." Genes Dev **20**(16): 2214-22.

Saito, K., Y. Sakaguchi, et al. (2007). "Pimet, the Drosophila homolog of HEN1, mediates 2'-O-methylation of Piwi- interacting RNAs at their 3' ends." Genes Dev **21**(13): 1603-8.

Sarot, E., G. Payen-Groschene, et al. (2004). "Evidence for a piwi-dependent RNA silencing of the gypsy endogenous retrovirus by the Drosophila melanogaster flamenco gene." Genetics **166**(3): 1313-21.

Schwarz, D. S., G. Hutvagner, et al. (2003a). "Asymmetry in the assembly of the RNAi enzyme complex." Cell **115**(2): 199-208.

Schwarz, D. S., G. Hutvágner, et al. (2003b). "Asymmetry in the assembly of the RNAi enzyme complex." Cell **115**(2): 199-208.

Schwarz, D. S., G. Hutvagner, et al. (2002). "Evidence that siRNAs function as guides, not primers, in the Drosophila and human RNAi pathways." Mol Cell **10**(3): 537-48.

Sen, G., T. S. Wehrman, et al. (2004). "Restriction enzyme-generated siRNA (REGS) vectors and libraries." Nat Genet **36**(2): 183-9.

Sen, G. L. and H. M. Blau (2005). "Argonaute 2/RISC resides in sites of mammalian mRNA decay known as cytoplasmic bodies." Nat Cell Biol **7**(6): 633-6.

Siolas, D., C. Lerner, et al. (2005). "Synthetic shRNAs as potent RNAi triggers." Nat Biotechnol **23**(2): 227-31.

Song, J. J., S. K. Smith, et al. (2004). "Crystal structure of Argonaute and its implications for RISC slicer activity." Science **305**(5689): 1434-7.

Tam, O. H., A. A. Aravin, et al. (2008). "Pseudogene-derived small interfering RNAs regulate gene expression in mouse oocytes." Nature **453**(7194): 534-8.

Taverna, S. D., R. S. Coyne, et al. (2002). "Methylation of histone h3 at lysine 9 targets programmed DNA elimination in tetrahymena." <u>Cell</u> **110**(6): 701-11.

Thermann, R. and M. W. Hentze (2007). "Drosophila miR2 induces pseudo-polysomes and inhibits translation initiation." <u>Nature</u>.

Tolia, N. H. and L. Joshua-Tor (2007). "Slicer and the argonautes." <u>Nat Chem Biol</u> **3**(1): 36-43.

Tomari, Y., T. Du, et al. (2007). "Sorting of Drosophila Small Silencing RNAs." <u>Cell</u> **130**(2): 299-308.

Tomari, Y., C. Matranga, et al. (2004). "A protein sensor for siRNA asymmetry." <u>Science</u> **306**(5700): 1377-80.

Ui-Tei, K., Y. Naito, et al. (2004). "Guidelines for the selection of highly effective siRNA sequences for mammalian and chick RNA interference." <u>Nucleic Acids Res</u> **32**(3): 936-48.

Vagin, V. V., A. Sigova, et al. (2006). "A distinct small RNA pathway silences selfish genetic elements in the germline." <u>Science</u> **313**(5785): 320-4.

Vella, M. C., E. Y. Choi, et al. (2004). "The C. elegans microRNA let-7 binds to imperfect let-7 complementary sites from the lin-41 3'UTR." <u>Genes Dev</u> **18**(2): 132-7.

Wakiyama, M., K. Takimoto, et al. (2007). "Let-7 microRNA-mediated mRNA deadenylation and translational repression in a mammalian cell-free system." <u>Genes Dev</u> **21**(15): 1857-62.

Wang, B., T. M. Love, et al. (2006). "Recapitulation of short RNA-directed translational gene silencing in vitro." Mol Cell **22**(4): 553-60.

Watanabe, T., Y. Totoki, et al. (2008). "Endogenous siRNAs from naturally formed dsRNAs regulate transcripts in mouse oocytes." Nature **453**(7194): 539-43.

Weston, A. and J. Sommerville (2006). "Xp54 and related (DDX6-like) RNA helicases: roles in messenger RNP assembly, translation regulation and RNA degradation." Nucleic Acids Res **34**(10): 3082-94.

Wienholds, E. and R. H. Plasterk (2005). "MicroRNA function in animal development." FEBS Lett **579**(26): 5911-22.

Wu, L., J. Fan, et al. (2006). "MicroRNAs direct rapid deadenylation of mRNA." Proc Natl Acad Sci U S A **103**(11): 4034-9.

Yekta, S., I. H. Shih, et al. (2004). "MicroRNA-directed cleavage of HOXB8 mRNA." Science **304**(5670): 594-6.

Yi, R., Y. Qin, et al. (2003). "Exportin-5 mediates the nuclear export of pre-microRNAs and short hairpin RNAs." Genes Dev **17**(24): 3011-6.

Yin, H. and H. Lin (2007). "An epigenetic activation role of Piwi and a Piwi-associated piRNA in Drosophila melanogaster." Nature **450**(7167): 304-8.

Zamore, P. D. and B. Haley (2005). "Ribo-gnome: the big world of small RNAs." Science **309**(5740): 1519-24.

Zamore, P. D., T. Tuschl, et al. (2000). "RNAi: double-stranded RNA directs the ATP-dependent cleavage of mRNA at 21 to 23 nucleotide intervals." Cell **101**(1): 25-33.

Zeng, Y. and B. R. Cullen (2004). "Structural requirements for pre-microRNA binding and nuclear export by Exportin 5." Nucleic Acids Res **32**(16): 4776-85.

Zeng, Y., R. Yi, et al. (2003). "MicroRNAs and small interfering RNAs can inhibit mRNA expression by similar mechanisms." Proc Natl Acad Sci U S A **100**(17): 9779-84.

# CURRICULUM VITAE

# Chia-Ying Chu

## Chia-ying.Chu@umassmed.edu

## Education

2002~Present     PhD Candidate
Department of Biochemistry and Molecular Pharmacology
Graduate School of Biomedical Sciences
University of Massachusetts, Worcester, MA

2000, B.S.     School of Pharmacy
National Taiwan University
Taipei, Taiwan

1997, M.S.     Graduate Institute of Zoology
National Taiwan University
Taipei, Taiwan

1995, B.S.     Department of Zoology
National Taiwan University
Taipei, Taiwan

## Work Experiences

08/2001~07/2002     Teaching Assistant
Department of Zoology, National Taiwan University
- Teaching Assistant, for the course of Animal Histology Lab. and General Zoology Lab.
- Lecturer, on General Zoology
-

08/2000 ~ 07/2001     Teaching Assistant
Department of Pharmacy, National Taiwan University
- Teaching Assistant, for the course of Pharmaceutics, Pharmacokinetics and Pharmaceutics Lab.

## Scholastic Awards/ Honors

1999     National Taiwan University Presidential Awards
1997     Te-Kuie Hsieh and Sung-Yan Feng Scholarship
1995-1997   The Ministry of Education Graduate Fellowship

1991-1995  Scholarship for Gifted Senior High School Students Studying Mathematics and Natural Sciences (Ministry of Education, R.O.C.)

## Publications

1. Nathans R, **Chu CY**, Serquina A, Lu C, Cao H, and Rana TM. "Defense against HIV-1 is mediated by P bodies and a cellular microRNA". *Molecular Cell* (submitted, under review).

2. **Chu CY**, and Rana TM, "Potent RNAi by short RNA trigger". *RNA* 2008 14: 1714-19.

3. **Chu CY**, Rana TM. "Small RNAs: regulators and guardians of the genome." *J Cell Physiol*. 2007 Nov;213(2):412-9. Review.

4. **Chu CY**, Rana TM. "Translation repression in human cells by microRNA-induced gene silencing requires RCK/p54." *PLoS Biol*. 2006 Jul;4(7):e210.

5. Chiu YL, Dinesh CU, **Chu CY**, Ali A, Brown KM, Cao H, Rana TM. "Dissecting RNA-interference pathway with small molecules." *Chem Biol*. 2005 Jun;12(6):643-8.

6. Brown KM, **Chu CY**, Rana TM. "Target accessibility dictates the potency of human RISC." *Nat Struct Mol Biol*. 2005 May;12(5):469-70.

7. Ping YH, **Chu CY**, Cao H, Jacque JM, Stevenson M, Rana TM. "Modulating HIV-1 replication by RNA interference directed against human transcription elongation factor SPT5." *Retrovirology*. 2004 Dec 27;1:46.

8. Chiu YL, Ali A, **Chu CY**, Cao H, Rana TM. "Visualizing a correlation between siRNA localization, cellular uptake, and RNAi in living cells." *Chem Biol*. 2004 Aug;11(8):1165-75.

9. **Chu, Chia-ying**. (1997) Expression of Heterologous Promoter Sequences in Fish cell Line and Zebrafich Embryos. Thesis for Master Degree. Graduate Institute if Zoology, National Taiwan University.